

Pathogenesis of Non-WNT, Non-SHH type Medulloblastoma

By

Pooja Panwalkar

[LIFE09200904016]

Tata Memorial Centre (TMC)

*A thesis submitted to the
Board of Studies in Life Sciences
In partial fulfillment of requirements*

For the Degree of

DOCTOR OF PHILOSOPHY

of

HOMI BHABHA NATIONAL INSTITUTE

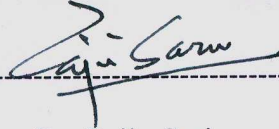


December 2015

HOMI BHABHA NATIONAL INSTITUTE

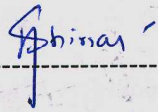
Recommendations of the Viva Voce Board

As members of Viva Voce committee we certify that we have read the dissertation prepared by Ms. Pooja Panwalkar entitled "Pathogenesis of non-WNT, non-SHH type medulloblastoma" and recommend that it may be accepted as fulfilling the thesis requirement for the award of Degree of Doctor of Philosophy.



Date: 23.12.15

Chairperson: -- Dr. Rajiv Sarin



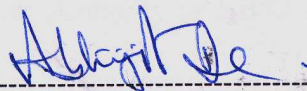
Date: 23-12-15

Convenor -- Dr. Neelam Shirsat



Date: 23/12/15

Member 1: -- Dr. Sorab Dalal



Date: 23/12/15

Member 2: -- Dr. Abhijit De



Date: 23/12/15

External Examiner: -- Dr. D. Karunakaran

Final approval and acceptance of this dissertation is contingent upon the candidate's submission of the final copies of the dissertation to HBNI.

I hereby certify that I have read this dissertation prepared under my direction and recommend that it may be accepted as fulfilling the dissertation requirement.

Date: 23.12.2015

Place: Navi Mumbai


Dr. Neelam Shirsat

(Guide)

STATEMENT BY AUTHOR

This dissertation has been submitted in partial fulfillment of requirements for an advanced degree at Homi Bhabha National Institute (HBNI) and is deposited in the Library to be made available to borrowers under rules of the HBNI. Brief quotations from this dissertation are allowable without special permission, provided that accurate acknowledgement of source is made. Requests for permission for extended quotation from or reproduction of this manuscript in whole or in part may be granted by the Competent Authority of HBNI when in his or her judgment the proposed use of the material is in the interests of scholarship. In all other instances, however, permission must be obtained from the author.



Pooja Panwalkar

DECLARATION

I, hereby declare that the investigation presented in the thesis has been carried out by me. The work is original and has not been submitted earlier as a whole or in part for a degree /diploma at this or any other Institution / University.



Pooja Panwalkar

List of Publications Arising From the Thesis

Article:

Pooja Panwalkar, Aliasgar Moiyadi, Atul Goel, Prakash Shetty, Naina Goel, Epari Sridhar and Neelam Shirsat. (2015). **MiR-206, a cerebellum enriched miRNA is down-regulated in all medulloblastoma subgroups and its overexpression is necessary for growth inhibition of medulloblastoma cells.** *J. Mol. Neurosci.* 56: 3, 673-680 PMID:25859932

Presentations at Conferences:

1. **Participated and presented** an abstract titled **‘Role of miR-206 in the pathogenesis of medulloblastoma’** as a poster presentation at **XXXVI All India Cell Biology Conference and International Symposium on "Stress Adaptive Response and Genome Integrity (SARGI)** held on 17-19th October 2012 at Bhabha Atomic Research Centre (BARC), Mumbai, India
2. **Participated and presented** an abstract titled **‘Role of miR-206 in the pathogenesis of medulloblastoma’** as an **oral presentation** at the **‘Joint meeting of Asian society of Neurooncology (ASNO) and Indian Society for Neurooncology (ISNO)’** held on 21st-24th March 2013 at Mumbai, India
3. **Participated and presented** an abstract titled **‘miR-206—A miRNA down-regulated in medulloblastoma, a common pediatric malignant brain tumor’**, as a **poster presentation** at **‘Mechanisms & Models of Cancer meeting’** held on 12th-16th August 2014 at Cold Spring Harbor Laboratory, New York, USA.

ACKNOWLEDGEMENT

“Silent gratitude isn’t much help to anyone” – G.B. Stern

Hence, here goes....

Firstly, I would like to thank my Ph.D. guide, *Dr. Neelam Shirsat*. Her insightful nature and deep understanding of the subject helped me successfully carry out my Ph.D. project. She taught me a number of things, knowingly and unknowingly and always pushed me to achieve the best. I am also grateful to all my doctoral committee members *Dr. Rajiv Sarin*, *Dr. Sorab Dalal* and *Dr. Abhijit De*, for their time, suggestions and encouragement.

I also thank our director *Dr. Shubhada Chiplunkar*, ex-director *Dr. Rajiv Sarin* and ex-Dy. Director *Dr. Surekha Zingde* for the excellent infrastructure and environment at ACTREC. This project would have been incomplete without the help of our clinical collaborators. I thank *Dr. Aliasgar Moiyadi*, *Dr. Prakash Shetty*, *Dr. Atul Goel* and *Dr. Naina Goel* for providing us with the tissues for this study. A special thanks to *Dr. Epari Sridhar* for his time and enthusiasm in help with the immunohistochemical analysis. I am extremely grateful to the patients and their parents. Their support is indeed invaluable.

ACTREC facilities provided me with all the necessary equipment and expertise for my work. I am thankful to *Mr. Uday Dandekar* from the Common instrument facility for his efforts in providing solutions to most instrument related problems. I owe a ‘thank you’ to *Dr. Arvind Ingle* and *Dr. Rahul Thorat* from the Laboratory animal facility. During the initial phases of animal related work, the painstaking efforts and patience of Dr. Thorat helped me achieve some interesting leads in my experiments. A very friendly interaction with the animal house staff including *Mahesh*, *Shashi*, *Chavan* and *Sakpal* always made work simpler.

I am also thankful to other facilities and their staff members whose support helped me understand and optimally use these facilities for my experiments. I especially thank, *Vaishali, Tanuja* and *Jayraj* from the Digital Imaging Facility, *Rekha* and *Shamal* from Flow cytometry and *Sharada and Naresh* from the Genomics facility.

It's difficult to do science with an empty head, but impossible with an empty stomach! I therefore thank ACTREC for the fellowship.

The journey of six years started with a small step into Shirsat Lab. I cannot thank enough all the people from the lab for making it an excellent environment to work. A big thank you to *Anantji, Umesh* and *Sadaf* for their help and support! The first few years in lab were tough. But I could always rely on my seniors *Amit, Pratibha, Shailendra* and *Ratika* for their advice. They made me feel comfortable in the new environment and always told stories of their experiences which encouraged me tremendously. *Kedar*, my batch mate and lab mate, deserves a special thank you for his help with my work and his constructive criticism that nudged me to improve significantly. I am also grateful to my colleagues *Shreyas, Annada* and *Sanket* for sometimes teaching me and at other times, helping me with my work. I am also thankful to all my juniors *Satish, Raikamal, Shalaka, Harish* and *Akash*. They were always there when I had to discuss work but also there to share a laugh. I am grateful to my trainees for being the unintended instruments of my learning course in teaching. Thank you *Sharayu, Swapnil* and *Yona*!

I made the best of friends in my roommates from Room nos. 50 and 54, Ketaki hostel. I cherish the friendship of *Rupa, Madhura, Abira, Sushmita* and *Snehal* who made my life at ACTREC so much better. The many moments of frustration and self doubt were quickly cured with a cup of hot tea and warm encouragements from this 'family' away from family. The many parties with my batchmates *Shafqat, Bhanu, Tanmoy, Srikanta, Rubina* and *Priyanka*, and friends *Sandeep, Avinash, Soundarya* and *Kaushal* made life out of lab extremely enjoyable. Thanks to *Bhawik* and

Gopal for the 'dabba' we shared at lunch every day. Each of these people truly enriched my experience at ACTREC.

I could always find solace in sharing my experiences with friends from school and college. Their moral support made a significant contribution to the successful completion of my thesis. Thank you to you all!

An exceptionally big thanks to my family- my Ajji, who used to always believe in me and my parents, who have been the pillars of support in my life with their words of love and encouragement. Last, but definitely not the least, words will not be enough to thank my husband, Atul for his contribution to the successful completion of my Ph.D. He taught me much of the lab work and we shared many exciting scientific discussions. His encouragement and support helped me immensely in reaching the final goal. Thank you for tolerating my absence and for always trusting me to make it right till the end!

Table of Contents

SYNOPSIS.....	1
<i>List of Figures</i>	15
<i>List of Tables</i>	16
<i>List of Abbreviations</i>	17
INTRODUCTION	19
REVIEW OF LITERATURE	25
2.1 Medulloblastoma- A Clinical Perspective.....	26
2.2 Mechanism of Pathogenesis- From History to Current Understanding	27
2.3 Challenges in Understanding the Biology of the Non-WNT Non-SHH Medulloblastoma	36
2.4 MicroRNA's: A Big Role for Small Molecules.....	38
2.5 MicroRNAs in Medulloblastoma	39
MATERIALS AND METHODS.....	45
Materials	46
Methods.....	48
3.1 Ethics Statement and Collection of Human and Mice Tissues	48
3.2 Extraction of RNA from Human or Mice Tissues	49
3.3 Extraction of RNA by the Guanidium Isothiocyanate (GITC) Method.....	49
3.4 Preparation of Denaturing Gels for RNA.....	52
3.5 Reverse Transcriptase PCR for conversion of RNA to cDNA	53
3.6 Stem loop Reverse Transcription for miRNA.....	55
3.7 Real Time PCR.....	57
3.8 Molecular Subgrouping of Medulloblastoma Tumor Tissues.....	59
3.9 Cloning of PCR Products into the Target Vector.....	62
3.10 Cell Culture	72

3.10.1 Tissue Culture Media and Reagents	72
3.10.2 Routine Maintenance of Cell Lines	73
3.10.3 Freezing and Revival	75
3.10.5 Transient Transfection of Medulloblastoma Cell Lines with miRNA Mimics	77
3.10.6 Generation of Lentiviral particles and Selection of Stable Polyclonal Populations of Medulloblastoma Cell Lines	78
3.10.7 MTT Reduction Assay	80
3.10.8 Soft agar Colony Formation Assay	81
3.10.9 Clonogenic and Radiation Sensitivity Assay	82
3.10.10 Synergistic Effect of All trans Retinoic Acid and miR-206 on the D283 Medulloblastoma Cell Line	83
3.10.11 Invasion Assay	83
3.11 In vivo Tumorigenicity Assay	86
3.11.1 In-vivo Tumorigenicity Assay by Subcutaneous Injection	86
3.11.2 In-vivo Tumorigenicity Assay by Orthotopic Injection in Mouse Cerebellum	86
3.11.3 Bioluminescence Imaging	91
3.12 Extraction of Proteins from Cultured Cells	93
3.13 Estimation of Protein Concentration	94
3.15 Western Blot Analysis and Immuno-detection	98
3.16 Immunohistochemical Analysis of Ezrin expression in Medulloblastoma Tumor Tissues	102
3.18 Luciferase Reporter Assay	116
3.18.1 Generation of Vector Constructs for the 3'UTR Luciferase Reporter assay	117
3.18.2 Luciferase Assay	120
3.19 Sodium Bisulphite Treatment of Genomic DNA and Sequencing of the PCR Amplified Gene Fragments	123
3.20 Survival Analysis for Group 3 and Group 4 Tumors using miR-204 as a Predictor	125
3.21 Statistical Analysis	126

RESULTS AND DISCUSSION	127
4.1: Molecular Subgrouping of Medulloblastoma Cell Lines.....	128
4.2: Role of miR-206 in the Biology of Medulloblastoma	131
4.2.1 Evaluation of miR-206 Expression in Human Medulloblastoma Tumor Tissues and Normal Cerebellum and Cerebrum Tissues by Real Time RT-PCR analysis.....	131
4.2.2 Evaluation of miR-206 Expression in Mouse Medulloblastoma Tumor Tissues from the <i>Smo</i> ^{+/+} Transgenic Mice and the <i>Ptch1</i> ^{+/-} Knock-out Mice and Normal Cerebellum Tissues by Real Time RT-PCR	132
4.2.3 Construction of a Lentiviral Plasmid Vector for Expression of miR-206.....	132
4.2.4 Effect of miR-206 Expression on the Growth, Clonogenic Potential, Radiation Sensitivity and Anchorage-independent Growth of the Established Medulloblastoma Cell Lines	134
4.2.5 Effect of Restoration of miR-206 Expression on the Level of OTX2 Protein in the Non-WNT Non-SHH Subgroup Cell Lines.....	138
4.2.6 Effect of miR-206 Overexpression on the Level of OTX2 Expression and Anchorage Independent Growth of Non-WNT, Non-SHH Medulloblastoma Cell Lines.....	140
4.2.7 Synergistic Effect of Restoration of miR-206 Expression and Treatment with All Trans Retinoic Acid (ATRA) on the Growth and OTX2 Expression in D283 Cell Line	142
DISCUSSION.....	144
4.3: Role of miR-204 in the biology of medulloblastoma.....	147
4.3.1 Differential expression of miR-204 in molecular subgroups of medulloblastoma	147
4.3.2 Correlation of miR-204 expression with survival in the non-WNT, non-SHH medulloblastoma patients	148
4.3.3 Effect of miR-204 expression on the proliferation, anchorage independent growth and tumorigenicity of medulloblastoma cell lines	149
4.3.4 Identification of the molecular mechanism underlying the effect of miR-204 by genome wide expression profiling.....	158
4.3.5 Ezrin expression in medulloblastomas and its correlation with molecular subgroups and survival.....	163
4.3.6 Identification of novel miR-204 target genes	164
4.3.7 CpG island methylation of miR-204 promoter region.....	168

DISCUSSION.....	170
SUMMARY AND CONCLUDING REMARKS	178
BIBLIOGRAPHY	184
PUBLICATIONS.....	193

SYNOPSIS



HOMI BHABHA NATIONAL INSTITUTE

PH. D. PROGRAMME SYNOPSIS OF PH.D. THESIS

- 1. Name of the Student: Pooja Panwalkar**
- 2. Name of the Constituent Institution: Tata Memorial Centre, ACTREC**
- 3. Enrolment No. : LIFE09200904016**
- 4. Title of the Thesis: Pathogenesis of non-WNT, non-SHH type medulloblastomas**
- 5. Board of Studies: Life Sciences**

1. INTRODUCTION

Medulloblastoma is the most common malignant brain tumor in children. It is a Grade IV tumor arising in the cerebellum or brain stem. Current treatment includes surgery, chemotherapy and radiation therapy. The five year survival rate is 80 % for average risk and 50-60% for high risk patients. However, neuro-cognitive deficits and other treatment related sequelae are often observed in survivors.¹ Hence, a better understanding of the biology of the tumor is required to explore new targets for therapy.

Expression profiling studies have identified four molecular subgroups of Medulloblastoma; WNT, SHH, Group 3 and Group 4. These four subgroups are also distinct in terms of demographics, histology, DNA copy number aberrations, and clinical outcome. The first two subgroups have a characteristic developmental pathway gene signature i.e. the WNT and SHH signalling pathway respectively. Group 3 and Group 4 tumors have an overlapping gene expression profile. The Group 3 and Group 4 (Non-WNT, non-SHH) tumors have the highest rate of metastases at diagnosis and Group 3 tumors are also associated with the worse overall survival within the four subgroups.² Group 3 tumors often show over expression of MYC, cell

cycle related genes and certain retina specific genes. The group 4 tumors on the other hand, show expression of neuronal differentiation related genes. Exome sequencing analysis has identified histone modification and chromatin remodelling genes to be mutated in tumors from all the four subgroups.⁴ Recent reports suggest that tetraploidy and copy number alterations are most commonly associated with Group 3 tumors followed by Group 4 tumors.⁵ However, the exact molecular mechanism of pathogenesis of non-WNT, non-SHH subgroup tumors is not known. MiRNAs are small non-coding molecules that regulate mRNA expression and have been shown to be deregulated in many cancers. Previous report from our lab has shown miRNA expression to be deregulated in medulloblastomas as compared to normal cerebellum and the four molecular subgroups of medulloblastomas show differential miRNA expression.^{3,6} In the present work, the role of two such miRNAs viz miR-206 and miR-204 in medulloblastoma biology has been studied.

2. OBJECTIVE: To study the role of miRNA coding genes in the pathogenesis of non-WNT, non-SHH medulloblastoma.

3. WORK DONE AND RESULTS

3.1. Characterization of medulloblastoma cell lines

The subgroup affiliation of medulloblastoma cell lines was studied by analyzing the expression of the genes specifically and differentially expressed in each of the four medulloblastoma subgroups in the medulloblastoma cell lines Daoy, D283, D425, D341 and D384 by real time RT-PCR analysis. Daoy shows reduced expression of *OTX2* and expresses *HHIP*, a SHH signaling pathway gene. It is derived from a tumor with desmoplastic histology and shows chromosome 9 alteration⁹, hence it is likely to belong to the SHH subgroup. All other cell lines show high expression of *MYC*, *IMPG2*, retinal specific genes like *CRX* and under-express neuronal differentiation genes like *GRM8*. They are reported to bear isochromosome 17q and

amplification of the *MYC* gene.¹⁰ Therefore these cell lines seem to belong to the group 3 of medulloblastoma.

3.2 Role of miR-206 in the pathogenesis of medulloblastoma

MicroRNA expression profiling shows a number of miRNAs to be downregulated in medulloblastomas as compared to the normal cerebellum. MiR-206 is one such miRNA. It was previously identified as a skeletal muscle specific miRNA. Its expression is 10,000 fold higher in skeletal muscle as compared to that in the brain. In brain it has been shown to be expressed exclusively in the cerebellum which is the site of medulloblastoma occurrence.⁷ MiR-206 has been reported to target OTX2, a known oncogene that is overexpressed in WNT, Group 3 and Group 4 medulloblastomas with focal amplifications reported in Group 3 tumors.⁸

3.2.1 Evaluation of miR-206 expression in medulloblastoma tumor tissues and normal cerebellum

MiR-206 expression was evaluated in human sporadic medulloblastoma tumor tissues (n=44) and in normal cerebellum (n=7) and cerebrum tissues (n=5) by real time RT-PCR. MiR-206 expression in the normal brain cerebrum was found to be 50-200 fold lower as compared to the normal developing and adult cerebellum consistent with its reported enriched expression in rat cerebellum.¹⁷ MiR-206 expression was found to be downregulated in medulloblastomas belonging to all the four subgroups by 10-10,000 fold ($p \leq 0.0001$) and by ~100 fold in five established medulloblastoma cell lines *viz.* Daoy, D425, D283, D384 and D341 ($p \leq 0.0001$).

The expression of murine homolog of human miR-206 was evaluated in medulloblastomas from the SHH subgroup mouse models *viz.* *Smo*^{+/+} transgenic mice and *Ptch1*^{+/-} knock-out mice.^{11, 12} MiR-206 expression was found to be downregulated by ~10 fold ($p \leq 0.05$) in *Smo*^{+/+} transgenic mice tumors and by 10-100 fold ($p \leq 0.01$) in *Ptch1*^{+/-} knock-out mice tumors as compared to their normal cerebellar counterparts.

3.2.2 Effect of miR-206 expression on the growth characteristics of medulloblastoma cell lines

The effect of restoration of miR-206 expression was studied in the Daoy, D425 and D283 medulloblastoma cell lines. These cell lines were transduced with lentiviral particles of pTRIPZ-miR-206 vector construct that expressed miR-206 in a doxycycline inducible manner. Two stable polyclonal populations (P1, P2) of each of the three cell lines expressing miR-206 upon doxycycline induction at levels comparable to those in the normal cerebellum were selected in the presence of puromycin. The effect of miR-206 expression on proliferation was studied by the MTT assay. Restoration of miR-206 expression upon doxycycline treatment of P1 and P2 populations of the Daoy, D425 and D283 cell lines showed a marginal (5-10%) growth inhibition. The clonogenic assay was carried out to study the effect of miR-206 expression on the clonogenic potential of Daoy cells. No significant difference was observed in the number of colonies formed by the vector control cells and the miR-206 expressing P1 and P2 populations of Daoy cells. The effect of miR-206 expression on the radiation sensitivity of Daoy cells was studied in a clonogenic assay after irradiation of the cells at a dose of 6 Gy. There was a marginal increase (~20%) in the radiation sensitivity of Daoy cells upon miR-206 expression. The effect of miR-206 expression on the anchorage independent growth potential of Daoy, D425 and D283 cells was studied by the colony formation in soft agar. There was no significant difference in the number or size of colonies formed in the P1 and P2 populations of miR-206 expressing cells as compared to the vector control cells. Thus, the expression of miR-206 at levels equivalent to that in the normal cerebellum did not have a significant effect on the growth characteristics of medulloblastoma cell lines Daoy, D425 and D283.

3.2.3 Effect of miR-206 on OTX2 expression

OTX2 has been reported to be a target of miR-206.¹³ *OTX2*, a homeobox transcription factor plays an important role in cerebellar development.¹⁴ In the fully developed cerebellum however, expression of the *OTX2* gene is silenced. On the other hand, it is over-expressed in all

medulloblastomas except SHH subgroup tumors.¹⁵ Restoration of miR-206 expression was not found to result in the down-regulation of OTX2 protein levels as studied by western blot analysis in the P1 and P2 populations of D425 and D283 cell lines.

3.2.4 Effect of overexpression of miR-206 on OTX2 expression and growth

OTX2 is overexpressed in the non-SHH medulloblastomas. Overexpression of miR-206 by ~100-500 fold by transfection of synthetic miR-206 mimics in D283 and D425 cells resulted in reduction in the OTX2 protein levels. MiR-206 overexpression also resulted in ~50% ($p \leq 0.001$) reduction in the colony formation as compared to the siGLO transfected control cells of D425 and D283 cell lines. The stable polyclonal populations (P3) of D425 and D283 cells overexpressing miR-206 (~ 80-150 fold) also showed ~50 % ($p \leq 0.01$) and ~30 % ($p \leq 0.002$) reduction in the soft agar colony formation respectively. Thus, miR-206 overexpression was found necessary to downregulate OTX2 protein levels and bring about growth inhibition of medulloblastoma cells.

3.2.5 Synergistic effect of miR-206 and ATRA treatment on OTX2 expression and growth

ATRA (All-trans retinoic acid) has been shown to downregulate OTX2 expression and inhibit proliferation of medulloblastoma cells.¹⁶ The effect of restoration of miR-206 expression in combination with ATRA treatment on the level of OTX2 expression and growth of medulloblastoma cells was analyzed. The western blot analysis showed reduction of OTX2 protein levels on treatment with 5 nM and 10 nM ATRA in the P1 population of D283 cells. However, no further reduction in the OTX2 expression levels was seen on restoration of miR-206 expression. The treatment of D283 P1 population with 5 nM/10 nM ATRA resulted in 40-50% growth inhibition as studied by MTT reduction assay. This did not change upon miR-206 expression, indicating no synergistic effect of ATRA and miR-206 at the levels studied.

3.3 Role of miR-204 in the pathogenesis of medulloblastoma

Previous studies in the lab have shown that miR-204 expression is down-regulated 10-100 fold in the SHH tumors and in most group 3 tumors as compared to the normal cerebellum. It is an intronic miRNA located at chromosome 9q22.1 within the *TRPM3* gene. In a large scale study on 3312 tumors, 1107 non-malignant tissues on miRNA profile in cancer, miR-204-211 family was found to be the top deleted family.¹⁷ The functional role of miR-204 as a tumor suppressor miRNA has been shown in various cancers.¹⁸⁻²² Expression of miR-204 brought about reduction in proliferation and anchorage independent growth of Daoy cell line. *In vivo* tumorigenicity in nude mice showed ~65-70% reduction in size of the tumors formed by subcutaneous xenografts from miR-204 expressing Daoy cells as compared to the vector control cells. (Pratibha Boga, Ph. D. thesis). MiR-204 expression was also found to be downregulated 10-100 fold in the D425 and D341 cell lines and 2-3 fold in the D283 cell line compared to the normal cerebellum (R.Q.= 25-35). Hence, the effect of expression of miR-204 on the growth, tumorigenicity and invasion potential of these cell lines was studied.

3.3.1 Effect of mir-204 expression on the proliferation, anchorage independent growth and tumorigenicity of medulloblastoma cell lines

Stable polyclonal populations of Daoy and D341 cells were obtained by transduction with miR-204-pTRIPZ construct viral particles, expressing miR-204 on doxycycline induction. The level of miR-204 expression was found to be in the range of R.Q.= 25-45, which is comparable to that in the normal cerebellum. Daoy cell line showed 35-45% reduction ($p \leq 0.01$) in proliferation while there was a marginal reduction in D341 cells on induction of miR-204 expression as compared to the uninduced control cells as judged by the MTT assay. The anchorage independence growth potential of miR-204 expressing Daoy cells showed 30-40% ($p \leq 0.01$) reduction and D341 cells showed ~40% ($p \leq 0.01$) reduction as studied by colony formation in soft agar. *In-vivo* tumorigenicity of Daoy cells was studied by injecting 4.5×10^5 cells

subcutaneously into NOD/SCID mice. There was ~70% ($p \leq 0.01$) reduction in the volume of tumor formed by miR-204 expressing cells as compared to that of vector control cells. In order to study the effect of miR-204 expression on the growth of D283 and D425 cell lines, the cells were transfected with synthetic miRNA mimics. Transfection with miR-204 mimic resulted in the level of expression (RQ = 50-100) which was comparable to that in the normal cerebellum or in the Group 4 tumors. There was no significant difference in the proliferation of D283 and D425 cells expressing miR-204 as compared to the siGLO transfected control cells. There was no significant difference in the colony formation in soft agar in D283 cells expressing miR-204 whereas there was 25-30% ($p \leq 0.01$) reduction in D425 cells expressing miR-204 as compared to the respective control siGLO transfected cells.

3.3.2 Effect of miR-204 expression on invasion potential of medulloblastoma cell lines

The effect of miR-204 expression on the invasion potential of Daoy and D283 cells was studied using matrigel coated Boyden chamber inserts. Doxycycline induction of miR-204 expression in the polyclonal populations of Daoy cells resulted in ~50% ($p \leq 0.001$) reduction in invasion as compared to the uninduced control cells. MiR-204 mimic transfected D283 cells also showed ~50% ($p \leq 0.001$) reduction in invasion as compared to the control siGLO transfected cells.

3.3.3 Gene expression analysis of miR-204 expressing medulloblastoma cell lines

In order to study the changes in gene expression profile on expression of miR-204 and to identify potential targets of this miRNA, gene expression analysis was carried out. It was analyzed for differential gene expression in the control cells as compared to that in miR-204 expressing Daoy and D283 cells. The validated targets of miR-204 such as *RAB22A*, *M6PR*, *EZR*, *AP1S2*, *EDEMI* and *BCL2L2* were found to be downregulated by 1.5 - 6 folds in miR-204 expressing Daoy cells as compared to the vector control cells. These changes were less evident in the miR-204 mimic transfected D283 cells. The validation of expression of the known target genes, *RAB22A*, *M6PR*, *EZR*, *AP1S2*, *EDEMI* and *BCL2L2* was studied by real time RT-PCR in

the Daoy and D341 cell lines. The expression of *RAB22A* and *M6PR* was found to be downregulated by ~1.5-2 fold in the miR-204 expressing Daoy and D341 cell lines. The expression of *AP1S2*, *BCL2L2* and *EDEMI* was found to be very low (R.Q. < 0.5) in Daoy cells and hence there was no significant difference in the expression of these genes in the control and miR-204 expressing Daoy cells. MiR-204 expressing D341 cells showed 2-10 fold downregulation of *AP1S2*, *BCL2L2* and *EDEMI* gene expression as compared to the uninduced control cells. Thus, *RAB22A* and *M6PR* are downregulated upon miR-204 expression in both Daoy and D341 cells while the *AP1S2*, *BCL2L2* and *EDEMI* are down regulated in D341 cells that have significant expression of these genes.

3.3.4 Identification of novel miR-204 target genes

The miRNA target prediction software 'targetscan' predicted *RAB10* and *ANGPTL2* as putative miR-204 target genes. These were also found to be downregulated by 1.5 fold and 3-5 fold respectively in miR-204 expressing Daoy cells as compared to the vector control cells in the gene expression analysis. The gene *NRPI* is also a predicted target gene of miR-204; hence 3' UTR of the *EZR*, *NRPI*, *RAB10* and *ANGPTL2* genes was cloned into a luciferase reporter vector to identify the direct targets of miR-204. *EZR* is a known target gene of miR-204 and was used as a positive control for the luciferase reporter assay.²⁰ The luciferase reporter activity for *EZR* was found to be reduced by ~30% ($p \leq 0.001$) on co-transfection of the *EZR* 3' UTR luciferase construct along with miR-204-pGIPz plasmid construct in 293T cells. Similarly, the luciferase reporter activity for *RAB10* was found to be reduced by ~30% ($p \leq 0.001$) while that of *NRPI* was found to be reduced marginally. There was no significant difference in the luciferase activity of the *ANGPTL2* 3'UTR luciferase reporter vector on cotransfection with miR-204-pGIPz plasmid construct. Thus, *RAB10* is a putative direct target of miR-204, while *ANGPTL2* and *NRPI* may not be direct targets of miR-204.

3.3.5 Ezrin expression in medulloblastomas and its correlation with molecular subgroups and survival

Ezrin, a validated miR-204 target gene, is a cytoskeletal crosslinker protein that has been reported to be overexpressed in medulloblastoma. SiRNA mediated downregulation of ezrin results into inhibition of invasion of medulloblastoma cell lines.²³ Ezrin expression was found to be downregulated in Daoy, D341 and D283 cells expressing miR-204 as compared to the control cells as studied by western blot analysis. Ezrin has been reported to be involved in metastasis in various cancers.^{23, 24} Immunohistochemical analyses for Ezrin expression was carried out in 108 medulloblastoma tumors tissues to determine its expression across the 4 subgroups which also show different degree of metastasis. The highest frequency of metastatic disease at diagnosis is seen for Group 3 and Group 4 medulloblastoma. The 108 medulloblastoma tumors include WNT (23), SHH (34), Gr 3(20) and Gr 4(30). Majority of the WNT (100%) and SHH (91%) tumors showed negligible to low expression of ezrin. On the other hand ~35% Group 3 and Group 4 tumors showed moderate to high level of Ezrin expression. However, Kaplan Meier analysis did not show significant correlation of Ezrin expression with survival across the subgroups.

3.3.6 Correlation of miR-204 expression with survival in the non-WNT, non-SHH medulloblastoma patients

MiR-204 expression across the medulloblastoma subgroups indicates downregulation of its expression in many Group 3 tumors and an upregulation in most of the Group 4 tumors. These subgroups are distinct in their clinical features such as prognosis and survival rate. Kaplan Meier analysis for survival of patients with group 3 (n=24) and Group 4 (n=35) tumors indicated significantly better survival ($p = 0.01$, hazard ratio = 3.76) for patients with high miR-204 expression as compared to low miR-204 expression. The expression level of miR-204 in the normal cerebellum was used as a median value.

4. SUMMARY AND CONCLUSIONS

In the present study the role of the two miRNAs; miR-206 and miR-204 in medulloblastoma biology was evaluated. MiR-206 was found to be downregulated in medulloblastomas from humans as well as murine tissues and medulloblastoma cell lines. Although restoration of its expression in medulloblastoma cell lines did not have a significant effect on their growth characteristics; overexpression of miR-206 was found to be necessary to downregulate its oncogenic target like *OTX2* and bring about growth inhibition of medulloblastoma cells.

MiR-204 showed differential expression across the medulloblastoma subgroups; however it was found to be downregulated in all medulloblastoma cell lines studied. Expression of miR-204 brought about reduction in the anchorage independent growth potential (Daoy D341 and D425), invasion (Daoy and D283) and tumorigenicity (Daoy) of the medulloblastoma cell lines. MiR-204 expression resulted in downregulation of the genes involved in metastasis (*EZR*), apoptosis (*BCL2L2*) and intracellular protein trafficking including *RAB22A*, *AP1S2*, *EDEM1*, *M6PR* as well as *RAB10*, a novel miR-204 target identified in the present study. MiR-204 target gene, Ezrin is differentially expressed across the molecular subgroups of medulloblastoma with higher expression in the metastatic non-WNT, non-SHH subgroups. Higher expression of miR-204 was found to correlate with better survival in the non-WNT, non-SHH subgroups supporting its role as a tumor suppressor miRNA.

5. REFERENCES

1. Biological background of pediatric Medulloblastoma and ependymoma: A review from a translational research perspective. De Bont J. *et.al.* (2006) *Neuro-Oncology* **10**:1040–1060.
2. Molecular subgroups of Medulloblastoma: the current consensus. Taylor M. *et. al.* (2012) *Acta Neuropathol* 123:465–472
3. Distinctive microRNA signature of medulloblastomas associated with the WNT signalling pathway Gokhale A. *et.al.*(2010) *J Can Res Ther*, 6:521-9
4. Dissecting the genomic complexity underlying Medulloblastoma. Lichter P. Pfister M. Eils R. *et al.* (2012) *Nature*, 488:100-105

5. Medulloblastoma exome sequencing uncovers subtype-specific somatic mutations. Pugh.T *et al.* (2012) *Nature*, 488:106-109
6. Real-time PCR assay based on the differential expression of microRNAs and protein-coding genes for molecular classification of formalin-fixed paraffin embedded medulloblastomas. Kunder, R., Jalali, R., Sridhar, E., et al. (2013) *Neuro-oncology* 15, 1644-1651.
7. MicroRNAs Show Mutually Exclusive Expression Patterns in the Brain of Adult Male Rats. Olsen L., *et.al.*(2009) *PLoS ONE* 4(10): e7225
8. OTX2 is critical for the maintenance and progression of classic Medulloblastoma. Adamson D. *et. al* (2010). *Cancer Res.* 70(1): 181–191
9. Establishment of a human medulloblastoma cell line and its heterotransplantation into nude mice. Jacobsen P, Jenkyn D and Papadimitriou J (1985) *J Neuropathol Exp Neurol.* 44(5):472-85.
10. Amplification of the c-myc Gene in Human Medulloblastoma Cell Lines and Xenografts Bigner S., Friedman H., Vogelstein B., et. Al. (1990) *Cancer Res* 50. 2347-2350, April 15. 1990
11. A mouse model for medulloblastoma and basal cell nevus syndrome. Corcoran, R.and Scott M. (2001). *J Neurooncol* 53(3): 307-318.
12. The SmoA1 mouse model reveals that notch signaling is critical for the growth and survival of sonic hedgehog-induced medulloblastomas. Hallahan A., Pritchard J, Hansen S *et al* (2004) *Cancer Res* 64:7794–7800
13. MiR-206 regulates neural cells proliferation and apoptosis via Otx2. Wang, R., et al. (2012). *Cell Physiol Biochem* 29(3-4): 381-390.
14. Otx1 and Otx2 define layers and regions in developing cerebral cortex and cerebellum. Frantz, G. D., et al. (1994). *J Neurosci* 14(10): 5725-5740.
15. OTX2 is critical for the maintenance and progression of Shh-independent medulloblastomas. Adamson, D. C., et al. (2010). *Cancer Res* 70(1): 181-191.
16. Evaluation of retinoic acid therapy for OTX2-positive medulloblastomas. Bai, R., et al. (2010). *Neuro Oncol* 12(7): 655-663.
17. Reprogramming of miRNA networks in cancer and leukemia. Volinia *et.al.* (2010) *Genome Res.* 20: 589-599
18. Network modeling identifies molecular functions targeted by mir-204 to suppress head and neck tumours metastasis. Lee Y. *et.al.* (2010) *PLoS computational Biology*, 6 (4):e1000730
19. MicroRNA-204 increases sensitivity of neuroblastoma cells to cisplatin and is associated with a favourable clinical outcome Stallings R. *et. al.*(2012) *British Journal of Cancer*, 107: 967–976
20. A microRNA contribution to aberrant Ras activation in gastric cancer, Lam *et. al.* (2011) *Am J Transl. Res.* 3(2):209-218
21. MicroRNA-204 critically regulates carcinogenesis in malignant peripheral nerve sheath tumours. Gong *et.al*, (2012)*Neuro Oncol* 14(8):1007–1017

22. VHL-Regulated MiR-204 Suppresses Tumours Growth through Inhibition of LC3B-Mediated Autophagy in Renal Clear Cell Carcinoma Mikhaylova *et. al.* (2012) *Cancer Cell*: 21, 532–546
23. The role of the membrane cytoskeleton cross-linker ezrin in Medulloblastoma cells Rutka.J. *et.al.* (2008) *Neuro Oncol* 11, 381–385

24. Dysregulation of Ezrin Phosphorylation Prevents Metastasis and Alters Cellular Metabolism in Osteosarcoma. Ren *et.al* (2011) *Cancer Res*;72(4); 1-12
25. OTX2 directly activates cell cycle genes and inhibits differentiation in medulloblastoma cells. Bunt, J., et al. (2012). *Int J Cancer* **131**(2): E21-32.

PUBLICATIONS:

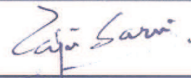
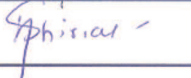


- a. **Published** - Pooja Panwalkar, Aliasgar Moiyadi, Atul Goel, Prakash Shetty, Naina Goel, Epari Sridhar and Neelam Shirsat. Mir-206, a cerebellum enriched mirna is downregulated in all medulloblastoma subgroups and its overexpression is necessary for growth inhibition of medulloblastoma cells. *J Mol Neurosci* 2015. DOI 10.1007/s12031-015-0548-z
- b. **Accepted** - NIL
- c. **Communicated** - NIL
- d. **Other publications** - NIL

Signature of Student:



Date: 27/5/15

Doctoral Committee:

S. No.	Name	Designation	Signature	Date
1.	Dr. Rajiv Sarin	Chairman		27-5-15
2.	Dr. Neelam Shirsat	Convener		27-5-15
3.	Dr. Sorab Dalal	Member		27/5/15
4.	Dr. Abhijit De	Member		27/5/15

Forwarded through



Dr. S.V. Chiplunkar
Director ACTREC
Chairperson,
Academic & Training Programme



Dr. K. Sharma
Director, Academics
T.M.C.

Prof. K.S. Sharma
DIRECTOR - ACADEMICS, TMC
Mumbai - 400 012

Dr. S. V. Chiplunkar
Director

Advanced Centre for Treatment, Research &
Education in Cancer (ACTREC)
Tata Memorial Centre
Kharghar, Navi Mumbai 410 210.

List of Figures

Figure 2.1: The mechanism of miRNA biogenesis.....	40
Figure 2.2: Heat map showing significantly differentially expressed miRNAs in four molecular subgroups of medulloblastoma and normal cerebellar tissues using SAM analysis.....	43
Figure 4.1.1: Expression of subgroup specific marker genes in medulloblastoma cell lines.	129
Figure 4.2.1: MiR-206 expression in the normal brain, medulloblastoma tumors, and in the established medulloblastoma cell lines.	133
Figure 4.2.2 : miR-206 pTRIPZ vector construct	134
Figure 4.2.4: Effect of miR-206 expression on the growth of medulloblastoma cell lines.	136
Figure 4.2.5: Effect of miR-206 expression on the anchorage independent growth of medulloblastoma cell lines.....	137
Figure 4.3.1: MiR-204 expression in the normal cerebellum, medulloblastoma tumors, and in the established medulloblastoma cell lines.	148
Figure 4.3.2: Kaplan Meier survival analysis	149
Figure 4.3.3: MiR-204 expression levels in stable polyclonal populations and miR-204 mimic transfected cells.	151
Figure 4.3.5: Effect of miR-204 expression on the anchorage independent growth of medulloblastoma cell lines.....	153
Figure 4.3.7: Effect of miR-204 expression on tumorigenicity of medulloblastoma cell lines.	156
Figure 4.3.8: Gene expression analysis of miR-204 expressing Daoy and D283 cells ...	160
Figure 4.3.9: Effect of miR-204 expression on the mRNA levels of the target genes. ...	161
Figure 4.3.10: Effect of miR-204 expression on the expression of target genes	162
Figure 4.3.12: <i>RAB10</i> is a direct target gene of miR-204.....	167
Figure 4.3.13: Methylation status of the miR-204 promoter region.	169

List of Tables

Table 2.1: Demographic characteristics of the four medulloblastoma subgroups.....	31
Table 2.2: Molecular and genomic characteristics of the four medulloblastoma subgroups.	32
Table 3.1: List of primers used for real time RT-PCR analysis of miR-204 target genes.	116
Table 3.2: List of primers for PCR amplification and cloning of 3'UTR regions of putative miR-204 target genes.	118
Table 3.3: Primer sequences used for Bisulphite PCR.	124
Table 4.1.1: Karyotypes of the medulloblastoma cell lines.....	129

List of Abbreviations

<i>APC</i>	Adenomatous Polyposis Coli, 28
<i>ATRA</i>	All Trans Retinoic Acid, 83
<i>CAT</i>	Computer Assisted Tomography, 26
<i>CGNPs</i>	Cerebellar Granule Neuron Progenitors, 33
<i>CNS</i>	Central Nervous System, 27
<i>CSF</i>	Cerebrospinal Fluid, 26
<i>CTNNB1</i>	Beta-catenin, 21
<i>DDX3X</i>	Dead box Helicase 3 X-linked, 21
<i>DEPC</i>	Diethylpyrocarbonate, 49
<i>DM's</i>	Double Minute chromosomes, 29
<i>DMEM</i>	Dulbecco's Modified Eagle's Medium, 74
<i>dNTP</i>	Deoxynucleotide Triphosphate, 55
<i>EZR</i>	Ezrin, 158
<i>FBS</i>	Fetal Bovine Serum, 74
<i>FFPE</i>	Formalin Fixed Paraffin Embedded, 48
<i>FOXC1</i>	Forkhead box C1, 159
<i>GAPDH</i>	Glyceraldehyde 3-phosphate dehydrogenase, 59
<i>HRP</i>	Horseradish Peroxidase, 101
<i>i17q</i>	Isochromosome 17q, 29
<i>LC/A</i>	Large Cell / Anaplastic, 27
<i>LFS</i>	Li-Fraumeni Syndrome, 28
<i>LRLP</i>	Lower Rhombic Lip Progenitor, 31
<i>M6PR</i>	Mannose-6-phosphate receptor, 158
<i>MAP1LC3B</i>	Microtubule-Associated Protein light chain 3B, 159
<i>MBEN</i>	Medulloblastoma with Extensive Nodularity, 27
<i>miRISC</i>	MicroRNA induced silencing complex, 39
<i>miRNA</i>	MicroRNA, 22
<i>MRI</i>	Magnetic Resonance Imaging, 26
<i>MYC</i>	V-Myc Avian Myelocytomatosis Viral Oncogene Homolog, 21
<i>MYOD1</i>	Myogenic Differentiation 1, 146

OTX2 Orthodenticle Homeobox 2, 21

PBS Phosphate Buffered Saline, 73

PNET Primitive Neuroectodermal Tumor, 28

PTCH1 Patched 1, 21

RAB10 RAB10, Ras Family Oncogene, 164

RAB22A RAB22A, Ras family oncogene, 158

RT Reverse Transcriptase / transcription, 53

SCNA Somatic Copy Number Aberrations, 36

SDM Site Directed Mutagenesis, 118

SHH Sonic Hedgehog, 21

SIRT1 Sirtuin 1, 159

SMO Smoothed, 21

SNV's Single Nucleotide Variations, 34

SUFU Suppressor of Fused, 21

TGN Trans Golgi Network, 172

TRPM3 transient receptor potential melastatin 3 cation channel, 170

UTR Untranslated Region, 23

VHL Von Hippel Lindau, 176

WHO World Health Organisation, 20

WNT Wingless, 21

INTRODUCTION

Medulloblastoma is the most common paediatric malignant tumor occurring in the cerebellar region of the brain. It constitutes of ~ 20% of all paediatric brain tumours [1]. World Health Organisation (WHO) classifies it as a grade IV tumor, which is the highest grade of malignancy [2]. These tumours have the capacity to metastasize to the leptomeninges or via the cerebrospinal fluid into the spinal cord. The symptoms of medulloblastoma include vomiting, headache, nausea and ataxia. The initial diagnosis is based on the location of the tumor in the posterior fossa region as judged by Magnetic Resonance Imaging or Computed Tomography scans and patient age. The final diagnosis is based on histopathological analysis of the tumor tissue, post surgery. The risk stratification of patients is carried out by taking into consideration the clinical features, including age at diagnosis, extent of surgical resection and metastatic status. Children ≤ 3 years of age, or with a $\geq 1.5 \text{ cm}^2$ size of residual tumour post surgery or those exhibiting leptomeningeal dissemination at the time of diagnosis are all considered to be high risk, and all other patients are considered as average risk [3]. Current treatment protocols that include a combination of surgery, cranio-spinal radiation therapy and chemotherapy have improved survival rates to 70-80 % in patients. Neuro-cognitive deficits are often seen in survivors' as a result of the cytotoxic treatments [4]. Secondary malignancies and increased mortality are also observed in patients with recurrent disease [5].

Gene expression profiling studies have identified medulloblastoma to be a heterogeneous disease consisting of four core molecular subgroups. The four core subgroups consist of the WNT, SHH, Group 3 and Group 4. These subgroups are not only distinct in their gene expression profile, but also in terms of their clinico-pathological correlates and demography [6]. These molecular subgroups are currently being explored to be used for better risk stratification [7].

The WNT and SHH subgroup tumours show a gene expression profile indicative of an activated WNT and SHH signalling pathway respectively. These signalling pathways are the drivers of pathogenesis in the tumours of these subgroups. Other subgroup specific characteristics of the WNT subgroup include mutations in the *CTNNB1* (Beta-catenin) gene and monosomy of chromosome 6. Similarly the SHH subgroup tumours show mutations in *PTCH1*, *SMO* or *SUFU* genes and loss of chromosome 9q [8]. Next generation sequencing studies have identified missense mutations in the RNA helicase gene *DDX3X* in about 50 % the WNT and 11 % of the SHH tumours. Mutations in other genes involved in epigenetic regulation of gene expression such as the SWI/SNF complex gene, *SMARCA4* and histone methyltransferase gene, *MLL2* have also been identified [9]. However, the mechanism by which these mutations contribute to the pathogenesis of these tumours is not completely understood.

The gene expression profiling does not reveal a specific signalling or developmental pathway activation in the non-WNT, non-SHH tumours i.e. the group 3 and group 4. The group 3 and group 4 tumors have an overlapping gene expression profile. The expression of the retinal genes in the group 3 tumours and that of the neuronal differentiation related genes in the group 4 tumours distinguishes them from each other. Neither the genetic basis nor the clinical significance of this gene expression signature is understood. The presence of an isochromosome 17q is most commonly associated with the group 3 and group 4 tumours [8]. The presence of higher rates of tetraploidy are also associated with these subgroups [10]. Similar to the gene expression signature, the nature of the contribution of these chromosomal alterations to the pathogenesis of these tumours are not clear. The group 3 tumours show amplification and / or overexpression of the known oncogenes like *MYC* and *OTX2*. Amplifications in some of the genes involved in TGF- β signalling pathway genes and deletions in genes that are

inhibitors of this pathway have been identified in about 20% of group 3 tumours. Deletions affecting regulators of the NF- κ B pathway have been reported in Group 4 tumours [11]. Next generation sequencing studies have revealed subgroup specific mutations in the genes involved in epigenetic regulation in these subgroups as well. Mutations in genes such as *SMARCA4*, *MLL2* and *CTDNEP1*, *LRP1B* etc are enriched in group 3 tumours while mutations in *KDM6A*, *MLL3*, *ZMYM3* etc are enriched in group 4 [9, 10]. This evidence may point to crucial steps in the pathogenesis of group 3 and 4 tumours; however it fails to pinpoint to an exact mechanism of pathogenesis for these subgroups that can unify these observations.

The subgroups of medulloblastoma are also distinct in terms of their clinical characteristics such as the degree of metastasis at diagnosis, age distribution, ratio of male to female patients, and most importantly the overall survival of the patients (Table 2.1). In terms of metastasis at diagnosis the highest prevalence is seen in the group 3 and 4 tumours with a frequency of 40-45 % and 35-40 % respectively. In terms of the overall survival the WNT subgroup patients fare the best with a survival rate of ~ 95 %. The group 3 patients have the poorest survival rate of ~ 50 % while the SHH and group 4 patients have an intermediate survival rate of ~ 75 % [8]. Thus the group 3 and 4 tumours show an overlapping gene expression profile, and have a similar rate of metastasis, however, the patients with group 4 tumours fare better in terms of survival as compared to the patients with group 3 tumours. A better understanding of the biology of these non-WNT, non-SHH tumours (group 3 and group 4 tumors) is required to understand their mechanism of pathogenesis, similarities and differences between these subgroups which may enable better approaches for the therapy of these patients.

MicroRNA's (miRNA's) are small, ~ 22 nucleotide long, non-coding RNAs that are known to regulate gene expression by binding to a specific sequence in the 3'

untranslated (UTR) region of their target mRNAs. This binding causes either inhibition of translation or degradation of the target mRNA resulting in down regulation of protein expression. MiRNAs play a key role in diverse biological processes, including development, cell proliferation, differentiation, and apoptosis [12]. Altered miRNA expression is also known to play an important role in the pathogenesis and progression of cancer [13]. MiRNA expression profiling of a small subset of medulloblastoma tumor tissues carried out in our lab could distinguish the tumours, into the four molecular subgroups [14]. The expression of a select set of differentially expressed miRNAs was validated in 160 medulloblastoma tissues. The WNT tumours show high expression of a distinct set of miRNA's which includes miR-193a-3p, miR-148a, miR-224, miR-204 and miR-365 as compared to the other subgroups. The SHH subgroup is characterised by the downregulation of three miRNAs miR-153, miR-204 and miR-135b as compared to the other subgroups. On the other hand, miR-135b is found to be overexpressed in group 3 and group 4 tumours. MiR-592, which is overexpressed in group 4 medulloblastomas, distinguishes them from the group 3 tumours. This differential expression has been used to develop a real time PCR based assay to classify medulloblastomas into the 4 molecular subgroups using a set of 12 protein coding genes and 9 microRNA's as markers [15].

The miRNAs overexpressed in the WNT subgroup, including miR-193a-3p, miR-148a and miR-224 have been found to inhibit growth, radiation sensitivity and invasion potential when expressed in non-WNT medulloblastoma cell lines indicating to their functional significance in medulloblastoma biology [14, 16]. Therefore, in the present study, the role of two differentially expressed miRNAs in the biology of medulloblastoma was explored, especially with the relevance to their role in the non-WNT, non-SHH subgroups. MiRNA expression profiling identified miR-206 to be downregulated 10-1000 fold in all the four subgroups of medulloblastoma as compared to the normal cerebellum

tissues. MiR-204 expression is found to be down-regulated 10-100 fold in all SHH tumours and in most group 3 tumours as compared to the normal cerebellum [15]. In the non-WNT, non-SHH subgroups, miR-204 expression was downregulated in the group 3 tumours and upregulated in the group 4 tumours. Hence, to understand the functional role of miR-206 and miR-204 in medulloblastoma, these miRNA's were expressed in medulloblastoma cell lines individually and their effect on the growth, tumorigenicity and invasion potential of these cell lines was investigated.

REVIEW OF LITERATURE

2.1 Medulloblastoma- A Clinical Perspective

Medulloblastoma is the most common malignant brain tumour of childhood, accounting for ~20 % of all paediatric brain malignancies [17]. Incidence of this disease peaks between ages 5 and 9 years, but patients of all ages can be affected. The disease occurs predominantly in males with a gender ratio of 1.5-2: 1 (male: female). Medulloblastoma is currently classified using WHO criteria as a grade IV tumour because of its invasive nature, metastatic capability and primitive cellular appearance [2].

Symptoms, Diagnosis, Risk Stratification and Treatment

Patients present with symptoms of headaches, vomiting, lethargy and drowsiness. Most of these are caused by an increased intracranial pressure resulting in hydrocephalus (an excessive accumulation of fluid in the brain). The hydrocephalus in turn is a result of the blockage of the flow of Cerebrospinal fluid (CSF) in the fourth ventricle. Ataxia and behavioural changes may also be seen especially in the older children which are a result of disruption in the cerebellar function due to the tumor mass. The diagnosis of patients is carried out primarily by using Computer assisted tomography (CAT) and Magnetic Resonance imaging (MRI). The imaging of the entire cerebrospinal axis as well as CSF cytology is frequently carried out to rule out metastatic disease [17]. The final diagnosis is based on histopathological analysis of the tissue resected by surgery. The current risk stratification scheme classifies patients as standard risk or high risk. Children ≤ 3 years of age or with a $\geq 1.5 \text{ cm}^2$ size of residual tumour post surgery or those exhibiting leptomeningeal dissemination at the time of diagnosis are all considered to be high risk, and all other patients are treated as average risk. The age of the patient is an important criterion in the risk stratification since the therapeutic approach for infants includes avoidance of cranio-spinal radiation to minimize the adverse effects on the developing

brain. WHO classifies medulloblastoma into four histological subtypes- classic, desmoplastic, large cell / anaplastic (LC/A) and medulloblastoma with extensive nodularity (MBEN). The LC / A histology is often associated with a poor prognosis. Additional risk factors such as amplification of the *MYC* gene are also taken into consideration [18]. With the advent of the molecular subgrouping of medulloblastoma, changes in the risk stratification protocol are currently being considered [7]. The primary treatment modality for all patients is surgery with the aim of maximal tumor resection sparing the surrounding normal tissue. This may be followed by cranio-spinal radiotherapy and / or chemotherapy. Radiotherapy involves radiation of the cranio-spinal axis plus a boost to the posterior fossa although the doses administered vary with the risk stratification. Adjuvant chemotherapy with vincristine, lomustine and cisplatin may also be administered [3]. The current risk stratification and treatment protocols have led to a survival rate of ~ 80 % for the standard risk patients and ~ 60 % for the high risk patients. This improved outcome however is accompanied by considerable side effects. The survivors suffer from long term intellectual impairment and neuro-endocrine damage as a result of the aggressive therapy administered during the development of the brain [4]. Secondary malignancies and late mortality in these patients has also been reported[5].

2.2 Mechanism of Pathogenesis- From History to Current Understanding

Originally identified in 1925 by Cushing and Bailey as a “spongioblastoma cerebelli”, medulloblastoma was described as an undifferentiated neuro-epithelial neoplasm of the cerebellar vermis (midline) or, infrequently the cerebellar hemispheres (lateral). Medulloblastoma was believed to arise from theoretical cells of origin termed ‘medulloblasts’ (Bailey and Cushing, 1925). It was earlier classified along with other tumors of the central nervous system (CNS) as primitive neuroectodermal tumors

(PNETs) due to the histological similarity between the cerebellar and cerebral embryonal tumors. However, the differences in the common chromosomal aberrations in the PNETs outside the posterior fossa and those inside it led to the classification of medulloblastomas separately from that of the cerebral PNETs [19]. Gene expression profiling of PNETs and medulloblastomas further confirmed them as distinct tumor types [20].

Initial evidence regarding the molecular basis of medulloblastoma came from the identification of mutations in the *PTCH1* gene in patients with Gorlins syndrome and subsequently in sporadic medulloblastomas [21]. Patients suffering from this familial syndrome were known to be susceptible to medulloblastoma and basal cell carcinoma. The *PTCH1* gene was known to be a part of the SHH signalling pathway, indicating to the role of this signalling pathway in the pathogenesis of medulloblastoma. Subsequently mutations in *PTCH1*, *SMO* and *SUFU* genes involved in the SHH signalling pathway were identified in sporadic medulloblastomas as well [22, 23]. Germline mutations in the adenomatous polyposis coli (*APC*) gene were identified in patients with Turcot's syndrome who also develop medulloblastoma [24]. While *APC* mutations predominantly occur in familial medulloblastomas they were also found in some sporadic medulloblastomas [25]. The *APC* gene belongs to the WNT signalling pathway. Sporadic medulloblastomas were found to carry mutations in additional WNT signalling pathway genes including activating mutations in *CTNNB1* and *AXIN* [26, 27]. Furthermore, Li-Fraumeni Syndrome (LFS), an autosomal disorder resulting from germ-line *TP53* mutations, was also found to predispose to medulloblastoma formation. However, subsequently it has been reported that the overall frequency of *TP53* mutations in medulloblastoma (both familial and sporadic cases) is relatively low (7-16 %) [28]. These familial syndromes assisted in the identification of the deregulated WNT and SHH developmental pathways as drivers of pathogenesis in a subset of medulloblastomas.

The studies on the cytogenetic aberrations in medulloblastoma identified the isochromosome 17q (i17q), in which loss of the p arm of chromosome 17 occurs in the context of a 17q gain, as the most frequent chromosomal abnormality in this disease [29]. Amplification of the *MYC* locus on 8q24, often in the form of Double Minute chromosomes (DM's), was reported in multiple medulloblastoma cell lines and confirmed in primary tumours [30, 31].

A series of gene expression profiling studies further investigated the molecular basis of medulloblastoma pathogenesis that led to identification of molecular subgroups of medulloblastomas. Thompson *et. al.* showed the existence of 5 molecular subgroups in a study of 44 medulloblastomas [19]. In this study Monosomy 6 and *CTNNB1* mutations were found to be mutually exclusive to *PTCH1* and *SUFU* mutations in medulloblastoma tumor tissues. The study by Kool *et.al.*, on 62 medulloblastomas, showed for the first time the existence of 5 unique molecular subgroups that segregated medulloblastomas having WNT or SHH signalling pathway activation as distinct subgroups and additional three subgroups of non-WNT non-SHH medulloblastomas [20]. The WNT and SHH tumors were shown to be distinct in their expression profiles. However, the non-WNT, non –SHH tumors were found to have an overlapping gene expression signature. This study also showed for the first time the association of increased metastasis rate in the non-WNT, non-SHH tumours. Gene expression profiling study by Northcott *et.al* (103 tumors) showed that medulloblastomas can be subgrouped with the highest confidence into four core molecular subgroups [21]. Northcott *et. al.* also showed the existence of subgroup association with the age, histology, chromosomal alterations and survival. The study by Cho and colleagues identified six subgroups. This included one WNT, one SHH and four non-WNT, non-SHH subgroups [22]. Notably, the tumors carrying *MYC* amplification were found to have the worse prognosis within the tumors with the retinal

gene expression signature commonly considered as group 3 tumors. This subclassification of tumors was found to be of significance in the risk stratification of tumors based on their molecular subgroup.

In 2012, a consensus regarding the molecular subgroups was reached. This supported the existence of four core molecular subgroups namely the WNT, SHH, group 3 and group 4 based on their gene expression profiles [6]. These subgroups were found to differ in terms of their demographics as well as clinical features including prognosis and overall survival (Table 2.1). They have now been reported to also have distinct cell of origin indicating to the heterogeneity of this disease. A recent study has shown that these subgroup associations are also retained in the recurrent cases of medulloblastoma [32]. Studies on the identification of the molecular mechanisms of pathogenesis now focus on identification of subgroup specific drivers of pathogenesis.

The current understanding of the molecular / genetic features of these four subgroups is briefly described below (Table 2.2).

WNT subgroup

The WNT subgroup constitutes ~10% of all medulloblastoma tumors according to an international meta-analysis study [8]. However its incidence is almost double in the Indian cohort studied in our lab [15]. These tumors frequently show classic histology. It has a 1:1 male to female ratio and is predominant in older children. It has the best prognosis with an overall survival rate of > 90 % and the tumors rarely show leptomeningeal dissemination. The activated WNT signalling pathway is the driver of tumorigenesis in these tumors as seen in the high expression of the WNT signalling pathway genes including *WIF1*, *DKK1*, *LEF1*, *CCND1* and *MYC*. > 90 % of WNT tumors have mutations in the *CTNNB1* gene resulting into a constitutively active protein. Presence of monosomy 6 is the most frequent (> 75 %) chromosomal alteration in these

tumors. The lower rhombic lip progenitor (LRLP) cells have been indicated as the cells of origin for this subgroup giving rise to tumors closer to the brain stem rather than in the cerebellar hemispheres, in a mouse model of this subgroup [6, 8]. Deep sequencing studies have identified mutations in the multifunctional RNA binding protein *DDX3X* in 50 % of WNT tumors [9]. These mutations have been shown to potentiate the effect of the *CTNNB1* mutations. Additionally, mutations in the SWI/SNF complex gene *SMARCA4*, the DNA methyltransferase gene *MLL2* and the well known tumor suppressor gene *TP53* are also seen in a subset of these tumors [9, 10]. The mutations in the epigenetic modifiers may result in disruption of chromatin remodelling at WNT-responsive genes thus contributing to the pathogenesis of these tumors. However this observation currently lacks functional evidence. The good prognosis of this subgroup has led to its clinical trials for de-escalation of the current aggressive therapy for treatment of WNT subgroup medulloblastomas [7].

	WNT	SHH	Group 3	Group 4
Survival	~95 %	~75 %	~50 %	~75 %
Metastasis	5-10 %	15-20 %	40-45 %	35-40 %
Age	Older children and adults	Infants, children and adults	Infants and young children	Older children and young adults
Histology	Classic, very rarely LCA	Classic > Desmoplastic > LCA	Classic > LCA	Classic, rarely LCA
Gender Ratio	1:1	1.5:1	2:1	3:1

Table 2.1: Demographic characteristics of the four medulloblastoma subgroups.

	WNT	SHH	Group 3	Group 4
Gene expression	WNT signaling	SHH signaling	Common gene expression signature (<i>LEMD1, FOXG1, EOMES</i>)	
			Photoreceptor genes	Neuronal Differentiation related genes
Chromosomal alterations	Monosomy 6 (85%)	9q loss (47%) 3q gain (27%)	i 17q (26%) 1q gain (35%) 7 gain (55%) 8p loss (33%) 16q loss (50%)	i17q (66%) 7 gain (47%) 8p loss (41%)
Mutations	<i>CTNNB1</i> (90%) <i>DDX3X</i> (50%) <i>SMARCA4</i> (25%) <i>MLL2</i> (13%) <i>TP53</i> (13%)	<i>PTCH1</i> (28%) <i>DDX3X</i> (11%) <i>MLL2</i> (12%) <i>TP53</i> (11%)	<i>SMARCA4</i> (11%) <i>MLL2</i> (5%) <i>SPTB</i> (6%) <i>CTDNBP1</i> (5%) <i>LRP1B</i> (5%) <i>TNXB</i> (5%)	<i>KDM6A</i> (12%) <i>MLL3</i> (5%) <i>ZMYM3</i> (5%) <i>CBFA2T2</i> (3%)
Focal Amplifications	-	<i>MYCN</i> (8%) <i>GLI2</i> (5%)	<i>MYC</i> (17%) <i>PVT1</i> (12%) <i>OTX2</i> (8%)	<i>SNCAIP</i> (10%) <i>MYCN</i> (6%) <i>CDK6</i> (5%)
Tetraploidy	1/7 (14%)	4/14 (29%)	7/13 (54%)	8/20 (40%)

Table 2.2: Molecular and genomic characteristics of the four medulloblastoma subgroups.

The table shows the differential gene expression signature, chromosomal alterations, mutations, focal amplifications and presence of tetraploidy in the tumors of the four medulloblastoma subgroups as has been reported by various studies. The percentage values describe the percentage of tumors showing the particular alteration within the subgroup. The genes in bold are those involved in epigenetic regulation of gene expression [33].

SHH subgroup

The SHH subgroup constitutes about 30 % of all medulloblastoma tumors. Desmoplastic histology is most commonly associated with the SHH subgroup although the tumors of this subgroup may show classic or less often LC / A histology as well. It also has a 1:1 male to female ratio. The age distribution for this subgroup is bimodal with frequent incidence in both infants (0–3 years) and adults (> 16 years). It has an overall survival rate of ~75 %. These tumors show metastasis at diagnosis, at a frequency of 15-20 % [6, 8]. The SHH tumors show high expression of the SHH pathway genes including *HHIP1*, *EYA1* and *PDLIM3* [34]. Common cytogenetic and mutational events include loss of chromosome 9q (harbouring the *PTCH1* gene), and 10q in addition to focal amplification of *GLI2*, *MYCN* and focal deletion of *PTCH1*. This is the most well studied subgroup due to its initial characterisation based on germline mutations in the *PTCH1* gene in Gorlin's syndrome patients and availability of mouse models of the disease. Two mouse models of this subgroup were the first of medulloblastoma mouse models to be established and have been extensively studied. The *Ptch1*^{+/-} mice with a tumor incidence of 15-20 % by six months of age and the *Smo*^{+/+} mice with an incidence of upto 90 % by 2-3 months of age are mouse models of medulloblastoma resulting from SHH pathway activation [35, 36]. The cerebellar granule neuron progenitors (CGNPs) have been identified as the cell of origin of these tumors [37, 38]. These are the cells that proliferate in response to the SHH signal during the normal cerebellar development and lead to tumor formation due to the deregulated SHH signalling. Recent studies have shown mutations in the *DDX3X* and *MLL2* genes in SHH subgroup tumors, however their role in the pathogenesis of these tumors is not understood [10]. The SHH tumors carrying *TP53* mutations, either germline (Li Fraumeni syndrome) or somatic carry significantly higher number of somatic copy

number variations (SNVs) and display complex chromosomal arrangements consistent with a phenomenon called chromothripsis (chromosome shattering) [39]. This has been proposed to be an early event in the process of tumorigenesis. Pharmacological small molecule inhibitors of *SMO* activity have been tested in phase 1 clinical trials, however the tumors were found to acquire additional mutations leading to rapid disease progression [40]. However, a combination therapy with the *SMO* inhibitor and PI3K inhibitors, have shown promise in pre-clinical studies of medulloblastoma [41].

Group 3

Group 3 is the molecular subgroup with the worse prognosis, accounting for one-quarter (25%) of all medulloblastomas. These tumors show a gender ratio of 2:1 occurring more commonly in males. They occur almost exclusively in infants (< 3 y) and young children (3-16 y). This molecular subgroup is associated with multiple markers associated with poor outcome, including large cell/anaplastic histology, focal *MYC* amplifications and metastatic dissemination. Group 3 medulloblastomas are highly metastatic (46.5 %) tumors with a 5-year survival of less than 50 %. The drivers of Group 3 pathogenesis remain to be fully elucidated. Genomic amplification and overexpression of *MYC* (17 %) and *OTX2* (11 %) are seen in a mutually exclusive pattern. Group 3 tumors have an overlapping gene expression signature with group 4 tumors. The overlapping gene expression profile includes transcription factors involved in brain development, viz. *EOMES* and *FOXP1*, a testes specific gene *LEMD1*, and genes involved in neuronal migration like *UNC5D* and *EPHA8*[14]. The photoreceptor gene expression is specific to the group 3 tumors which distinguishes it from the group 4 tumors. Cytogenetically, Group 3 medulloblastomas have the largest number of both broad and focal copy number alterations, including loss of chromosome 8p, 16q as well as gains of 1q and 7 among others. The most commonly observed chromosomal aberration is the isochromosome 17q,

seen in ~26 % of group 3 tumors [6, 8]. Next generation sequencing has shown subgroup-enriched SNVs, targeting *SMARCA4* (11 %) and *MLL2* (5 %) as well as structural rearrangements generating *PVT1-MYC* fusions seen in ~50 % of *MYC* amplified group 3 tumors. The region of the *PVT1* gene undergoing the amplification carries a cluster of miRNAs which have been shown to potentiate the oncogenic properties of *MYC* [11]. Currently patients belonging to this subgroup are treated with high risk treatment protocols.

Group 4

This subgroup constitutes ~ 35 % of all medulloblastomas. The group 4 tumors have an intermediate prognosis (5-year overall survival of 75 %) and predominantly classic histology, affecting children (age 3-16 y) and adults (> 16 y), while rarely occurring in infants (< 3 y). There is a substantial gender skew observed in Group 4 tumors in which this molecular subgroup occurs three times more frequently in males than in females in the international cohort [6, 8]. In the Indian cohort this ratio reaches even higher to 9:1 male to female patients [15]. The mechanism of pathogenesis of this subgroup is least understood. Group 4 medulloblastomas demonstrate an overlapping gene expression signature with that of the group 3 tumors as described above. In addition these tumors show a neuronal signature including many genes associated with neuronal differentiation and glutamate/GABA signalling which is distinct from the group 3 tumors. Cytogenetically, group 4 medulloblastomas frequently display loss of Chr.11p, Chr.8 and the X-chromosome, along with gains of Chr.7 and 18q. The i17q is observed in 66 % of patients. Additionally, focal amplifications of *CDK6* and *MYCN* are also observed. Recently, Northcott *et. al.*, identified a tandem duplication of *SNCAIP*, a gene associated with Parkinson's disease and neurodegeneration in these tumors. *SNCAIP* is among the most highly expressed genes in group 4 medulloblastomas and its expression (and

duplication) has been suggested as a means to further separate Group 4 medulloblastomas into two distinct subtypes [11].

2.3 Challenges in Understanding the Biology of the Non-WNT Non-SHH Medulloblastoma

The familial syndromes *viz* the Gorlin's and Turcot's syndrome gave the first indication of deregulation of WNT and SHH signalling in the pathogenesis of medulloblastomas. The gene expression profiling and the mutational analysis have now confirmed the role of the deregulation of these developmental pathways in two distinct subgroups of medulloblastomas. However, the non-WNT, non-SHH medulloblastomas still remain very poorly understood in terms of the drivers of their pathogenesis. These medulloblastoma subgroups account for > 50 % of medulloblastoma cases and show an overlapping gene expression signature. The classification of these tumors is challenging due to their overlapping gene expression profile and occurrence of certain tumors which show characteristics of both subgroups.

The group 3 tumors show presence of tetraploidy (54 %) and an unstable genome showing multiple focal and broad SCNA's [10, 11]. Neither the biological relevance nor the clinical importance of these alterations is understood. The amplification of the *MYC* and *OTX2* genes in the group 3 tumors maybe a crucial step in the pathogenesis of some of these tumors, however not all group 3 tumors carry this amplification, many group 3 tumors show overexpression of *MYC* and *OTX2* through an as yet unknown mechanism. In a mouse model of the group 3 medulloblastoma concomitant knockout of *TP53* and overexpression of *MYC* in the cerebellar neuronal progenitor cells led to the development of tumors mimicking the gene expression signature of human group 3 tumors [42]. However, the human group 3 tumors very rarely show the loss of the *TP53* gene. The

genome sequencing data has shown consistent somatic structural variations at the chromosome 9q34.13 region in ~ 6.6 % of group 3 and group 4 tumors. The *GFII* / *GFII**B* gene activation was observed in the tumors carrying this somatic variation as a result of its relocation in the proximity of enhancers regions. The transduction of neural stem cells with *MYC* and *GFII* / *GFII**B* resulted in formation of tumors when xenografted in the cerebella of nude mice. Thus, *GFII* / *GFII**B* may represent one of the genes that cooperate with *MYC* in a small subset of group 3 tumors [43, 44]. However, the drivers of tumorigenesis that may cooperate with *MYC* in the majority of group 3 tumors are not understood.

In case of group 4 tumors, amplifications in the *CDK6*, *SNCAIP* and *MYCN* gene are seen albeit only in a small subset of tumors. As compared to the group 3 tumors this subgroup carries fewer SCNA's. The overexpression of *MYCN* under the *GLT1* (glutamate transporter gene) promoter has been shown to give rise to both SHH dependent and SHH independent medulloblastomas. The *MYCN* gene expression is deregulated in both the SHH and Group 4 tumors. However, it is not clear if the *MYCN* over expressing, SHH independent tumors recapitulate the group 4 tumors [44]. The recent next generation sequencing studies have identified the mutations in a variety of genes involved in epigenetic regulation. Mutations in the *KDM6A* gene, a histone demethylase is postulated to maintain the trimethylation marks on H3K27, retaining the stem-like state of cells [45]. Although this is a novel finding, the numbers of tumors that actually show alterations in epigenetic modifiers are few (Table 2.1- genes in bold) and hence are unlikely to be the drivers of tumorigenesis.

The poor survival rates and presence of metastasis in these tumors necessitates the identification of novel mechanisms that may be used for targeted therapy and / or risk stratification of the non-WNT non-SHH medulloblastomas.

2.4 MicroRNA's: A Big Role for Small Molecules

MicroRNAs are ~20 nucleotide long non-coding RNA molecules that regulate gene expression at the post transcriptional level. Since their discovery by Victor Ambros and colleagues in *C.elegans* in 1993, multiple studies have focussed on searching for new microRNAs and elucidating their function in normal cellular functioning as well as in disease, especially cancer [46]. A single miRNA can potentially regulate several genes while a single gene may be regulated by multiple miRNAs thus creating a complex interaction network [47]. The identification of target genes of miRNAs has indicated to their role in various cellular processes including proliferation, growth, metabolism, apoptosis etc. MiRNAs may express in a ubiquitous manner or maybe tissue specific e.g. the miR-1 family of miRNAs is known to be muscle specific and has been reported to be important for muscle differentiation [48]. Similarly the miR-155 and miR-150 have been shown to play an important role in the differentiation of B and T lymphocytes [49, 50].

MiRNA biogenesis and mechanism of action

The miRNA coding genes are located either within the introns of protein coding genes or outside any known coding genes in the intergenic regions. The transcription of these genes by the RNA-polymerase II enzyme generates double stranded primary transcripts (pri-miRNA) (Figure 2.1). In the pri-miRNA the region encoding the miRNA forms an imperfect stem-loop hairpin structure. The pri-miRNA is converted to a pre-miRNA. This process is mediated by a complex of Drosha type II RNase, the double strand RNA binding protein DGCR8 and other proteins which cleave the hairpin-loop to generate the pre-miRNA. This pre-miRNA is then exported to the cytoplasm by exportin 5. In the cytoplasm, the pre-miRNA is processed into the mature miRNA by the Dicer type III

RNase. Only a single strand of the pre-miRNA is retained as the mature miRNA while the other stand gets degraded [51].

The miRNA brings about downregulation of its targets by becoming associated with the microRNA induced silencing complex (miRISC) which contains an Argonaute family protein. The region of the miRNA that binds to its target is called as the seed region (generally from the 2nd nucleotide to the 8th nucleotide). This is important for pairing of the miRNA with the target mRNA although unlike siRNAs they form imperfect complementary stem-loop structures and pair imperfectly with sites in the 3' UTR region of their target mRNAs. They may act by decreasing the level of target mRNAs due to their degradation or by interfering with the process of translation resulting in decrease in the level of protein [12].

2.5 MicroRNAs in Medulloblastoma

In cancer, a global downregulation of miRNAs has been reported [13]. However, certain oncogenic miRNAs such as miR-21 and miR-17-92 cluster have also been reported to be upregulated in cancers [52]. These miRNAs have been shown to promote the tumorigenic properties of cancer cells. The initial evidence of miRNAs as tumor suppressors came from the identification of the miR-15, miR-16a cluster of miRNAs at the breakpoint region on chromosome 13q14 that is frequently lost in chronic lymphocytic leukaemia (CLL) [53]. Further studies on the role of miRNAs downregulated in cancer have led to the identification of a number of tumor suppressor miRNAs.

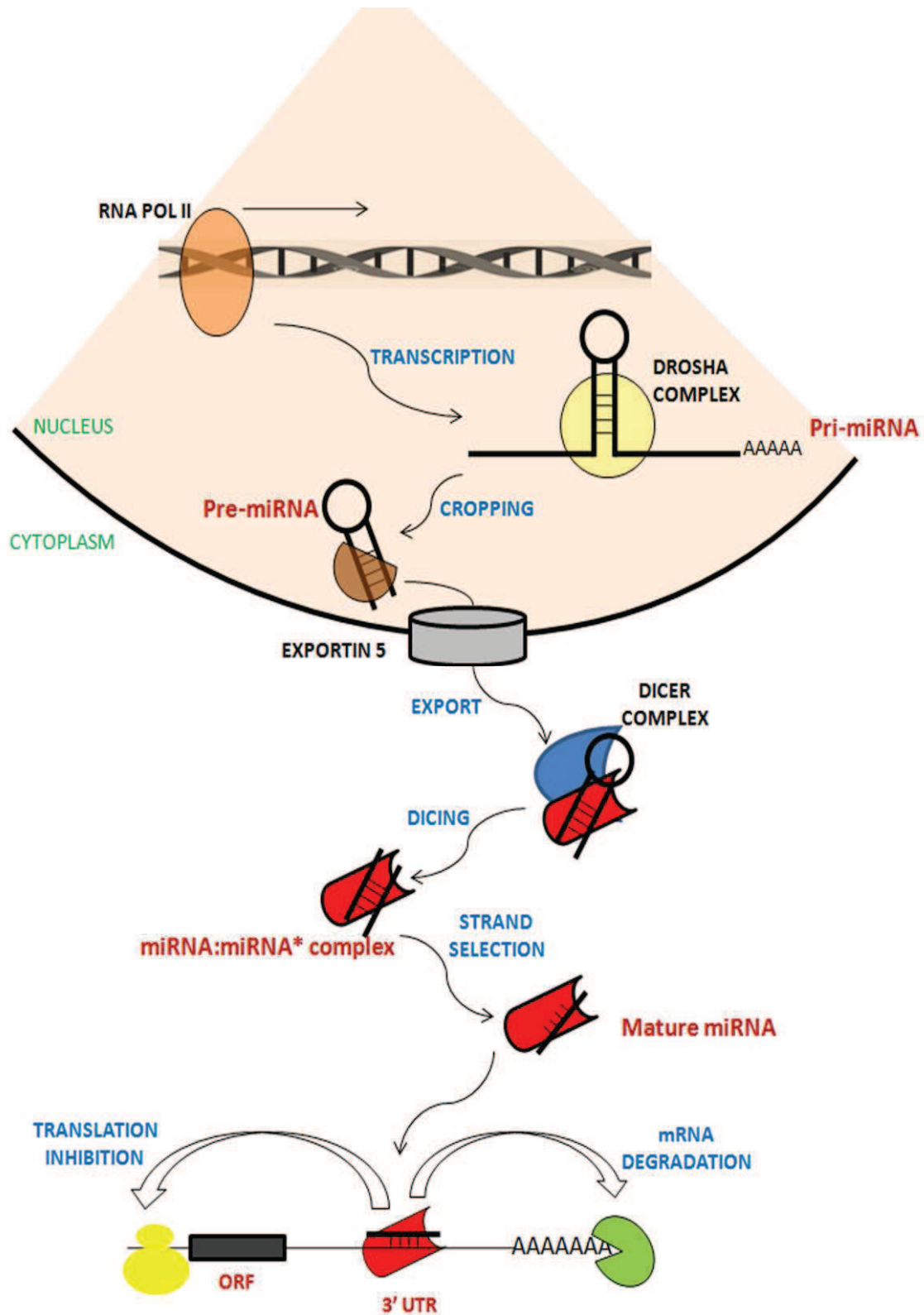


Figure 2.1: The mechanism of miRNA biogenesis

Schematic diagram showing the mechanism of miRNA biogenesis from transcription to its maturation and mechanism of action. Adapted from [54].

MicroRNA profiling of medulloblastoma and the functional role of some differentially expressed miRNAs

In medulloblastoma the first evidence for the role of deregulation of miRNAs came from the miRNA expression profiling study by Ferretti *et.al.* [55]. They found consistent downregulation of a number of miRNAs in medulloblastomas as compared to normal cerebellum. Functional studies on two of the downregulated miRNAs miR-9 and miR-125a showed inhibition of proliferation and anchorage independent growth upon expression of these miRNAs in medulloblastoma cell lines D283 and Daoy. This study however was carried out before the advent of the molecular subgrouping of medulloblastomas. Hence subgroup specific expression of miRNAs was not studied. The miRNA profiling by Cho *et. al.* showed upregulation of miR-21 in all medulloblastomas as compared to the normal cerebellum [56]. The miR-17-92 cluster was also upregulated in subgroups parallel to the WNT, SHH and Group 3. The downregulation of miR-17-92 cluster was shown to inhibit medulloblastoma cell growth indicating to its oncogenic role in medulloblastoma [57, 58]. Similarly the miR-182-183 cluster has also been shown to be high in the *MYC* positive medulloblastomas and to promote tumorigenesis [59, 60]. MiRNAs that are found to be downregulated in medulloblastoma may play a tumor suppressive role. Indeed, expression of miRNAs such as miR-199b-5p, miR-218, miR-124 etc in medulloblastoma cell lines has been shown to reduce xenograft tumor formation in immunocompromised mice [61-63].

MiRNA expression profiling carried out in our lab on a set of 4 normal cerebellum tissues and 19 medulloblastoma tumor tissues could successfully classify the normal cerebellum from the tumors. Interestingly, the miRNA expression profile could also independently classify the tumors into the four core molecular subgroups [14] (Figure 2.2). The WNT subgroup showed a distinct set of highly expressed miRNAs including

miR-193a, miR-224, miR-148a, miR-204, miR-365 etc. The SHH subgroup showed downregulation of miR-153, miR-204 and miR-135b. MiR-135b was found to be upregulated in the non-WNT, non-SHH tumors. Furthermore, miR-182 and miR-183 were found to be upregulated and miR-204 downregulated in most group 3 tumors. The miR-379/miR-656 and miR-127/miR-432/miR-433 cluster present in an imprinted region on chromosome 14 was found to be highly expressed in the normal cerebellum and group 4 tumors. This differential expression was validated on 101 medulloblastoma tissues. A set of 12 protein coding and 9 miRNA coding genes have been used to develop an assay to classify medulloblastoma tumor tissues into the molecular subgroups [15].

The miRNAs overexpressed in the WNT subgroup medulloblastomas including miR-193a, miR-224 and miR-148a have been shown to inhibit growth of the non-WNT medulloblastoma cell lines [14, 16]. This indicates that the upregulation of these miRNAs in the WNT subgroup medulloblastomas may contribute to the excellent survival of this subgroup. The differential expression of some of these miRNAs was also found to correlate with the survival of the patients. In the combined cohort of Group 3 and Group 4 medulloblastomas cases, those with miR-592 overexpression were found to have significantly better survival (72 % vs. 25 %) while those with miR-182 overexpression were found to have significantly worst survival (45 % vs. 70 %) [15]. These data indicate to the important role for miRNA's in the biology of medulloblastoma.

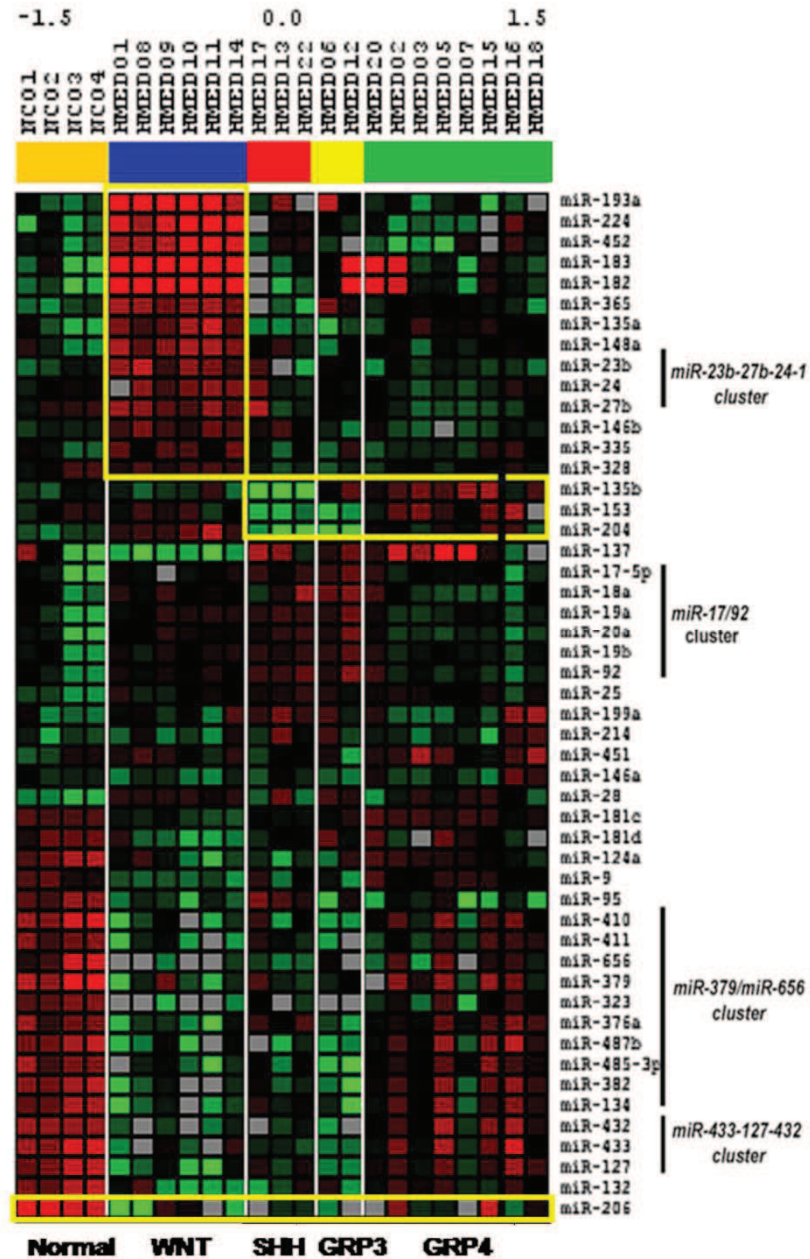


Figure 2.2: Heat map showing significantly differentially expressed miRNAs in four molecular subgroups of medulloblastoma and normal cerebellar tissues using SAM analysis.

The miRNAs indicated with the yellow box represent the highly differentially expressed miRNAs. Ochre: normal, blue: WNT, red: SHH, yellow- Group 3 and green: Group 4 [14].

In the present study the role of two such miRNAs in the pathogenesis of medulloblastoma was investigated. MiR-206 is a miRNA that was found to be downregulated in all the medulloblastoma tissues irrespective of their subgroup affiliation. This miRNA has been shown to target the *OTX2* gene which is overexpressed in all non-SHH tumors. *OTX2* is also known to be amplified in a subset of group 3 tumors [64]. Additionally, miR-206 shows cerebellum specific expression in the normal rat brain [65]. Hence, the effect of miR-206 expression on medulloblastoma cell growth characteristics was studied.

MiR-204 is another miRNA that is found to be differentially expressed in the medulloblastoma subgroups. In the non-WNT, non-SHH subgroup medulloblastomas, miR-204 was found to be down regulated in most group 3 tumors and upregulated in most group 4 tumors. Further analysis showed that the higher expression of this miRNA correlates with better survival of patients within the group 3 and group 4 subgroups. (See results section). This indicates to its importance as a prognostic marker. Hence, the functional role of this miRNA in the biology of medulloblastoma was studied by expressing this miRNA in medulloblastoma cell lines and studying the effect of miR-204 expression on their growth characteristics. Furthermore, multiple target genes of this miRNA in medulloblastoma were also identified in order to understand its mechanism of action.

MATERIALS AND METHODS

Materials

The following chemicals were obtained from **Life technologies, Thermo Fischer Scientific** Carlsbad, CA, USA:

Exonuclease I, Gene Ruler 1 Kb DNA ladder, Shrimp Alkaline Phosphatase (SAP) (Cat. No. EF0511), Taq DNA polymerase (1 U/ μ l) (Cat. No. EP0404), T4-DNA ligase (Cat. No. E0011), Dpn I restriction enzyme (Cat. No. ER1701), SuperSignal® West Pico chemiluminescent substrate (Pierce-Thermo scientific, Cat. No. 34077).

The following chemicals were obtained from **Applied Biosystems, Thermo Fischer Scientific** Carlsbad, California, USA.

MicroRNA Reverse Transcription Kit (Cat No. 4366596), 2 X Taqman PreAmp Master Mix (Cat. No. 4391128), 2 X Taqman PCR Master Mix (Cat. No. 4304437), 2 X Power SYBR Green Master Mix (Cat. No. 4367659), Taqman miRNA Assays (Cat. No. 4427975), 384-well Real time PCR plates and optical adhesive sheets.

The following chemicals were obtained from **Invitrogen, Thermo Fischer Scientific** Carlsbad, CA, USA:

MMLV-RT 200 U / μ l (Cat No. 28025-013), Dulbecco's modified Eagle medium (Cat No. 12800-058), Fetal bovine serum (Cat No. 16140-071), Trypsin, L-Glutamine, Formamide, LMP (low melting point) agarose,

The following chemicals were obtained from **Dharmacon, GE Healthcare**, Lafayette, CO, USA.

miRIDIAN microRNA mimics, siGLO RISC-Free Control siRNA, and Dharmafect 2 transfection reagent.

The following chemicals were obtained from **Sigma Aldrich**, St. Louis, MO, USA:

All trans retinoic acid (ATRA Cat. No. R2625), Agarose, Proteinase K, DEPC, DMSO, EDTA, Ethidium bromide, BES (Cat. No. B4554).

The following chemicals were obtained from **Merck millipore**, Darmstadt, Germany; **Qualigens**, Thermo Fischer Scientific India Pvt Ltd, Mumbai, India or **S D fine-chem. limited**, Mumbai, India:

Xylene, Methanol, Glacial Acetic Acid, Potassium Acetate, Sodium Acetate, N-laurylsarcosine. Sulfuric Acid (LR), Potassium dichromate (LR), Tri-Sodium citrate (LR), Citric Acid (LR), Hydrogen peroxide, Methanol.

The following reagents were obtained from **New England Biosciences (NEB)**, Ipswich, MA, USA: Standard Taq DNA polymerase (Cat No.M0273L)

The following reagents were obtained from **S D fine-chem. limited**, Mumbai, India:

NaCl (Cat No.20241 AR), Na₂HPO₄.2H₂O (Product no. 20383 AR), CaCl₂.2H₂O (C-3306)

The following **kits** were obtained from the companies specified in brackets:

Recover All RNA extraction kit (Ambion, Life Technologies, Carlsbad, CA, USA; Cat No.AM1975)

EZ DNA Methylation-Gold Kit (Zymo-Research, Irvine, CA, USA; Cat No.D5005)

QiaAmp DNA mini kit (Qiagen, Limburg, Netherlands; Cat No.51304)

Qiagen Plasmid Midi kit (Qiagen, Limburg, Netherlands; Cat No.12143)

QIAquick PCR purification Kit (Qiagen, Limburg, Netherlands; Cat No. 28104)

The water used for the preparation of all solutions and reagents was Ultrapure water (Resistivity = 18 MΩ cm) obtained from a Milli-Q water plant (**Millipore**, Billerica, MA, USA).

Disposable plastic ware (certified DNase, RNase, and protease-free) was obtained from **Axygen**, California, USA.

Disposable sterile plastic ware for tissue culture was obtained from **Nunc**, Rochester, NY, USA.

Primers:

All PCR primers were obtained from **Sigma Genosys** in lyophilized form.

Methods

3.1 Ethics Statement and Collection of Human and Mice Tissues

This study was approved by TMC-ACTREC Institutional Ethics Committee III of the Tata Memorial Centre. Formalin fixed paraffin embedded (FFPE) medulloblastoma tumor tissues were obtained with written informed consent of the patient or the parent in case of patients less than 18 yr of age. In case of patients in the age group 7 to 18 yr, an assent was also obtained from the minor patient, in addition to the parent's consent. The consent form, assent form and the information sheet were approved by the Institutional Ethics committee. Normal cerebellar tissues were obtained from Brain Tissue Repository, NIMHANS, Bangalore that include two normal developing cerebellar tissues from children less than 1 yr of age and six normal adult cerebellar tissues.

This part of the study was approved by the institutional animal ethics committee. The normal cerebellar tissues at various stages of development (Day 7, 14 and 21) were obtained from C57 / BL6 mice after administration of euthanasia with overexposure to CO₂. *Ptch1*^{+/-} mice and *Smo*^{+/+} mice were obtained from Dr. Matthew Scott (Stanford School of Medicine, Stanford, CA, USA) [36] and Dr. James Olson (Fred Hutchinson Cancer Research Centre, Seattle, WA, USA) respectively [66]. The tumors formed in these SHH subgroup medulloblastoma mouse models were obtained in a similar manner. The tissues were flash frozen in liquid nitrogen and then stored at -80°C until use.

3.2 Extraction of RNA from Human or Mice Tissues

Five µm sections of fresh frozen tumour tissues or of FFPE tumour tissues were stained with hematoxylin and eosin and examined by light microscopy to ensure at least 80 % tumour content. RNA was extracted from the fresh frozen tissue samples using the Qiagen Rnaeasy kit or by the Guanidium Isothiocyanate (GITC) Method described below. RNA was extracted from FFPE tissues using the RecoverAll™ Total Nucleic Acid Isolation kit.

3.3 Extraction of RNA by the Guanidium Isothiocyanate (GITC) Method

All solutions were DEPC treated, unless otherwise stated. Only RNase free sterile plasticware were used.

Reagents

Preparation of DEPC-treated Milli-Q water: Water was collected from the Milli-Q plant directly in sterile 50 ml NUNC tubes. 50 µl DEPC was added to 50 ml Milli-Q water, mixed vigorously and left over night at 37 °C, with the tubes loosely capped. The tubes were autoclaved on the following day. This water was used for preparing all the reagents required for RNA extraction.

1 M Sodium citrate, pH 7.0: 14.7 g Sodium citrate dihydrate was dissolved in about 35 ml of autoclaved Milli-Q water. The pH was adjusted to 7.0 with a few drops of 1 M citric acid and the volume was made up to 50 ml. (1 M Citric acid was prepared by dissolving 10.5 g powder in 50 ml DEPC-treated water.) 50 µl of DEPC was added to both 1 M citrate and citric acid solution, tubes were mixed vigorously and left at 37 °C overnight. The solutions were autoclaved on the next day, and stored at room temperature.

10 % N-lauryl-sarcosine: 5 g N-lauryl-sarcosine was dissolved in DEPC-treated water and the final volume was made up to 50 ml. The resulting solution was neither treated with DEPC, nor autoclaved. It was kept at 65 °C for 1 h, and stored at room temperature.

4 M Guanidinium Isothiocyanate (GITC): (Prepared in 25 mM Sodium citrate pH 7.0, 0.5 % Sarcosyl). 23.6 g of guanidine isothiocyanate was dissolved in 40 ml DEPC-treated water. 1.25 ml of 1 M sodium citrate and 2.5 ml of 10 % sarcosine were added and the final volume was made up to 50 ml with DEPC-treated water. The final solution was neither treated with DEPC nor autoclaved. Solution D was prepared from GITC by adding β-mercaptoethanol at a final concentration of 0.1 M. This solution is stable at room temperature for one month.

Phenol (Saturated with DEPC-treated water): 25 ml DEPC-treated water was added to 25 ml distilled phenol at room temperature in a sterile NUNC tube. The tube was mixed vigorously by inverting several times. The tube was kept at 4 °C until the two phases separated (30-60 min). The upper phase of water was replaced with fresh DEPC-treated water, mixed once again and stored at 4 °C.

2 M Sodium acetate, pH 4.0: 13.6 g sodium acetate was dissolved in about 25 ml of Milli-Q water and pH was adjusted to 4.0 with glacial acetic acid. Final volume was made up to 50 ml with Milli-Q water. 50 µl DEPC was added to the solution, mixed vigorously and left at 37°C over night. The solution was autoclaved the following day and stored at room temperature.

Method

1. For tissue samples: approximately 30-50 mg of frozen tumour tissue was collected in a chilled homogenizer collection tube. This was homogenized at low-medium intensity with approximately 2-3 ml of Solution D. The tissue lysate was collected in a microcentrifuge tube and immediately passed through a 26-gauge needle at least ten times. The lysate was triturated until it loses its viscosity, resulting in complete shearing of genomic DNA.
2. For cultured cells: The medium was poured off and the cells were washed with 1 X PBS. 0.5 ml of Solution D was added per well of a 24-well plate. The cell lysate was collected by tilting the plate and was passed immediately through a sterile syringe fitted with a 26 gauge needle. This was done at least ten times until the lysate lost its viscosity, resulting in complete shearing of the genomic DNA. At this stage the lysate was either stored at - 20 °C or processed further immediately.
3. 50 µl of 2 M Sodium acetate pH 4.0 was added per 0.5 ml solution D in an eppendorf tube and mixed by inverting the tube.
4. Next, 0.5 ml of DEPC water-saturated phenol and 0.2 ml chloroform were added successively, and the contents of the tube were mixed thoroughly by vortexing for 1 min. The cap of the tube was loosened to release the developed pressure, and the tube was vortexed again for 30 seconds.
5. The tube was kept on ice for 15-20 min, and centrifuged at 10,000 rpm at 4° C for 10 min in a table top centrifuge (Rota 4-R). The upper aqueous phase was transferred to a fresh eppendorf tube, and centrifuged once again to settle any traces of phenol.

6. The supernatant aqueous phase was transferred to a fresh eppendorf tube and an equal volume of isopropanol (approx. 0.5 ml) was added. The tube was vortexed briefly, and the mixture was kept at -20 °C overnight to precipitate the RNA.
7. On the next day, the tube was centrifuged at 10,000 rpm at 4 °C for 20 min, to pellet down the precipitated RNA. Supernatant was decanted carefully, so as not to disturb the RNA pellet.
8. The RNA pellet was washed with 70 % ethanol (0.5 ml prepared in DEPC-treated water), kept at room temperature for 2 min, and centrifuged at 10,000 rpm at 4 °C for 10 min. The supernatant was decanted, and the drops were allowed to drain off by keeping the tubes inverted on folds of a clean dry tissue paper. The RNA pellet was also dried using vacuum (speedvac) and dissolved in minimum volume of DEPC-treated water, (e.g. 10 µl for RNA from 5×10^5 cells). For dissolving the RNA, it was first kept on ice for about 50 min with intermittent vortexing and spinning down, and then it was heated at 65 °C for 10 min and chilled on ice. It was then stored at -80 °C.
9. The extracted RNA was quantified by spectrophotometry analysis (O.D. at 260/280 nm) using the Nanodrop spectrophotometer (Thermo Scientific) and by loading it on a denaturing gel. The ratio of 28s rRNA to 18s rRNA is approximately 2:1 in a good quality RNA.

3.4 Preparation of Denaturing Gels for RNA

Reagents

10 X MOPS: 41.6 g MOPS, 16.7 ml of 3 M sodium acetate pH 5.0, 20 ml of 0.5 M EDTA pH 8.0. Adjust pH to 7.0 with 5 M NaOH; make up the volume to 1 litre with Milli-Q water and autoclave.

10 X RNA loading dye: 1 mM EDTA pH 8.0, 50 % v / v glycerol, 0.4 % bromophenol blue.

Method

1. 1 % agarose gel was prepared as follows: agarose was weighed into the appropriate volume of autoclaved Milli-Q water. The slurry was heated in a microwave oven until the agarose was dissolved completely. MOPS was added to a final concentration of 1 X and the slurry was mixed properly and placed at 60 °C for 10 min.
2. Then, formaldehyde (37 % solution) to a final concentration of 20 % was added and the gel solution was kept at 60°C for 20 min. Ethidium bromide to a final concentration of 0.5 µg / ml was added, the gel was poured in a gel tray and was allowed to set at room temperature for 30-45 min.
3. After the gel had completely set, it was placed in the electrophoresis tank filled with 1 X MOPS buffer, just enough to cover the gel to a depth of about 3 mm.
4. RNA samples were mixed with half the volume of 10 X MOPS, and double the volume of freshly prepared formamide: formaldehyde (3:1) mixture and the samples were placed at 60 °C for 15 min.
5. The RNA samples were mixed with 10 X RNA loading dye at 1 X final concentration and loaded into the wells of the gel. The electrophoresis of the gel was at 60 mA constant current, till the dye had migrated almost to the bottom of the gel.
6. The gel was placed in Milli-Q water overnight to wash off excess of ethidium bromide, RNA was visualized by observing the gel on a UV transilluminator.

3.5 Reverse Transcriptase PCR for conversion of RNA to cDNA

Reagents

5 X First Strand Buffer, M-MLV RT enzyme (200 U / µl), 0.1 M DTT (all three from Invitrogen), 10 mM dNTP mix, RNase Inhibitor (20 U / µl), p (dN) 6 prime (100 ng / µl)

Method

1. A 10 μ l reaction was set up for the cDNA synthesis from 500 ng of total RNA
2. First, the following components were added to a nuclease-free microcentrifuge tube:

Components	Volume	Final Concentration
Total RNA	-	500 ng
10 mM dNTP Mix	0.5 μ l	1 mM
100 ng / μ l random primers p(dN)6	0.5 μ l	0.5 mM
DEPC treated Milli-Q water	Make up volume to 6 μ l	

3. RNA was heated at 65 °C for 5 min to denature RNA secondary structures and chilled on ice for 2 minutes.
4. Reaction mix was prepared on ice by adding the following component

Components	Volume	Final Concentration
5 X First strand buffer	2 μ l	1X
0.1 M DTT	1 μ l	0.01 M
RNase Inhibitor (20 U / μ l)	0.25	5 U
DEPC treated Milli-Q water	Make up volume to 3.5 μ l	

5. The reaction mix was added to the RNA, mixed by gentle pipetting, and incubated at 37 °C for 5 min to allow annealing of random primers to the RNA.
6. 0.5 μ l (100 U) of M-MLV RT was added to the reaction tube and mixed by gentle pipetting. The tubes were transferred to the thermal cycler (Eppendorf) and thereafter the following conditions were followed:

Temperature	Time
25 °C	10 min
37 °C	50 min
70 °C	15 min
4 °C	∞

7. The cDNA synthesized was then used for analyzing gene expression levels by real time PCR or stored at -20 °C.

3.6 Stem loop Reverse Transcription for miRNA

Mature miRNAs are only 20-23 nucleotides in length. The stem-loop RT primers hybridized to mature miRNA molecule and then reverse transcribed with a reverse transcriptase. The RT product is then quantified by Taqman PCR with miRNA specific forward primer, reverse primer corresponding to part of the Stem loop RT primer (excludes the loop region) and the taqman probe.

Reagents

10 X RT Buffer, 100 mM dNTP mix, RNase Inhibitor (20 U / μ l) Multiscribe M-MLV RT enzyme (50 U / μ l), (All from miRNA reverse transcription kit, ABI. DEPC- treated Milli-Q water

Multiplex 5 X RT Primer pool: 98 μ l of 1 X T.E. pH 8.0 was added with 1 μ l of the 5 X RT primer of the miRNA of interest (miR-206 or miR-204) and 1 μ l of RNU48 5 X RT primer. 20 μ l aliquots of the pooled primers were made and stored at -20 °C. Repeated freeze thaw cycles were avoided.

Method

1. All the reagents required were thawed and mixed well by tapping and pulse spinning.
MiRNA RT primers were thawed on ice.
2. 0.2 µl – 2 µl pipettes were used for pipetting volumes below 2 µl including RNA dilutions.
All the enzymes were added directly from -20 °C freezer.
3. The master mix was prepared in a 0.5 ml tube as follows: The RT primer Pool is a mixture of stem loop RT primer for multiple miRNAs

Component	Volume	Final concentration
10 X RT Buffer	0.5 µl	1 X
100 mM dNTP mix	0.1 µl	0.5 mM
Multiplex RT primer pool	2 µl	1 X
RNase inhibitor (20 U / µl)	0.1 µl	2 U
Multiscribe MMLV-RT (ABI)	1 µl	50 U
Total RNA	50 ng/ 200 ng	
DEPC treated MQ water	Make up volume to 5 µl	

4. Before adding MMLV-RT, the PCR machine was set and kept on hold 16 °C and the lid temperature was set to 105 °C. The contents of the tube were gently mixed by tapping followed by a pulse spin.
5. 3 µl of master mix was dispensed into each of the 0.2 ml tube. 2 µl of the diluted RNA sample (25 ng / µl) was added to the respective tubes. Gently tapped and pulse spun the contents. The Reverse transcription was done in a thermal cycler using the conditions given below.

Temperature	Time
16 °C	30
42 °C	30
85 °C	5 min
4 °C	Hold

3.7 Real Time PCR

Reagents for Taqman chemistry

2 X Taqman PCR Master Mix (Applied Biosystems), 20 X Probes and Primer mix (Applied Biosystems)

Reagents for SYBR chemistry

2 X SYBR green (Applied Biosystems), 10 pmol / μ l gene specific forward primer, 10 pmol / μ l gene specific reverse primer

Method

1. The cDNA obtained from the stem loop RT reaction or RT reaction using random primers was diluted to 5 ng / μ l with DEPC-treated autoclaved Milli Q water for use in the PCR reaction. A total of 10 ng cDNA was used per reaction.
2. The PCR reaction for the Taqman chemistry was set up as follows:

Components	Volume per well
2 X Taqman PCR Master Mix	2.5 μ l
20 X Probe-Primer Mix	0.25 μ l
DEPC MQ	0.25 μ l
cDNA (5 ng / μ l)	2.0 μ l
Total volume	5 μ l

3. The PCR reaction for the SYBR green chemistry was setup as follows

Components	Volume per well
2 X SYBR green PCR Master Mix	2.5 μ l
10 pmol / μ l Forward primer	0.25 μ l
10 pmol / μ l Reverse primer	0.25 μ l
cDNA (5 ng / μ l)	2.0 μ l
Total volume	5 μ l

4. The 5 μ l PCR reaction mix were loaded into the wells of a 384-well microtitre optical plate. The plate was covered with an optical cover sheet and sealed with the help of a plastic applicator. The applicator was pressed evenly over the optical cover sheet several times to ensure proper sealing of the wells. The sealed plate was centrifuged briefly at 2000 rpm for 2 min to spin down the reaction mixes ensuring no air bubbles.
5. The plate was loaded in the Real Time PCR machine. PCR was carried out in Avant 7900HT Sequence Detection machine or the QuantStudio™ 12K Flex Real-Time PCR System both from Applied Biosystems, NY, USA with default cycling parameters.

The default PCR cycling parameters are:

Temperature	Time	No. of cycles
50 °C	2 min	1
95 °C	10 min	1
95 °C	15 s	40
60 °C	1 min	

6. The initial 50°C incubation is to activate the hot start AmpliTaq Gold DNA polymerase enzyme, followed by an initial denaturation step for 10 min and then 40 cycles of denaturation-annealing-extension step. After completion of 40 cycles, the dissociation step of the amplified products was performed. Amplification data was collected in real

time by the machine and stored in the SDS 2.1 software or the Quant studio 12Kflex software. After completion of the runs, the data was analyzed using the same software's. (Applied Biosystems, NY, USA).

GAPDH or RNU48 were used as a housekeeping gene internal control for protein-coding genes and miRNAs respectively. The expression of the gene of interest, relative to *GAPDH* or RNU48 levels were quantified and expressed as Relative Quantity (RQ), calculated as $Ct(\text{gene of interest}) - Ct(\text{GAPDH/RNU48}) = \Delta Ct$. The Relative quantity was calculated as $[2^{-(\Delta Ct)} \times 100]$. Ct = Threshold cycle as automatically determined by the SDS 2.1 software / Quant studio 12Kflex software.

3.8 Molecular Subgrouping of Medulloblastoma Tumor Tissues

The differential expression of the 12 protein-coding genes and 9 miRNAs in FFPE tissues was analyzed by real-time RT-PCR assay developed in the lab [15]. The protein coding gene expression was assessed using the reverse transcription protocol described in *section 3.5*. In case of RNAs extracted from FFPE tissues, 100 ng of cDNA was used for the real time PCR using the SYBR green chemistry. (*Please refer section 3.7*)

A modification to the published protocol was made for the study of miRNA expression in the FFPE tissues by inclusion of a pre-amplification reaction post the stem loop RT-PCR for miRNAs. A pre-amplification step prior to real time PCR was carried out. The pre-amplification is beneficial when working with limiting amounts of RNA such as those obtained from FFPE tissues. For the preamplification reaction, a multiplexed RT reaction for pools of the 9 miRNAs and RNU48 RT primers and Taqman miRNA Assays were used.

a) Preparation of custom RT pool

Note: Each Taqman MicroRNA Assay contains one 5 X RT primer. Up to 96 of these primers can be pooled into one RT reaction as follows:

1 μ l of each individual 5 X RT primer were combined and 1 X T.E was added to make the final volume to 100 μ l. Thus the final concentration of each RT primer in the RT primer pool was 0.05 X each. 20 μ l aliquots of the RT primer pool were made and stored – 20 °C for up to two months.

b) Preparation of custom pre-amplification (Pre-Amp) primer pool

The Pre-Amp primer pool was prepared similar to the custom RT primer pool. 1 μ l of each individual 20 X Taqman MicroRNA Assay was combined and 1 X T.E. was added to make the final volume to 100 μ l, with the final concentration of 0.2 X for each assay in the pool. Aliquot and Store the Pre-Amp primer pool at – 20 °C.

c) Preparation of the RT reaction mix

1. In a 0.2 μ l PCR tube, the following reaction components were added. The reaction mix was prepared on ice. The custom RT pool (thawed on ice) or Multiscribe Reverse Transcriptase should not be vortexed. A single PCR reaction contained the following components:

Components	Volume	Final Concentration
10 X RT Buffer	0.5 μ l	1X
100 mM dNTP mix	0.1 μ l	0.5 mM
Custom RT primer pool	2.0 μ l	0.02X each
RNase inhibitor	0.1 μ l	2 U
Multiscribe MMLV-RT	1.0 μ l	50 U
DEPC treated Milli-Q water	Make up volume to 4 μ l	

2. The components were mixed thoroughly by inverting 6 times followed by pulse spin. The reaction mix should not be vortexed.
3. 1 μ l of 25 ng total RNA was added to the reaction mix for a total reaction volume of 5 μ l. The components were mixed by inverting followed by pulse spin.
4. The reaction was incubated on ice for 5 min and subsequently transferred into a thermal cycler. The cycling parameters were same as that for stem- loop RT-PCR. The RT product can be stored at -20°C for up to one week.

d) Preparation of the Pre-Amp reaction mix

1. In a 0.2 μ l PCR tube, the following components were added:

Components	Volume	Final Concentration
Taqman Pre-Amp Master Mix	2.5 μ l	1X
Pre-Amp primer pool	0.75 μ l	0.03X each
RT Product	0.5 μ l	2.5 ng
DEPC treated MQ water	Make up volume to 5 μ l	

2. The reaction components were mixed thoroughly followed by pulse spin. The tubes were then transferred to a thermal cycler.

PCR cycling parameters:

Temperature	Time	No. of Cycles
95 $^{\circ}\text{C}$	10 min	1
55 $^{\circ}\text{C}$	2 min	1
72 $^{\circ}\text{C}$	2 min	1
95 $^{\circ}\text{C}$	15 sec	1
60 $^{\circ}\text{C}$	4 min	1
99.9 $^{\circ}\text{C}$	10 min	1
4 $^{\circ}\text{C}$	∞	Hold

3. After the Pre-Amp PCR the tubes were spun briefly. 2 µl of the Pre-Amp product was diluted to 16 µl (1:8 dilution) using 0.1 X T.E., pH 8.0. This is the diluted Pre-Amp product which can be stored at – 20 °C for up to one week.

e) Preparation of the real time PCR reaction mix- *Please refer section 3.7*

3.9 Cloning of PCR Products into the Target Vector

This section describes the general protocol for molecular cloning. It was used for cloning of the miR-206 and miR-204 genomic region in the pTRIPZ lentiviral vector, miR-204 genomic region in the pGIPZ vector and the 3' UTR regions of putative miR-204 target genes in the pcDNA 3.0 luciferase reporter vector.

(a) PCR amplification and Phenol-Chloroform method of DNA purification

Reagents for PCR: 5 X phusion HF buffer, 10 mM dNTP mix, Phusion polymerase,

Reagents for Phenol-chloroform DNA purification: Tris saturated phenol, Chloroform

Tris Saturated Phenol: Distilled phenol kept at –20 °C was carefully thawed to RT by keeping it at 60 °C preferably in waterbath. The cap of the bottle was loosened to release any pressure built on thawing the phenol. As phenol is acidic, it needs to be neutralised to avoid degradation of DNA. 25 ml of phenol was taken and equal volume of autoclaved Milli-Q in sterile Nunc tube. It was mixed thoroughly by shaking the tube and allowed to rest until two phases separate. Upper phase was removed. This was repeated once to saturate phenol with water. To the water saturated phenol, equal volume of 1 M Tris, pH 8.0 was added and mixed thoroughly by shaking the tube and left undisturbed to allow the two phases to separate. The upper phase was removed and the same sets of steps were repeated with 0.1 M Tris, pH 8.0. The pH of the phenol phase was subsequently achieved to be 7.0 or above. 10-15 ml of 10

mM Tris, pH 8.0 was added on top of the phenol phase for long-term storage in refrigerator and exposure to light was avoided by covering the tube with aluminium foil.

Method

1. All the reagents required for the reaction except the enzyme were thawed and kept on ice.
2. For each PCR reaction 25 ng of human lymphocytic genomic DNA was added in the end to the 0.2 ml tube containing the PCR components.
3. The PCR Reaction mix was prepared as follows

Components	Volume	Final Concentration
5 X Phusion buffer (HF)	2 μ l	1 X
10 mM dNTP mix	0.2 μ l	0.2 mM
Forward primer (10 pmol / μ l)	0.2 μ l	2 pmol
Reverse primer (10 pmol / μ l)	0.2 μ l	2 pmol
Phusion Polymerase (2 U / μ l)	0.1 μ l	0.2 U
Genomic DNA		25 ng
Autoclaved Milli-Q water		Make up volume to 10 μ l

4. Reactions were carried out in Eppendorf Master Cycler 5333 (Eppendorf, Germany). All precautions were taken to avoid PCR related contamination. All reagents and PCR products were handled using filter tips. The PCR cycling parameters were as follows:

Temperature	Time	Cycles
98 °C	5 min	1
98 °C	30 sec	30
Annealing temperature	45 sec	
72 °C	30 sec	
72 °C	10 min	1
4 °C	∞	Hold

5. 5 μ l of the PCR product was run on a 1 % agarose gel and visualized using an UV transilluminator. The PCR product was further purified using phenol: chloroform method, before using it for cloning.
6. The PCR product was diluted with approximately $\frac{3}{4}$ th volume of T.E. pH 8.0. An equal volume of Tris Saturated phenol was added to the diluted PCR product, mixed and centrifuged at 12,000 rpm, 20 °C for 15 min.
7. The upper aqueous layer was transferred to a fresh eppendorf tube and an equal volume of phenol: chloroform (1:1) was added to it, mixed and centrifuged at 12,000 rpm, 20 °C for 15 min
8. The aqueous was again collected in a fresh eppendorf tube. An equal volume of chloroform was then added to the tube, mixed and centrifuged at 12,000 rpm, for 15 min, at 20 °C.
9. The upper layer was again separated and $\frac{1}{10}$ th volume of 3 M sodium acetate pH 5.2 was added to it and mixed by inverting the tube.
10. 2.5 X volume of chilled absolute alcohol (kept at -20 °C to chill) was added to the tube, mixed well and kept overnight at -20 °C to precipitate the DNA.
11. Next day, the mixture was centrifuged at high speed (16,000 rpm) for 20 min at 4 °C and the pellet was washed with 500 μ l of 70 % alcohol for two times and centrifuged at 12000 rpm for 10 min at 4 °C
12. The pellet was air-dried and dissolved in minimum of 10 μ l T.E buffer pH 8.0.

(b) Agarose Gel Electrophoresis

Reagents

50 X Tris-acetate-EDTA (TAE) buffer: 121 g Tris and 18.6 g EDTA was dissolved in 300 ml of Milli-Q water followed by addition of 28.55 ml glacial acetic acid. Volume was made up to 500 ml and was autoclaved.

Ethidium Bromide stock solution (10 mg / ml): Dissolve 10 mg Ethidium Bromide in 1 ml of autoclaved Milli-Q water.

6 X DNA loading dye: Dissolve 0.25 % bromophenol blue, 40 % (w / v) sucrose in Milli-Q water.

Method

1. The appropriate amount of agarose was weighed into a measured volume of 1 X TAE buffer to make a 1 % gel. The slurry was heated in a microwave oven until the agarose was dissolved completely and ethidium bromide to a final concentration of 0.5 μg / ml (from a 10 mg / ml stock) was added when the gel solution had cooled to about 40 °C.
2. A gel tray was cleaned, the gel was poured into the gel tray and a clean comb was inserted in the slot provided in the tray. The gel was allowed to set at room temperature for 30-45 minutes.
3. After the gel had completely set, the gel was placed in the electrophoresis tank filled with 1 X TAE buffer. The buffer should be just enough to cover the gel to a depth of about 3 mm and the comb was carefully removed.
4. The DNA samples were mixed with 6 X loading buffer at 1 X final concentration and loaded into the wells of the gel. The gel was run in electrophoresis chamber at 40 mA constant current, till the dye had migrated about three-fourths of the gel.

5. The DNA was visualized on an UV transilluminator.

(c) Restriction digestion

Reagents: 10 X buffer, Restriction Enzyme

Method

1. All the reagents required for the reaction except for the enzyme were thawed and kept on ice.
2. For a typical restriction enzyme reaction, 2-3 U of enzyme was used to digest ~1 µg DNA in a reaction volume of 20 µl; at the recommended temperature for at least 4 hr. (If more than one reaction was performed a master mix was prepared containing the buffer, enzyme and Milli-Q water).
3. The reaction was heat inactivated at the recommended temperature for 15-20 min (most enzymes are inactivated at 65 °C for 15 min).
4. For cloning the digested product, the volume of the reaction was made to 200 – 300 µl with TE. The mixture was purified by phenol-chloroform method and precipitated with ethanol as described for PCR products.

(d) Dephosphorylation of Vector using Shrimp Alkaline Phosphatase (SAP)

The digested vector was treated with Shrimp Alkaline Phosphatase to remove the 5'-phosphate from the last base to avoid religation between the ends of vector molecules

Reagents: 10 X Restriction Enzyme digestion buffer, Shrimp Alkaline Phosphatase (1 U / µl)

Method

1. All the reagents required for the reaction except for the enzyme were thawed and kept on ice.

2. The reaction was set up as follows and incubated at 37 °C for 60 min.

Components	Volume
10 X R.E digestion buffer	3 μ l
Shrimp Alkaline Phosphatase (1 U / μ l)	1 μ l (1 U)
RE digested DNA mixture	10-20 μ l (1-10 pmol termini)
Autoclaved Milli-Q water	Make up volume to 30 μ l

3. The reaction was terminated by heat inactivation at 65°C for 15 minutes.

(e) Ligation

Reagents: 10 X Ligation buffer, T4 DNA Ligase (5 U/ μ l), 50 % PEG 4000 solution.

Method

1. All reagents required for the reaction except for the enzyme were thawed and kept on ice.

The reaction was setup as follows

Components	Blunt-end Ligation	Sticky-end Ligation
	Volume/ amount	Volume/amount
Linear vector DNA	60 fmol vector ends	30 fmol vector ends
Insert DNA (PCR product)	180 fmol insert ends	90 fmol insert ends
10 X Ligation buffer	2 μ l	2 μ l
50 % PEG 4000 solution	2 μ l	-
T4 DNA Ligase (5 U/ μ l)	1 μ l (5 U)	0.4 μ l (2 U)
Autoclaved Milli-Q water	Make up volume to 20 μ l	Make up volume to

2. The mixture was incubated for 16 hour at 22 °C (cold bath) and inactivated by incubating at 65 °C for 10 min.

(f) Preparation of competent cells

Reagents

Transformation buffer (TB): 0.3 g PIPES, 0.22 g of $\text{CaCl}_2 \cdot 2\text{H}_2\text{O}$, 1.86 g of KCl were dissolved in 95 ml Milli-Q and pH was adjusted to 6.7-6.8 with 5 M KOH. The initial white precipitate may form at low pH, however once the right pH is adjusted, solution should become clear. 1.09 g of MnCl_2 was added in this solution and final volume was made up to 100 ml and filter-sterilised using 0.22 μm filter.

Super Optimal Broth (SOB): 20 g of tryptone, 5 g of yeast extract was dissolved in 995 ml of Milli-Q water. 2 ml of 5 M NaCl and 1.25 ml of 2 M KCl was added to achieve final concentrations of 10 mM and 2.5 mM respectively. Solution was autoclaved and 5 ml of 2 M MgCl_2 solution prepared and sterilised separately was added just before use.

Luria Broth (LB): 1 g of tryptone, 0.5 g of yeast extract and 0.5 g of NaCl was dissolved in 100 ml of milli-Q water and autoclaved

SOB agar plates: 1.5-2 g Agar was dissolved in 100 ml of SOB (or LB), autoclaved and poured in pre-sterilised plastic plates.

Method

1. *Escherichia coli* strains DH5 α or stb13 cells were freshly streaked from the glycerol stocks on the SOB agar plates one day prior to inoculation into SOB for preparation of competent cells.

2. 200 ml of SOB medium (10 % of flask volume) was prepared and autoclaved in wider neck 2 L flask. All the steps here onwards are performed under aseptic conditions in laminar air flow system.
3. A single colony from the freshly streaked SOB plate was inoculated into the 200 ml SOB and the flask was incubated at 18°C at 150-200 rpm till the O.D at 600 nm reaches to 0.4. The O.D was checked at regular intervals using a spectrophotometer by removing 1ml of the growing culture under aseptic conditions.
4. The culture was centrifuged at 3000 rpm for 15 min at 4 °C when O.D reaches 0.4 or in when it's in between 0.4 to 0.7.
5. The supernatant was discarded and one third volume of ice cold transformation buffer (134 ml for 200 ml culture) was added slowly onto the pellet so as to gently resuspend the pellet.
6. It was completely resuspended in TB with gentle pipetting for 5-10 min and was incubated on ice for additional 10 min. Care was taken to avoid formation of bubbles during the re-suspension of the cell pellet.
7. The resuspended pellet was centrifuged at 3000 rpm for 15 min at 4 °C. The cell pellet was again resuspended in 16 ml of TB (1 / 12.5 volume of the initial culture volume i.e. for 200 ml) as described in the earlier step.
8. 1.12 ml of DMSO (at a final concentration of 7 %) was added on the walls of suspension tubes slowly and was mixed by shaking or by gentle pipetting once or twice.
9. The cells in this solution were made into aliquots of 100 µl in 1.75 ml pre-chilled sterile eppendorf tubes and snap-frozen in liquid nitrogen.
10. The competent cell vials were stored at -80 °C and were thawed on ice just before use.

(g) Transformation of competent cells

Reagents: *Stbl3* or DH5α ultra-competent cells, SOC broth, LB broth

Method

1. *Stbl3* or DH5 α ultra-competent cells, stored at -80 °C were thawed on ice by tap-mixing intermittently and kept on ice.
2. 2-10 μ l of the DNA ligation mixture was added to the cells and incubated on ice for 30 min, followed by a heat shock for 45 sec at 42 °C (90 sec for DH5 α)
3. Then the transformation mixture was subjected to cold shock by immediately transferring to ice for 5 min.
4. 900 μ l of SOC broth was added to the transformation mixture and incubated on a shaker incubator for 1 hr at 37 °C. The mixture was spread on a LB agar plate containing ampicillin (100 μ g / ml) and incubated at 37 °C for 16-18 hr
5. The colonies obtained were then inoculated in LB broth containing ampicillin (100 μ g / ml) and plasmid DNA was extracted from the cultures using alkaline lysis method.

(h) Plasmid extraction by alkaline lysis method

Reagents

Solution I: Glucose Tris EDTA solution:

Components	Volume	Final concentration
2 M Glucose	1.25 ml	50 mM
0.5 M EDTA	1.0 ml	10 mM
2 M Tris, pH 8.0	0.625 ml	25 mM
Final volume	Make up to 50 ml with autoclaved Milli-Q water	

Solution II: (Freshly prepared)

Components	Volume	Final concentration
5 M NaOH	0.2 ml	0.2 N
20 % SDS	0.25 ml	1 %
Final Volume	Make up to 5 ml with autoclaved Milli-Q water	

Solution III/ (3 M Potassium 5 M acetate, pH 4.8):

14.7 g of Potassium acetate was dissolved in 20 ml Milli Q water and volume was made upto 30 ml. To this, 5 M Potassium acetate, 5.5 ml of glacial acetic acid and 10 ml of Milli-Q water was added. pH was checked. If it is not ~ 4.8 more acetic acid was added and finally the volume was made to 50 ml with Milli-Q water and the solution was autoclaved.

Method

- 1-2 ml of bacterial culture in a 1.5 ml eppendorf tube was centrifuged at 3000 rpm for 5 min at room temperature. The cell pellet was resuspended in ice cold 100 µl solution I by vortexing and incubated for 5 min at room temperature.
- 200 µl of freshly made solution II was added and mixed by gently inverting the tube followed by incubation on ice for 5 min.
- 150 µl of solution III was added and immediately mixed by vortexing for 10 sec, followed by incubation on ice for 5 min.
- The tube was centrifuged at 13000 rpm for 5 min at 4 °C and the clear supernatant was removed in a fresh tube without disturbing the pellet.
- An equal volume of phenol-chloroform (1:1) was added to the supernatant. (for example, 250 µl of tris-saturated phenol and 250 µl of chloroform were added for 500 µl of supernatant.)

6. The tube was vortexed for 2 min and centrifuged at 12000 rpm for 5 min. The aqueous layer was removed carefully into a fresh tube.
7. Equal volume of chloroform was added to the aqueous layer and tube was vortexed to thoroughly mix the contents. Step 6 was repeated.
8. 1 ml (or double the volume) of absolute ethanol was added to the supernatant, mixed by inversion and allowed to precipitate at room temperature for 5 min.
9. The tube was centrifuged at 13000 rpm at room temperature for 5 min and the supernatant was decanted carefully so as to not disturb the DNA pellet. 1 ml of 70 % ethanol was added to the DNA pellet and re-spun at 13000 rpm for 5 min. The ethanol was aspirated and the DNA pellet was air dried.
10. The DNA pellet was dissolved in 10-25 μ l TE containing RNaseA (1 μ g / ml) and then analysed for successful cloning by restriction digestion.
11. The constructs generated were purified on a larger scale using the Qiagen DNA Midi kit according to manufacturer's protocol.

3.10 Cell Culture

Medulloblastoma cell lines Daoy and D283 were obtained from ATCC. D341, D425 and D384 medulloblastoma cell lines were a kind gift from Dr. Darell Bigner (Duke University, Durham, USA.). HEK293FT cells were obtained from Invitrogen (Carlsbad, CA, USA)

3.10.1 Tissue Culture Media and Reagents

Tissue culture medium: Commercially available powdered medium, Dulbecco's Modified Eagle Medium (DMEM) and DMEM with F12 nutrient mixture (DMEM/ F12) containing high glucose, pyridoxine hydrochloride and sodium pyruvate (Catalog No. 12800-058, and 12500-062 Thermo Fischer Scientific) was prepared as per the manufacturer's instructions. The powdered medium was reconstituted by dissolving it in ~800 ml autoclaved Milli-Q

water under sterile conditions. 3.5 g Sodium bicarbonate was added and the pH was adjusted to 7.5 using 1N HCl (about 11 ml). The volume was made up to 1 L in a sterile volumetric flask and the medium was filter sterilized through a 0.22 µm pore size filter membrane (Cat no. GSWP04700) fitted in a sterile filtration assembly. The filtered medium was stored in 500 ml aliquots at 4 °C.

The Complete medium contained DMEM supplemented with 10 % fetal bovine serum (FBS, Invitrogen, and Cat. No. 16140-071). 1 ml of the 100 X antibiotic (Penicillin and streptomycin) stock solution was added per 100 ml of complete medium if required.

100 X antibiotic mix: 10,000 units Penicillin G (Alembic Ltd, Vadodara, India) and 10,000 µg Streptomycin sulphate, available as injection vials (Abbott Healthcare Pvt. Ltd, Ahmadabad, India) were dissolved per ml in Milli-Q water, filter sterilized and stored at 4 °C.

10 X phosphate buffered saline (PBS): 80.8 g NaCl, 2.0 g KCl, 12.6 g Na₂HPO₄ · 2 H₂O, 2.0 g KH₂PO₄, and 10 g glucose was dissolved in autoclaved Milli-Q water and the volume made up to 1 L. The solution was filter sterilized and stored at 4 °C.

10 X Trypsin (0.25%): 2.75 g of trypsin was added to 110 ml of autoclaved Milli-Q water and allowed to dissolve overnight on a magnetic stirrer. The solution was sterilized by filtering through a 0.22 µm pore size filter. The solution was stored in 10 ml aliquots at -20 °C. 10 X stocks were diluted to 1 X working solution with 1 X PBS. The working solution was stored at 4°C.

3.10.2 Routine Maintenance of Cell Lines

All the reagents, glassware and plasticware used for tissue culture work were sterile and of tissue culture grade.

The adherent cell lines Daoy and HEK293FT cells were routinely cultured in 1X Dulbecco's Modified Eagle's Medium(DMEM) with 10 % fetal bovine serum (FBS). They were passaged as follows-

1. The spent media was aspirated out using a Pasteur pipette and the cells in the plate were rinsed twice with 1 X PBS.
2. 1 X trypsin was added to the plate and was removed after the cells started to round up but just before the cells started to detach. The cells were collected in 1 X PBS and the cell suspension was transferred to a centrifuge tube containing 1 ml complete medium and tightly corked.
3. The cell suspension was centrifuged for ~2 min at 1000 rpm in a REMI benchtop centrifuge. The supernatant was discarded and the cell pellet was loosened by tapping the tube gently.
4. The cells were resuspended in an appropriate volume of complete medium, cell count was taken using a haemocytometer, and the required cell number was seeded in to tissue culture plates. The cells were incubated in a humidified incubator at 37 °C in an atmosphere of 5 % CO₂. The cells were passaged when the density reached ~ 75-80 % or were frozen. The cells were not passaged for too long and a fresh vial of frozen cells was revived at regular intervals.

D283, D341, D425 and D384 are semi-adherent cell lines and they were routinely cultured in 1X DMEM + F12 nutrient mixture containing 10% FBS in the following manner.

1. The cells were directly collected from the tissue culture plate using a Pasteur pipette. The use of trypsin is not required for these cells. The cell suspension was transferred to a centrifuge tube which was tightly corked.

2. The cell suspension was centrifuged for ~2 min at 1000 rpm in a REMI benchtop centrifuge. The supernatant was discarded and the cell pellet was loosened by tapping the tube gently.
3. The cells were resuspended in an appropriate volume of complete medium. The cell suspension was triturated 3-4 times using a Pasteur pipette to obtain a single cell suspension. The cells were counted using a haemocytometer, and the required cell number was seeded in tissue culture plates.

3.10.3 Freezing and Revival

1. The cell lines were grown to a density of 75-85% after which the Daoy and 293 FT cells were trypsinised as described above and the D283, D425, D341 and D384 cell lines were centrifuged to obtain the cell pellet. The cell pellet was loosened by gently tapping the tube and the centrifuge tube was placed on ice for 1-2 minutes. Pre-chilled freezing medium (FBS +10% DMSO) was added dropwise to the cells ($\sim 1 \times 10^6$ cells per ml of freezing medium) on ice, with constant shaking to ensure as even cell suspension and transferred to pre-chilled freezing vials. These vials were cooled gradually by transferring them from ice to -20 °C for 2 hours and to -80 °C overnight and finally stored under the vapour of liquid nitrogen.
2. To revive the frozen cells, a vial containing frozen cells was removed from liquid nitrogen and immediately thawed in a water-bath at 37 °C. As soon as the cell suspension thawed, it was transferred to a centrifuge tube containing 3-4 ml complete medium and centrifuged at 1000 rpm for 2 min. The supernatant was discarded and the cell pellet was loosened by tapping the tube gently. The cells were resuspended in 4 ml of complete medium and centrifuged again. The supernatant was discarded and the cells were resuspended in an appropriate volume of complete medium. The medium was replaced after the cells had

adhered or on the next day after microscopically confirming the presence of live cells.

3.10.4 Transient transfection of HEK293T cells using BES buffered saline

Transfection of plasmid DNA into HEK 293T cells was carried out using calcium phosphate precipitation method. This method of transfection was used to validate expression of miRNA from the miR-206 / miR-204 pTRIPz construct, for generation of lentiviral particles and for validation of luciferase reporter assay as described in the further sections.

Reagents

2 X BBS (BES buffered saline): [50 mM BES, 280 mM NaCl, 1.5 mM Na₂HPO₄]

For 50 ml BBS, 0.533 g BES(Sigma B4554-25G), 0.818 g NaCl (S.D. Fine Chemicals Product No.- 20241 AR) and 0.0134 g Na₂HPO₄.2H₂O (S.D. Fine Chemicals Product No. 20383 AR) were dissolved in 45 ml of autoclaved milli-Q water and the pH was adjusted to 6.95 using 5 M NaOH. The final volume was made up to 50 ml and the pH was checked again. The solution was filtered through a 0.22 µm filter (Millipore) and stored as 0.5 ml aliquots at -20 °C.

0.5 M Calcium Chloride [CaCl₂]: 3.675 g CaCl₂ .2H₂O (Sigma C-3306) was dissolved in 45 ml of autoclaved Milli-Q water. The volume was made up to 50 ml and filter sterilized using 0.22 µm filter and stored as aliquots of 0.5 ml at -20 °C.

The reagents were thawed at R.T. beforehand. Plasmid DNA used for transfection were purified using QIAGEN plasmid purification midi kit (QIAGEN, Hilden, Germany)

Method

1. 2×10^5 HEK293 cells were seeded in a 35 mm tissue culture plate one day prior to the day of transfection.

2. On the next day, the medium of the plate was changed 4 hrs prior to transfection.
3. The required volume for 6 µg of Qiagen column purified plasmid DNA was added to a sterile eppendorf tube and the volume made up to 50 µl with sterile M.Q. water. 50 µl of 0.5 M CaCl₂ was added dropwise to the tube. 100 µl of 2 X BBS was then added dropwise to the tube and mixed by gently pipetting it up and down for 2-3 times. The mixture was then incubated at R.T. for 20 min.
4. The mixture was added on the cells and the plate was swirled gently to allow proper mixing.
5. 16 hrs after transfection, the medium of the plate was changed. The cells were used for further assays or for extraction of RNA. The number of cells and the amount of DNA is scaled up proportionately and used for transfection in 55 mm plates or 90 mm plates.

3.10.5 Transient Transfection of Medulloblastoma Cell Lines with miRNA Mimics

The effect of overexpression of miR-206 / miR-204 in D283 and D425 cell lines on their malignant behaviour was studied by transient transfection of these cell lines with miRNA mimics using Dharmafect-2 transfection reagent. The non-targeting RISC-free control siGLO was used as a negative control.

Reagents: miR-206 / miR-204 mimic or siGLO (Dharmacon), Dharmafect 2 transfection reagent (Dharmacon), 5 X siRNA buffer (Thermo Fischer Scientific), Nuclease free water (Sigma)

Method

1. The miRNA mimics (5 nmol stock) were initially dissolved in 250 µl of 1 X siRNA buffer (5 X siRNA buffer is diluted to 1 X using the nuclease free water) to achieve a stock concentration of 20 µM. Aliquots of 20 µl were made and stored at -20 °C to avoid repeated freeze-thaw cycles.

2. 1×10^5 D425 and 1.5×10^5 D283 cells were seeded in a 35 mm dish one day prior to the transfection.
3. In separate tubes, the miRNA mimic or siGLO and the DharmaFECT 2 transfection reagent were diluted with serum-free 1 X DMEM / F12.
4. The required concentration of the miRNA mimic / siGLO (2 μ l) and 4 μ l of DharmaFECT 2 transfection reagent was diluted in 200 μ l of serum-free 1 X DMEM / F12 and mixed by gently pipetting up and down. These mixtures were incubated separately at R.T. for 5 min.
5. After the incubation 200 μ l of both the tubes were mixed (total volume 400 μ l) by pipetting gently and incubated at R.T. for 20 min.
6. 1.6 ml of 1X DMEM + 10 % FBS was added to the mixture and again mixed by pipetting. The existing medium from the D283 and D425 cells was then replaced by this transfection medium.
7. The D425 and D283 cells were incubated with the transfection mix for 48 h and 24 h respectively after which the medium was changed. D283 cells were incubated for lesser time since they showed toxicity on incubation for longer duration.
8. 72 h post transfection, the cells were used for further analysis. RNA was extracted from the cells to determine the level of miRNA expression by real time RT-PCR

3.10.6 Generation of Lentiviral particles and Selection of Stable Polyclonal Populations of Medulloblastoma Cell Lines

The effect of miR-206 / miR-204 expression on the growth characteristics of medulloblastoma cells was studied by generation of stable polyclonal populations of these cell lines. Lentiviral particles containing miR-206/ miR-204 pTRIPZ or pTRIPZ vector alone were generated and used to transduce medulloblastoma cells which were then selected in the presence of puromycin. The lentiviral particles were generated as follows-

All lentiviral procedures were carried out in Bio safety level 2 cabinets (Esco technologies, Hatboro, PA, USA.). Disposable rubber gloves, mask, cap and apron was worn when handling the lentivirus. Infected cultures, spent medium, contaminated disposables were treated with 10% sodium hypochlorite and autoclaved in biohazard bags prior to disposal.

1. 8×10^5 HEK293 FT cells (Invitrogen) were seeded in a 55 mm dish one day prior to transfection.
2. 6 μ g of miR-206 / miR-204 pTRIPZ vector along with the lentiviral packaging plasmid pMD2G (1.5 μ g) and psPAX2 (4.5 μ g) were transfected using calcium phosphate precipitation method.
3. 48 h post transfection the medium supernatant containing viral particles was collected and fresh complete medium was added to the plate. 72 h post transfection, the virus containing supernatant was collected again.
4. The supernatant was centrifuged at 1000 rpm at 4 °C for 2-5 min to remove the cell debris. The clear supernatant was then filtered through a 0.45 μ m filter. It was either concentrated 10-30 fold by ultracentrifugation at 25000 rpm at 4 °C for 90 min or stored at -80 °C.
5. In order to determine the viral titre 50,000 HEK293 cells were seeded in a 35mm dish. The filtered viral supernatant was serially diluted from 1:10 to 1:1000 and 1 ml of the different dilutions was used for transduction. The medium was changed 16 hrs post transduction and cells were induced with 4 μ g / ml of doxycycline. 48 hrs post induction, RFP expression was confirmed by microscopic examination of the cells. The cells were then processed for flow cytometry analysis (FACS Calibur, B.D. Biosciences, USA) to determine the number of RFP positive cells. The viral titre was determined by the formula $[(50,000 \times \% \text{ of RFP positive cells}) / 100] \times \text{dilution factor}$.
6. The selection of miRNA expressing clones was carried out by transduction of the medulloblastoma cell lines with the neat, diluted or concentrated viral supernatant. 1ml of

viral supernatant was added to a 35 mm dish containing 50,000 Daoy or D425 cells or 1×10^5 D283 or D341 cells. $4 \mu\text{g} / \text{ml}$ polybrene was added to the plate to increase the efficiency of transduction. 16 hrs post transduction the medium was changed and fresh complete medium was added to the cells.

7. 48 h after transduction the cells were trypsinised and added to a 55mm dish and the necessary amount of puromycin (250 ng / ml for Daoy, 200 ng / ml for D283, D425 and D341 cells) was added to select the cells.
8. After 3 doses of puromycin the selected cells were induced with $2\text{-}4 \mu\text{g} / \text{ml}$ doxycycline to determine the level of expression of miRNA in the cells. RNA was extracted from the cells and the level of miRNA expression was studied by real time RT-PCR as described in section 3.7. Stable polyclonal populations of pTRIPZ vector alone were also selected in a similar manner. These cells were used for studying the effect of the miRNA expression on the growth characteristics of the cells in the soft agar assay, MTT assay, clonogenic and radiation sensitivity assay, invasion assay and in-vivo tumorigenicity assay.

3.10.7 MTT Reduction Assay

The effect of miR-206 or miR-204 expression on the proliferation of the cells was studied by the MTT reduction assay.

Reagents

MTT [Methylthiazolyldiphenyl-tetrazolium bromide]: 5 mg / ml in 1 X PBS

50 mg MTT powder was dissolved in 10 ml 1 X PBS and mixed by vortexing. The solution is stored in dark at 4°C

Acidified SDS: 10 % SDS in 0.01 N HCl

10 g SDS was dissolved in 80 ml autoclaved Milli-Q water and heated at 60 °C for 1 hr to assist the dissolution. 88.4 µl of con. HCl was added and the final volume was adjusted to 100 ml. The solution was stored at R.T.

Method

1. The cells were seeded in a 96 well plate.(500 cell/well for Daoy, 1000 cells / well for D283, D425 and D341)
2. The medium from the wells was replenished every 3 days.
3. On day 0, 3, 6 and 9, 20 µl of MTT solution was added to 4 wells of each set and the cells were incubated at 37 °C in a CO₂ incubator for a period of 4 hrs.
4. After 4 hrs of incubation, formazan crystals were dissolved by adding 100 µl of acidified SDS to each well.

3.10.8 Soft agar Colony Formation Assay

The effect of miR-206 or miR-204 expression on the anchorage independence growth of the cells was studied by colony formation in soft agar

Reagents: LMP agarose (Sigma Cat. No.), 2X DMEM / DMEM F12 + 20 % FBS

Method

1. For the soft agar medium, 2X DMEM containing 20% FBS was mixed with an equal volume of molten 2% low melting point (LMP) agarose, and 1 ml of this mixture was poured into a sterile 35 mm dish to obtain a basal layer of 1% agarose in complete medium (DMEM + 10% FBS). The agarose was allowed to set for temperature before seeding the cells.
2. The control cells and doxycycline induced cells (10,000 Daoy or 1000 cells of D283, D425 and D341) were suspended in 1X DMEM supplemented with 20% FBS.

3. 2 % LMP molten agarose and 2X DMEM + 20% FBS were added to the cell suspension such that the final concentration of agarose in the suspension was 0.3 % and serum content was 10 %.
4. The contents were mixed properly using a micropipette and 1 ml of this mixture was added to a 35 mm dish pre-coated with the basal layer.
5. The agar was allowed to solidify for about 1 – 2 h at room temperature and then the plates were incubated at 37 °C under an atmosphere of 5 % CO₂.
6. The cells were fed with 0.1 - 0.2 ml complete medium (with or without doxycycline) every 3 days throughout the duration of the experiment.
7. After ~4 weeks of incubation, colonies with 10-15 cells per colony were counted under microscope from the entire plate. Average colony count from three plates was represented as histograms.

3.10.9 Clonogenic and Radiation Sensitivity Assay

Clonogenic assay was performed to study the clonogenic potential and radiation sensitivity of Daoy cells on expression of miR-206.

Method

1. 72 h post induction with doxycycline, the cells were trypsinized and 1000 cells were seeded in triplicates per 55 mm plate
2. Next day the cells were irradiated at a dose of 6 Gy (Cobalt-60 gamma irradiator, Bhabhatron, developed by Bhabha Atomic Research Center, India).
3. The medium was changed 24 h later. The cells were allowed to grow for 8-10 days until microscopically visible colonies formed.
4. The cells were fixed by incubation in chilled methanol: acetic acid (3:1) overnight at 4 °C, stained with 0.5% crystal violet dye and the colonies were counted using a stereomicroscope. Average colony count from three plates was represented as histograms.

3.10.10 Synergistic Effect of All trans Retinoic Acid and miR-206 on the D283

Medulloblastoma Cell Line

Reagents: All trans Retinoic Acid (ATRA) (stock solution 20mM). Appropriate amount of the ATRA powder was dissolved in 100 % ethanol by thorough vortexing. 20 µl aliquots were made and stored at -80 °C for upto one month.

Method

1. 1500 cells of polyclonal population of D283 (Both empty pTRIPZ and miR-206-pTRIPZ) with or without induction with doxycycline were seeded in a 96-well plate
2. On the next day, the necessary dilutions of the stock solution of ATRA were made and added to the cells at a dose of 5 nM / 10 nM. The control cells were added with an equivalent volume of 100 % ethanol. The dilutions were made such that the volume of the drug added remains < 10 % of the volume of the medium.
3. 72 hrs post treatment , the cells were added with MTT and the protocol for MTT reduction assay was carried out as described above to determine the cell viability.

3.10.11 Invasion Assay

The effect of miR-204 expression on the in-vitro invasion capacity of the Daoy and D283 medulloblastoma cell lines was studied by their using matrigel coated transwell inserts.

All pipette tips, eppendorf tubes and cell culture inserts were pre-cooled to 4 °C in a refrigerator for handling of matrigel.

Materials

1. Matrigel (Cat. No. 356234) stock 1mg/ml- This was diluted to 1 mg/ml in plain 1X DMEM and stored as 100 µl volume aliquots. The diluted matrigel was stored at -70⁰C. Care was taken to avoid reusing the same aliquot.
2. Cell culture inserts (0.8 µm pore, Cat. No. 353097)
3. 24 well cell culture plates with notch.

All above reagents were from BD Biosciences, San Hose, USA

4. Calcein (Cat. No- 206700, Molecular probes, Life technologies)
5. Cotton buds.

Method

1. The cell culture insert was carefully placed using sterile forceps into a well of the 24-well plate such that it fits into the notch of the well. The insert was then washed twice with chilled 1 X DMEM / F12 without FBS. The matrigel stock (1 mg / ml) was thawed on ice and diluted to 300 ng / µl with chilled 1X DMEM. 100 µl of this diluted matrigel was added to the insert (total 30 µg). Care was taken to avoid formation of any air bubbles. The plate was then incubated at 37 ⁰C for 1 hr.
2. The unpolymerised matrigel was removed from the well and 50,000 Daoy cells / 75000 D283 cells suspended in 1 X plain DMEM or DMEM / F12 were seeded on top of the matrigel coated insert. 750 µl of 1 X DMEM or DMEM / F12 +10 % FBS was carefully added along the wall of the well such that the insert got immersed in the complete medium. The cells were then incubated at 37 ⁰C for 36 hrs (Daoy) and 56 hrs (D283).
3. Five thousand cells from the mastermix of cells prepared for seeding in the transwell insert were seeded per well of 96-well black plate, in duplicates. This was done to determine initial cell number seeded for the invasion assay.

4. After ~6-8 hr, the medium in the 96-well plate was replaced with fresh medium supplemented with Calcein AM (1 μg / μl stock concentration) with a final concentration of 2 $\mu\text{g}/\text{ml}$ of medium. The plate was incubated for minimum of 30 min at 37⁰C.
5. Fluorescence was read with excitation at 485 nm and emission at 535 nm with 0.1 or 0.5 sec as exposure time, Lamp energy 5000, position-top, reading by plate as additional settings, using Mithras LB940 multimode reader (Berthold Technologies, Germany).
6. 35 h (55 h for D283 cells) post incubation; the wells of the 24-well plate with the transwell insert were added with 2 μg / ml of Calcein fluorescent dye and incubated for 1hr.
7. The insert was removed from the plate and the medium in the insert was discarded. Using a cotton bud the inner surface of the insert was carefully wiped to remove all the cells that have not invaded.
8. Images of the invaded cells were captured using the Zeiss Axiovert 200M fluorescence microscope by placing the insert back into the well of the 24-well plate.
9. The membrane of the insert was then cut using a scalpel blade. Care was taken to ensure that the bottom surface of the insert is not touched. The membrane was then placed in a well of a black walled 96-well plate and covered with 100 μl of plain medium. The fluorescence intensity of the calcein labelled cells was quantified using a luminometer using the FITC filter and an exposure time of 1 sec or 5 sec as described above.
10. In case of D283 cells, some proportion of invaded cells does not remain adhered to the membrane but remain in the lower chamber medium. To account for this population of invaded cells, lower chamber medium was centrifuged at 3000 rpm at 5 min to pellet down the cells. The cell pellet was resuspended in 100 μl of complete medium and the fluorescence was read as described above. The total fluorescence was calculated from the fluorescence values belonging to lower chamber cells and cells from insert membrane.

3.11 In vivo Tumorigenicity Assay

3.11.1 In-vivo Tumorigenicity Assay by Subcutaneous Injection

The effect of miR-204 expression on the in-vivo tumorigenic potential of Daoy medulloblastoma cell lines was studied by subcutaneous injection of this cell line in immunocompromised mice.

Method

1. The vector control and miR-204 expressing Daoy polyclonal populations (Daoy 204-C) were induced with 4 µg / ml of doxycycline for 72 hrs. The cells were suspended in 150-200 µl of sterile 1 X PBS for the injections.
2. 6-8 week old NOD / SCID mice were used. 4.6×10^6 Daoy vector control and miR-204 expressing cells on either flank of the same mouse using a 21 gauge needle.
3. The mice were fed with 1 mg / ml of Doxycycline in 5 % sucrose for induction of miRNA expression or with sucrose alone for the control animals.
4. The tumors formed were measured weekly for their length and breadth using a vernier calliper upto 3-4 weeks after the tumors formed. The tumor volume was calculated as $(W^2 \times L) / 2$.
5. The mice were euthanized by overdose of CO₂ and the tumors were resected from the flanks. The tumours were fixed in a 10 % formalin solution for atleast 24 hr prior to embedding in paraffin.

3.11.2 In-vivo Tumorigenicity Assay by Orthotopic Injection in Mouse Cerebellum

D283 cells were transfected with a pcDNA3.1 vector expressing firefly luciferase under CAG (CMV early enhancer/chicken beta-actin promoter) promoter and selected in presence of neomycin. These cells, stably expressing luciferase were transfected with either siGLO or

miR-204 mimic as described earlier. Tumorigenic potential of these firefly luciferase expressing cells was studied by generating orthotopic xenograft in immunodeficient mice using stereotactic method of intracranial injection. Following procedure was approved by Institutional Animal Ethics Committee.

Reagents

1. Anaesthetic agent (Ketamine and Xylazine)
2. Analgesic (Buprenorphine, Neon Laboratories, India)
3. Sterile ocular lubricant (Neosporin, Neon Laboratories, India)
4. Sterile phosphate-buffered saline
5. 70 % ethanol
6. Bone wax (Cat. No. W810, Ethicon Inc, Johnson & Johnson Ltd)
7. Tissue adhesive- VetBondTM (n-butyl cyanoacrylate) Cat. No. 1469SB, 3M Animal care products, St Paul, MN, USA)

Equipments

1. Syringe needle 30G
2. Glass Syringes, 5 µl Hamilton Co, Model 75 RN Syringe, 700 Series; volume 5µl; Cat. No. 7634-01)
3. Needles, 26 G, 2” compatible for 5 µl syringes (26GA RN 70mm PT3 6PK, Cat. No. 7804-03, Hamilton)
4. Sterile cotton buds
5. Surgical instruments include Fine forceps, Iris Scissors, Blunt forceps, sterile scalpel blades
6. Small animal stereotaxic frame (Harvard Apparatus, MA, USA)
7. Electric microdrill and bits (Cat. No.67-1000, Ideal Micro Drill Kit, Cell Point Scientific, Gaithersburg, MD, USA)

8. Heating pad/chamber (with thermometer)
9. Electric hair clippers

Animals Used: Immunodeficient mice: 6 to 8 week old BALB/c Nude mice (CAnN.Cg-Foxn1nu/Crl strain) or NODSCID (NOD/NcrCrl-Prkdc^{scid}) received from Charles River, USA.

Method

A) Preparation of cells

1. The cells were collected in medium by triturating using glass pipette. A short spin at 1500 rpm for 1 min was given to remove any dead cells. The cell pellet was resuspended in fresh medium.
2. The cells were counted using a haemocytometer and the required volume of culture suspension containing 2×10^5 cells was spun down at 2000 rpm for 3 min.
3. The cells were washed once with sterile 1 X PBS and resuspended in 5 μ l final volume of 1 X PBS.
4. The cell suspension was kept on ice till the time of injection.

B) Equipment and specimen setup

1. The small animal stereotaxic frame was assembled as per the manufacturer's instructions.
2. The heating pad necessary for post-procedural care is switched on to maintain the temperature at 37 °C.
3. The animals were weighed in order to decide the dosage of anaesthesia. Typically, 6-8 weeks old animals with minimum of 20 g body weight were used for the intracranial injections.
4. Ketamine and Xylazine were diluted 1:1 in sterile 1X PBS and were mixed to get a final concentration of 90-120 mg / kg body weight (ketamine) and 20 mg / kg body weight

(xylazine). Diluted stocks of ketamine and xylazine were preserved at 4 °C for up to one week.

C) Surgical procedure

Preoperative animal preparation

1. The mouse was anesthetized by administering ketamine-xylazine mixture through intra-peritoneal route by using a sterile 30 G needle syringe.
2. The lubricating ophthalmic ointment (Neosporin) was applied on both the eyes of mouse to prevent drying of the cornea.
3. Hair from the surgical site was removed with electric clipper or razor and the surgical site was disinfected by wiping the area by cotton tipped buds soaked in 70 % ethanol.
4. The anesthetized mouse was positioned appropriately in stereotactic apparatus with the incisors of the animal locked in the mouth fixture at front and the ears in ear holders. Ear bars were adjusted gently in ears at occiput of head level and then were tightened firmly. Height of the mouth fixture and ear bars was adjusted so that the head remains steady and flat.

Preoperative cell preparation

1. Hamilton syringes and needles (26 G) was washed several times by rinsing it with sterile PBS before aspirating cell culture.
2. Cells in microcentrifuge tube were re-suspended by tapping gently or by pipetting prior to each injection to prevent cell clumping.
3. 5 µl of cell suspension was drawn into Hamilton syringe with great care to avoid aspiration of bubbles.

Surgical opening of skull

1. 1.0-1.5 cm midline sagittal incision was given with a sterile disposable scalpel blade or iris scissors along the superior aspect of the cranium from intra-aural line towards the anterior aspect of head.
2. Bregma (intersection of coronal and sagittal sutures) on the anterior side and lambda (conjunction of sagittal and lambdoid sutures) on the posterior side was identified as they are used to serve as landmarks for the stereotactic localization prior to injection.
3. Fascia over area of skull was removed by using forceps and scalpel blade. This was done to make the injection site easily accessible to drill into the skull.

D) Injection of cells

1. A guiding needle was attached to the holder attached to the dorso-ventral (DV) axis of the stereotactic apparatus and was adjusted to 2.5 mm posterior to lambda at midline by using a vernier scale on the antero-posterior (AP) axis. DV and AP coordinates required to achieve injection precisely in the cerebellum were chosen by referring to Paxinos and Franklin's the Mouse Brain in Stereotaxic Coordinates: An Atlas of the stereotaxic coordinates of mouse brain.
2. Using a microdrill with a sterile drill bit, a small burr hole was made as per the coordinates set by the guiding needle. Sufficient care was taken so as to keep drilling superficially in order to avoid traumatic injury to the brain.
3. The 5 µl Hamilton syringe was attached to the stereotactic apparatus holder and cautiously inserted into the brain through the drilled burr hole.
4. The needle was maintained perpendicular to the skull and slowly inserted 3 mm deep into the brain. After waiting for 1 min, the needle was moved back by 0.5 mm and the cell suspension was delivered slowly over a period of 2-3 min.

5. The skull was kept dry during injection, using sterile cotton buds to remove any tissue fluid that may have refluxed out of the burr hole.
6. The syringe was kept in place for 1-2 min upon completion of injection and then slowly withdrawn.
7. The site of the burr hole was plugged with bone wax, and the skin was closed with the help of tissue adhesive VetBond.
8. The ear holders were unscrewed from the ears of the animal and incisors were removed from mouth fixture. The animal was transferred to a heating pad maintained at 37 °C till it regained consciousness.
9. Animals were sacrificed at 4th week by using over-exposure to CO₂ as a method of euthanasia. Whole brain of each animal was collected by surgically opening the skull. Whole brain of each animal was incubated separately in 10 % formalin solution overnight and cut in sagittal fashion by using blade to separate two hemispheres. This was then followed by paraffin embedding of both the hemispheres separately to prepare paraffin blocks. 5 µm sections were taken using microtome and stained for haematoxylin and eosin to visualise tumour cells in cerebellum.

3.11.3 Bioluminescence Imaging

Instruments

Xenogen IVIS spectrum imaging system (Caliper Life Sciences, MA, USA).

Reagents

D-luciferin, potassium salt (Cat. No.L8220 Biosynth AG, Switzerland) (30 mg /ml): 30 mg of

D-luciferin powder is dissolved in 1X PBS and can be stored in -20 °C.

Isoflorane (Forane 250 ml Inj, Abbott laboratories, India)

Method

1. The exhaust of the gas anaesthesia system was switched on and the animals were put in the incubation chamber and exposed to 3 % isoflurane till animals were anaesthetized and breathing rate was regularised.
2. 100 μ l of 30 mg / ml of D-luciferin (prepared fresh in 1 X PBS) at (150 mg / kg body weight) was administered to anesthetised mice via the intra-peritoneal route using sterile a 30 G syringe needle and the animal was placed in the imaging chamber of the IVIS system. 3 % isoflurane was delivered through nose cones provided inside the imaging chamber.
3. The image was acquired ~5 min after injection on auto exposure setting so as to determine optimal exposure time using Living Image 4.0 software provided with the instrument. Images were always captured so that count of photons was detected in the recommended detectable range for the instrument i.e. 600 to 60,000. Exposure time and Camera aperture (f stop) settings were adjusted as required.
4. 8-10 serial images at interval of 2 min wherein luminescence counts gradually increase attain peak and reduce subsequently. Image showing peak luminescence counts indicates peak enzyme activity that can be achieved and hence is used as a representative of tumour growth at that time point in a particular animal.
5. Region of interest (ROI) was precisely drawn over site of luminescence (represents site of the tumour) in overlay images using the Living Image 4.0 software (Caliper Life Sciences) and the total normalised photon output was represented as average radiance (photons / sec / cm^2 / steradian).
6. All the animals were imaged on 1st and 4th week post intracranial injection. Increase in tumour growth from 1st week to 4th week was represented as fold change in radiance. Significance of difference in increase in tumour growth between mice injected with either

siGLO transfected or miR-204 mimic transfected D283 cells was calculated using Student's t test.

3.12 Extraction of Proteins from Cultured Cells

Reagents

10X phosphate-buffered saline (PBS): (1.5 M NaCl, 89.8 mM Na₂HPO₄·2H₂O, 28.8 mM NaH₂PO₄·2H₂O). 90 g NaCl, 16 g Na₂HPO₄·2H₂O, 4.5 g NaH₂PO₄·2H₂O per litre; pH adjusted to 7.5 with 5 N NaOH, autoclaved and stored at room temperature. 10 X stock was dilute to 1 X with autoclaved Milli-Q water and stored at room temperature.

Lamelli buffer or 1 X sample buffer: 62.5 mM Tris-HCl pH 6.8, 2 % SDS, 10 % glycerol.

Method

1. The medium was poured off from the culture plates and the cells were rinsed twice with 1X PBS gently.
2. The PBS was drained off completely and cells were lysed in 1 X sample buffer. About 0.5 – 0.6 ml sample buffer was used for protein extraction from 90 mm plates with 80-90 % cell density. The viscous lysate, due to release of genomic DNA along with proteins from the cells, was collected by swirling the plate several times and transferred into a 1.75 ml eppendorf tube.
3. The tubes were immediately kept in a boiling water bath for 7 min, cooled to room temperature and centrifuged in Rota-4 R at 15,000 rpm for 1.5 h at 20°C to pellet down the genomic DNA. The DNA pellets were discarded.
4. The supernatant lysates containing protein were carefully transferred to fresh tubes and stored at -20 °C until further use.

3.13 Estimation of Protein Concentration

The proteins extracted in sample buffer from cultured cells were estimated using this method. [67]

Reagents

1 mg / ml BSA: 10 mg BSA was weighed and dissolved in 1 ml autoclaved Milli-Q water to obtain a stock of 10 mg/ ml. This stock was further diluted 1:10 in water to obtain a working stock of 1 mg / ml. BSA stocks were stored at -20°C.

Solution A: Cu-tartrate CO₃ (CTC)

- a) 20 % Na₂CO₃: 20 g was dissolved in 100 ml Milli-Q water.
- b) 0.2 g CuSO₄ was dissolved in 40 ml Milli-Q water.
- c) 0.4 g potassium tartarate was dissolved in 40 ml Milli-Q water.

CuSO₄ and potassium tartarate were mixed (b + c) and the volume was made up to 100 ml with Milli-Q water. Final concentration of CuSO₄ is 0.2 % and potassium tartarate is 0.4 %. To this, 100 ml of 20 % Na₂CO₃ (a) was added slowly with constant stirring. This solution 'A' was stored in dark at room temperature.

Solution B: 10% SDS.

10 g of SDS was dissolved in 80 ml Milli-Q water, heated at 60 °C to assist dissolution. The final volume was adjusted to 100 ml and stored at room temperature.

Solution C: 0.8 N NaOH.

16 g of NaOH was dissolved in 100 ml of Milli-Q water, and the volume made up to 500 ml and was stored at room temperature (Note: Do not autoclave).

Reagent A: Prepared by mixing solutions A, B, C, and Milli-Q water in a proportion of 1:1:1:1 just before use. (Note: Mixing NaOH with 10 % SDS results in a glue like insoluble precipitate. Therefore dilute the SDS first in the required volume of water and then add NaOH and CTC to it.)

Reagent B: Folin-Ciocalteu reagent was diluted 1 + 5 in Milli-Q water just before use.

Method

1. 2 µl of protein sample to be estimated was diluted in 1 ml of Milli-Q water in duplicates.
2. BSA standards, ranging from 1 µg to 20 µg were prepared in duplicate by appropriately diluting from 1 mg/ml stock of BSA, in 1 ml of Milli-Q water. 2 µl of the sample buffer used for extraction of protein to be estimated was also added. “Blank” tubes were prepared by adding only 2 µl of the sample buffer.
3. 1 ml of freshly prepared reagent A was added to each tube, immediately mixed on a vortex mixer, and kept in dark at room temperature for 10 min. Then 0.5 ml of freshly diluted reagent B was added to each tube, immediately mixed on a vortex mixer and incubated in dark at room temperature for 30 min.
4. The absorbance of the blue colour developed was read at 750 nm against blank in a spectrophotometer (Shimadzu UV-160A, UV-visible recording spectrophotometer), and the concentration of the unknown protein samples was calculated by using the BSA standard plot

3.14 SDS-Polyacrylamide Gel Electrophoresis (SDS-PAGE).

The proteins extracted in sample buffer were separated by SDS-PAGE for western blotting.

[68]

Reagents

30 % acrylamide solution: 29.2 g acrylamide, 0.8 g bis-acrylamide were dissolved in approximately 50-60 ml autoclaved Milli-Q water and the final volume was made up to 100 ml. Solution was filtered through ordinary filter paper and stored in an amber colored bottle at 4 °C.

20 % SDS: 20 g SDS was dissolved in 80 ml of Milli-Q water, heated at 60 °C to assist the dissolution. The final volume was made up to 100 ml, and stored at room temperature.

1 M Tris pH 8.8 and pH 6.8: 60.55 g Tris was dissolved in 400 ml Milli-Q water. pH was adjusted to 8.8 and 6.8 with concentrated HCl, the final volume was made up to 500 ml with Milli-Q water and autoclaved. Solutions were stored at 4 °C.

10 X electrode buffer: 30 g Tris, 143 g glycine, 20 g SDS were dissolved in approx. 700 ml Milli-Q water and the final volume was made up to 1 L. Stock solution was diluted to 1 X with Milli-Q water before use (1 X buffer is 25 mM Tris, 190 mM Glycine, 0.2 % SDS).

0.5 % Coomassie Blue staining solution: 0.5 g of Coomassie Blue staining dye was dissolved in 50 ml of methanol (LR grade) by constant stirring. The final volume was adjusted to 100 ml by adding 40 ml of Milli-Q water and 10 ml of glacial acetic acid. The staining solution was filtered through filter paper and stored at room temperature for 1 month.

Destainer: Methanol (LR), glacial acetic acid (AR) and Milli-Q water mixed in the proportion 5:1:4 and stored at room temperature.

Loading Dye: 0.025 % Bromophenol Blue in 1 X Sample Buffer.

Method

- Two clean glass plates (one of which was notched), separated by 1.5 mm thick spacers were clamped together. The sides and the bottom of the plates were sealed using 2 % agar.

The resolving gel of the required percentage was prepared by mixing the following

Final concentration of acrylamide (gel percentage)	10 %	12 %
30% acrylamide solution	10 ml	12 ml
1 M Tris-HCl pH 8.8	11.2 ml	11.2 ml
20% SDS	0.15 ml	0.15 ml
Milli-Q water	8.65 ml	6.65 ml
TEMED	0.02 ml	0.02 ml
20% Ammonium persulphate (APS)	0.05 ml	0.05 ml

- The gel solution was poured between the two glass plates taking care to avoid air bubbles.

Water was carefully layered over the gel and it was allowed to polymerize (approximately 20 – 30 min).. Following polymerization, the water layer was removed and a 5 % stacking gel was prepared and overlaid over the resolving gel.

5 % stacking gel composition	
30 % acrylamide solution	1.67 ml
1 M Tris-HCl pH 6.8	1.75 ml
20 % SDS	0.10 ml
Milli-Q water	6.98 ml
TEMED	0.01 ml
20 % ammonium persulphate (APS)	0.025 ml

3. A comb of 1.5 mm thickness was inserted immediately into the stacking gel solution between the two plates to form wells. After polymerization of the stacking gel, the comb was gently removed and the wells were cleaned by flushing first with water and then with 1 X electrode buffer (using a syringe-needle). The gel plates were clamped to the electrophoresis unit and the upper and lower tanks were filled with 1 X electrode buffer.
4. The proteins to be resolved were mixed with 1 X sample buffer containing 5 % v / v BME and 0.01 % bromophenol blue, boiled for 3 min and loaded into the wells of the gel. Three couloured prestained protein ladder (Puregene) was loaded along with the protein as the molecular weight marker.
5. Electrophoresis was carried out at 22 mA constant current till the dye reached the bottom of the gel. The gel was removed carefully and either stained with Coomassie blue to check equal loading of the proteins or processed for western blotting as described later.
6. For Coomassie blue staining, the gel was stained by immersing it in 0.5 % Coomassie Blue staining solution for 2 h. The gel was washed several times in destainer until a clear background was obtained and then transferred to 50 % methanol for 2-3 h. The gel was dried between gelatin papers (pre-soaked in 50 % methanol) at room temperature for 24 h.

3.15 Western Blot Analysis and Immuno-detection

The proteins separated by SDS-PAGE, were transferred to a PVDF membrane by western blotting technique.

Reagents

1 X transfer buffer: 25 mM Tris, 192 mM Glycine, 20 % Methanol.

3 g Tris and 14.4 g Glycine were dissolved in Milli-Q water and volume was made up to 800 ml with Milli-Q water. 200 ml Methanol was added to make 1 L. Buffer was chilled to 4 °C before use. (1 L transfer buffer is sufficient for western blotting in Biorad's mini trans-blot electrophoretic transfer cell)

10 X Tris-buffered saline (TBS): 0.1 M Tris, 1.5 M NaCl

12.1 g Tris and 87.6 g NaCl were dissolved in Milli-Q water, pH was adjusted to 8.0 with concentrated HCl and the final volume was made up to 1 L. Solution was autoclaved and stored at room temperature.

1 X Tris-buffered saline with Tween-20 (TBST): 10 X TBS was diluted to 1 X with Milli-Q water (1 liter), 1 ml Tween-20 was added to the solution and kept on magnetic stirrer for 1 h.

Ponceau-S staining solution: (0.2 % Ponceau-S in 1 % glacial acetic acid)

SuperSignal[®] West Pico chemiluminescent substrate (Cat. No. 34077 Pierce Biotechnology)

Method

1. The protein samples to be blotted were resolved by SDS-PAGE and the gel was kept in 1 X transfer buffer for 15-20 min until the gel was free from the smell of β - mercapto ethanol (BME).
2. The PVDF membrane (Merck-Millipore), to be used for blotting, was cut to the size of the gel to be blotted. The membrane was pre-wet in methanol for about 30 seconds, kept in Milli-Q water for 10 min. to wash off excess methanol and then placed in 1X transfer buffer for 20 min. Two pieces of a Whatman 3mm filter paper little bigger than the size of the gel, were also cut.
3. The transfer assembly was prepared according to the manufacturer's instructions. The cassette was assembled in a tray containing 1 X transfer buffer by arranging the components in the following sequence: First the cassette was placed, with the gray side down in a tray containing transfer buffer. A Scotch-Brite pad was placed over the grey

portion of the cassette, and a piece of Whatman paper was placed over it. Then the transfer buffer equilibrated gel was carefully placed over the Whatman paper and the PVDF membrane was juxtaposed to the gel without trapping any air bubbles between the gel and the PVDF membrane. A small cut was given at one corner of the membrane and the gel for correct orientation. Another piece of Whatman paper and a Scotch-Brite pad were placed over the PVDF membrane. The cassette was closed firmly and locked with the white latch on top of the cassette, and slid into the grooves for holding the cassette in place with the black portion (gel side) towards the cathode (negative electrode) and the transparent portion (membrane side) towards the anode (positive electrode). This whole assembly was placed inside the tank containing transfer buffer, and the electrodes were connected to the power supply. Transfer was carried out at 45 mA constant current at 4 °C for 16 h.

4. After the transfer, the membrane was carefully removed from the cassette using a pair of forceps, rinsed once with Milli-Q water, and kept in destainer for 30 min (to aide in staining with Ponceau-S). Then the membrane was washed twice with TBST for 5 min each and stained with Ponceau-S till the protein bands were visible. The molecular weight marker positions were marked on the membrane with a soft lead pencil and then the Ponceau-S was completely removed by washing the membrane with TBST. It was either probed immediately or stored at 4 °C in TBST, for later use.
5. For probing, the membrane was first blocked with a 5 % milk solution prepared in TBST. The membrane was kept in the milk solution for 1 h at room temperature on a rocker with gentle shaking.
6. The blocking solution was drained off and the membrane was washed 3 times for 5 min each with TBST, on the rocker with vigorous shaking.

7. TBST was drained off completely and the membrane was incubated with appropriately diluted antibody, with gentle shaking on the rocker. The working conditions of various antibodies used is given below –

Name	Company	Type	Dilution	Duration
OTX2	Santacruz biotechnology	Anti-Rabbit polyclonal	1:200 in 2 % BSA	O / N at 4 °C
EZR	Cell signaling technology	Anti-Rabbit polyclonal	1:1000 in 5 % milk	O / N at 4 °C
RAB10	Cell signaling technology	Anti-Rabbit polyclonal	1:1000 in 5 % BSA	O / N at 4 °C
SirT1	Cell signaling technology	Anti-Rabbit polyclonal	1:1000 in 5 % BSA	O / N at 4 °C
FOXC1	Cell signaling technology	Anti-Rabbit polyclonal	1:1000 in 5 % BSA	O / N at 4 °C
LC3B	Cell signaling technology	Anti-Rabbit polyclonal	1:1000 in 5 % BSA	O / N at 4 °C
γ -tubulin	Sigma-Aldrich	Anti-Rabbit polyclonal	1:4000 in 5 % BSA	1 hr at R.T.

8. The antibody solution was drained off (or stored at –20 °C for those diluted in BSA), and the membrane was washed six times for 5 min each with 1X TBST, on the rocker with vigorous shaking.
9. Then the membrane was incubated with appropriately diluted horseradish peroxidase (HRP) conjugated secondary antibody (anti IgG) for 1 h at room temperature on the rocker with gentle shaking. Anti-rabbit and anti-mouse HRP-conjugated antibodies (Amersham) were diluted 1:1000 and 1:400 respectively in 2 % milk-TBST. The antibody solution was

drained off and the membrane was washed vigorously six times for 5 min each with 1 X TBST and then three times with 1 X TBS.

10. The excess buffer was drained off and the membrane was placed on a clean cling film and covered with chemiluminescence substrate(Super Signal West Pico from Pierce Biotechnology) for 5 min at room temperature
11. Quickly, the detection solution was drained off; the membrane was wrapped in cling film, placed in an X-ray film cassette and exposed to X-ray film (Ref no.4908364, Kodak Companies). The membrane was exposed to X-ray film for 1-2 min depending on the signal intensity. The signal was visualized after developing the X-ray film in the developing machine.

3.16 Immunohistochemical Analysis of Ezrin expression in Medulloblastoma Tumor Tissues

Reagents

Chromic Acid solution: Potassium dichromate (40 g, 920 ml Milli Q water, 80 ml Con. Sulphuric Acid)

40g Potassium dichromate was dissolved in 920 ml of Milli Q water in a glass beaker. The beaker was kept in ice. Slowly and carefully, 80 ml of con. Sulphuric acid was added to this solution.

Poly-L-Lysine solution: 1 mg / ml poly-l-lysine in sterile Milli Q water

Dissolve 50 mg of poly-L-Lysine (Sigma, Cat. No. P2636) in 50 ml sterile Milli-Q water. Add a pinch of sodium azide (0.02%)

1 M Citrate Buffer pH 6.0:

Take 58.82 g of trisodium citrate (LR) Qualigens. Dissolve in about 150 ml of Milli Q water. Adjust pH to 6.0 with 1 M Citric acid solution. [21. 01g for 100 ml]. Make up the volume to

200 ml. Autoclave both the buffer and citric acid solution. Before use, dilute 1M Citrate buffer 1 in 100 in sterile MQ water and check the pH again. If required adjust the pH with 1 M Citric acid.

10X phosphate-buffered saline (PBS): (1.5 M NaCl, 89.8 mM Na₂HPO₄·2H₂O, 28.8 mM NaH₂PO₄·2H₂O). 90 g NaCl, 16 g Na₂HPO₄·2H₂O, 4.5 g NaH₂PO₄·2H₂O per litre; pH adjusted to 7.5 with 5N NaOH, autoclaved and stored at room temperature. 10X stock was dilute to 1X with autoclaved Milli-Q water and stored at room temperature

Hematoxylin solution for counterstaining

Method

a) Pretreatment and poly-L-lysine coating of the slides:

1. MicroAid glass slides size 75 X 25 mm \pm 1 mm, thickness 1.2 mm \pm 0.1 mm were taken and dipped in chromic acid solution for 1 h. Slides were kept in running tap water for 1 h to remove chromic acid.
2. The acid treated glass slides were boiled in MQ water for 5 min at high power in a microwave oven. This procedure was repeated two-three times with fresh water. Excess water was drained on tissue paper and slides were air dried.
3. Slides were dipped in Poly-L-lysine solution (1mg/ml) and kept for coating for 15 minutes. Slides were dried in a slide jar overnight at 37°C. 5 μ m thick paraffin sections were collected on dry poly-lysine coated glass slides. Sections were separated using diamond marker and labeled appropriately.

b) Deparaffinisation of sections:

1. Sections were deparaffinised by dipping the slides sequentially in three glass Koplin jars filled with Xylene for 10 min each.

2. Slides were dipped for 5 min in Koplin jar filled with fresh 100% alcohol. Slides were transferred to a second Koplin jar containing fresh 100% alcohol and again dipped for 5 minutes.
3. For inhibiting endogenous peroxidases, slides were dipped in Koplin jar containing 50 ml of fresh methanol and 500 µl of H₂O₂ for 15 minutes.
4. Sections were rehydrated by passing the slides through an alcohol gradient (100% alcohol, 70% alcohol and 50% alcohol) and finally rinsing them with Milli Q. Sections were incubated for 5 min in each alcohol concentration.
- 5.

c) Antigen retrieval by microwave method:

1. Slides were kept in a glass or plastic slide box filled with 400 ml of 10 mM Citrate buffer pH 6.0. Buffer level was marked on the box.
2. The slides were boiled in Microwave for 5 min at high power, twice. Slide box was removed from the microwave and kept at room temperature for 5 min. The lost volume of the buffer was made up with Milli Q water.
3. The slides were again boiled in a microwave at low power (90°C) for 5 min, twice and the slide box was taken out and kept at room temperature for 20 min.
4. Slides were then given three washes of 1X PBS for 5 min each.

d) Immunohistochemistry

1. For blocking non specific binding, each tissue section was covered with 100 µl of 3% BSA prepared in 1X PBS and incubated for 30 min.
2. Two washes of 1 X PBS were given to sections for 5 min each.
3. Sections were covered with anti-Ezrin rabbit polyclonal antibody (Cell signaling) that was diluted 1:100 in 1% BSA, prepared in 1X PBS. The slides were incubated overnight in a humidified chamber kept in a refrigerator.

4. Next day, antibody solution was drained off carefully and two quick rinses of 1X PBS were given to slides by putting PBS directly onto the sections.
5. 5 X 5 min washes of 1X PBS in a Koplins jar were given to remove non-specifically bound primary antibody.
6. Sections were covered with HRP-conjugated anti rabbit secondary antibody (Thermo scientific) and were incubated for two hours at room temperature. Secondary antibody was diluted 1:100 in 1% BSA.
7. 5 X 5 min washes of 1X PBS were given to remove nonspecifically bound secondary antibody.
8. Sections were further treated with 1mg/ml Diaminobenzidine (Sigma) in PBS and 1 μ l/ml H₂O₂ for 10 min. Reaction was terminated by giving five quick rinses with lots of Milli Q water. DAB is carcinogenic, care was taken while handling. DAB was inactivated by adding sodium hypochlorite.
9. Sections were counterstained with haematoxylin. Haematoxylin solution was filtered before use. Fresh haematoxylin was layered on the sections for 1 min. The nuclei stained light blue in colour.
10. The sections were dehydrated by passing through series of alcohol gradients (50%, 70% and 100% followed by xylene for 5min each). The sections were then mounted in DPX mountant.
11. The slides were observed under light microscope and images were captured on Olympus upright microscope using Axiocam software (Olympus).

3.17 Genome wide Expression Profiling of miR-204 Expressing Daoy and D283 cells

The changes in the gene expression profile of miR-204 expressing Daoy and D283 cells were studied for identification of direct targets of miR-204 in medulloblastoma cells. The gene

expression profiling was carried out using the Whole-Genome Gene Expression Direct Hybridization Assay (WGGEX direct hybridisation assay, Cat. No.BD-901-1002, Illumina, San Diego, USA)

PART A: Sample labelling using the Ambion Illumina Total Prep RNA Amplification kit (Cat. number: AMIL1791)

Reagents (provided with the kit)

T7 Oligo(dT) Primer, 10X First Strand Buffer, dNTP Mix, RNase Inhibitor, ArrayScript™ 10X Second Strand Buffer, DNA Polymerase, RNase H, T7 10X Reaction Buffer, T7 Enzyme Mix, Biotin-NTP Mix, Nuclease-free Water, Wash Buffer (Add 24 mL 100% ethanol before use), cDNA Binding Buffer, cRNA Binding Buffer

Materials

cRNA Filter Cartridges, cRNA Collection Tubes, cDNA Filter Cartridges + Tubes, cDNA Elution Tubes

Other requirements

1. 100% Ethanol (to prepare the Wash Buffer), ACS reagent grade or equivalent proof
2. Thermal cycler with a temperature-adjustable heated lid or hybridization ovens or incubators set at 70°C, 42°C, 37°C, and 16°C.
3. Heat block set at 55°C, for preheating the water for cDNA and RNA purification
4. Vacuum centrifuge concentrator
5. Vortex mixer
6. Microcentrifuge

All the procedures were performed using RNase-free eppendorf tubes and pipette tips. Precise incubation times were followed throughout the procedure.

Reverse Transcription to Synthesize First Strand cDNA

Pre-preparation:

1. Total RNA was extracted from tissue cultured cells using the RNeasy mini kit .The RNA was quantitated using the Nanodrop spectrophotometer and its integrity was verified by running it on a RNA gel.
2. 24ml 100% ethanol to the wash buffer bottle. It was mixed well and labelled to indicate addition of ethanol.
3. The following program was set on the PCR machine

Temperature	Time	Cycle
42°C (50°C lid)	2 Hr	1
4°C	Hold	

Method

1. 500 ng of total RNA was added to a 0.5 ml eppendorf tube and the total volume was made upto 11 µl
2. The Reverse Transcription Master Mix was prepared at room temperature in a nuclease-free tube. The required volumes for one reaction and the order of addition are shown in the table below. Multiply the number of reactions being performed by the volume of the component in the table, and by 1.05 to account for the necessary overage. The tubes were mixed well by gentle vortexing followed by a quick spin to collect the contents of the tube at the bottom. The tubes were then placed on ice.

Component	Volume for 1 reaction
T7 Oligo(dT) primer	1 µl
10X first strand buffer	2 µl
dNTP mix	4 µl
RNAse inhibitor	1 µl
Arraysript™	1 µl

3. 9 μL of Reverse Transcription Master Mix was added to each RNA sample and mixed thoroughly by pipetting up and down 2–3 times, flicking the tube 3–4 times followed by a quick spin to collect the contents of the tube at the bottom. Place the samples in the thermal cycler. Incubate for 2 hr at 42°C.

Second strand cDNA Synthesis

Pre-preparation:

The thermal cycler was programmed as follows. The lid was heat disabled.

Temperature	Time	Cycle
16°C (Heat disable lid)	2 hr	1
4°C	Hold	

Method

1. On ice, the second strand master mix was prepared in a 1.5 ml nuclease-free tube. By adding the components in the order listed below. Multiply the number of reactions being performed by the volume of the component in the table, and by 1.05 to account for the necessary overage. Mix well by gently vortexing. Centrifuge briefly (~5 sec) to collect the mixture at the bottom of the tube and place on ice.

Component	Volume for 1 Reaction
Nuclease free water	63 μl
10X Second strand buffer	10 μl
dNTP mix	4 μl
DNA polymerase	2 μl
RNase H	1 μl

2. 80 μ L of Second Strand Master Mix was added to each sample. The contents were thoroughly mixed by pipetting up and down 2–3 times, then flicking the tube 3–4 times, and centrifuge briefly to collect the reaction in the bottom of the tube.
3. The tubes were placed in a 16°C thermal cycler and the run was started. It is important to cool the thermal cycler block to 16°C before adding the reaction tubes because subjecting the reactions to temperatures >16°C will compromise cRNA yield.

After the 2 hr incubation at 16°C, the reactions were placed on ice. At this point, the reactions can be immediately frozen at –20°C. They should not be left on ice for more than 1 hr.

cDNA purification

1. The heating block was set at 55°C before beginning the procedure. 250 μ l of nuclease free water was placed at 55°C for heating.
2. 250 μ l of cDNA binding buffer was added to each sample and mixed thoroughly by pipetting up and down.
3. The cDNA filter cartridge was placed in the wash tube and 350 μ l of each sample-buffer mix is added onto the cartridge and centrifuged at 12000 rpm for 1 min. The flow-through was discarded and the cartridge was replaced into the same wash tube.
4. 500 μ l of wash buffer was added to the cartridge and centrifuged at same speed for 1 min ensuring that filter is devoid any remnants of the wash buffer. The flow-through was discarded and the tube was spun for additional 1 min. The filter cartridge was now transferred into the cDNA elution tube.
5. 20 μ l of nuclease free water (pre-warmed to 55°C) was added to the centre of the filter cartridge and incubated for 2 min at RT and then centrifuged for 1 min at 12000 rpm. The double-stranded cDNA will now be in the eluate (~17.5 μ L). The purified cDNA can be stored overnight at –20°C at this point if desired.

In Vitro Transcription (IVT) to Synthesize cRNA

1. The following program was set on the thermal cycler

Temperature	Time	Cycle
37 °C (lid at 105°C)	14 hr	1
4 °C	Hold	

2. Each cDNA sample (~17.5 µl) was added to a 0.5 ml eppendorf tube.
3. The IVT mastermix was prepared at room temperature in a 0.5 ml eppendorf tube in following manner.

Component	Volume for 1 reaction
T7 10X reaction buffer	2.5 µl
T7 Enzyme Mix	2.5 µl
Biotin-NTP mix	2.5 µl

4. 7.5 µl of IVT mastermix was added to each cDNA sample and mixed well by pipetting. It was then incubated in the thermal cycler at the set program for 14 hr.
5. The reaction was stopped by adding 75 µl of Nuclease free water to each tube to bring final volume to 100 µl.

cRNA Purification

1. 200 µl of nuclease free water was preheated to 55 °C.
2. 350 µL of cRNA Binding Buffer was added to 100 µl of each cRNA sample.
3. 250 µL of ACS reagent grade 100% ethanol was added to each cRNA sample and mixed by pipetting the mixture up and down 3 times. Do not vortex to mix and do not centrifuge.
4. The sample mixture was immediately added onto the centre of the filter in the cRNA filter cartridge and centrifuged for ~1 min at 12,000 rpm. This was continued until the mixture

had passed through the filter. The flow-through was discarded and the cRNA filter cartridge was placed back into the cRNA collection tube.

5. 650 μ L Wash Buffer was added to each cRNA Filter Cartridge and centrifuge for \sim 1 min at 12,000 rpm, or until all the Wash Buffer passed through the filter. The flow-through was discarded and the cRNA Filter Cartridge is spun for an additional \sim 1 min to remove trace amounts of Wash Buffer. The Filter Cartridge was then transferred to a fresh cRNA Collection Tube
6. 200 μ L of Nuclease-free Water (preheated to 55°C) was added to the centre of the filter and the tubes were incubated in the 55°C heat block for 10 min. The tubes were then centrifuged for \sim 1.5 min at 12,000 rpm, or until the Nuclease-free Water is through the filter. The cRNA is now in the cRNA Collection Tube in \sim 200 μ L of Nuclease-free Water.
7. The cRNA concentration was determined using the Nano-drop spectrophotometer. The size distribution of cRNA was evaluated using an Agilent 2100 bioanalyzer and by conventional denaturing agarose gel analysis.

PART B: Hybridisation of the bead chip and detection of signal using the Illumina HumanHT-12 v4 Expression BeadChip Kit

Reagents (provided with the kit)

HumanHT-12 v4 BeadChips , Wash E1 BC Buffer , BeadChip Tweezers, Wash Trays and Wash Tray Lids, High-Temperature Wash Buffer, Blocking E1 Buffer, Hybridization E1 Buffer (HYB), Humidity Control Buffer (HCB)

Other requirements:

100 % ACS grade ethanol, DEPC treated water, Two 1L glass measuring cylinder, 1L glass beaker, 500 ml glass bottle, 2 L glass bottle, 10 ml disposable serological pipettes, Slide rack with handle, Glass staining plates, Cy3-Streptavidin (company catalogue no), BeadChip

Hybridisation Chamber with gasket and inserts (Illumina), Hybridisation oven (Illumina), Hi-scan array scanner

All the glassware used was first treated with acid, thoroughly cleaned with water, followed by treatment with DEPC containing water. It was then sterilised at 180 °C for 1.5 hrs before use.

Method

1. The hybridization oven was preheated to 58°C and allowed to equilibrate for 30 min.
2. The HYB and HCB tubes were incubated at 58⁰C to dissolve the salt precipitates formed during storage. The bead chips were also removed from the cold storage and allowed to reach room temperature.
3. The cRNA sample tube was preheated at 65°C for 5 minutes. It was vortexed briefly and pulse centrifuged. The cRNA tube was allowed to cool to room temperature.
4. The cRNA-HYB buffer mix was made by adding 750 ng of cRNA with a total volume of 5 µl with 10 µl of HYB and mixed by pipetting up and down.
5. The bead chip hybridization (HyB) chamber was assembled as per the instructions given in the manual and 200µl of HCB was added in the eight humidifying buffer reservoirs in the Hyb Chamber. The BeadChip Hyb Chamber lid was closed and locked. It was left on the benchtop until the beadchips were loaded.
6. The beadchip was removed from the package and placed in the HyB chamber orienting the barcode end so that it matches the barcode symbol on the Hyb Chamber Insert. 15 µl of the cRNA-HYB mix was loaded on the beadchip from the sample inlet port ensuring that there is no bubble formation and that the sample covers all sections of the strip.

7. The 4 Hyb Chamber Inserts containing sample-laden BeadChips were loaded into each Hyb Chamber. The barcode end is positioned over the ridges indicated on the Hyb Chamber. Secure seating of the inserts was ensured.
8. The Hyb Chamber was then placed into the 58°C Illumina Hybridization Oven so that the clamps face the left and right sides of the oven and the Illumina logo on top of the Hyb Chamber facing you. The BeadChips were incubated for 14 hours at 58°C.
9. The high temperature wash buffer was made on the same day. The water-bath is set at 55°C and allowed to equilibrate for 30 min. 50 ml of 10X High temp-wash buffer was added with the help of a 10 ml serological pipette to a 500 ml glass cylinder. The volume was made up to 500 ml using DEPC treated water. The 1X High temp-wash buffer was then transferred to a 500 ml glass bottle and incubated overnight in the water bath at 55°C.
10. On the next day, 6 ml of E1BC buffer was added to 2 L DEPC treated water to make the Wash E1BC solution. 1 L of diluted Wash E1BC buffer was added to a 1 L glass beaker. 250 ml of Wash E1BC buffer was poured into two glass wash trays. 250 ml of 100% EtOH was poured into a separate glass wash tray and 250 ml of the high temperature was poured into a third staining dish and again placed in the water bath.
11. Using powder-free gloved hands, one beadchip was removed at a time from the Hyb Chamber and submerged face up at the bottom of the beaker containing the Wash E1BC buffer. Using powder-free gloved hands, the coverseal was removed from the first BeadChip under the buffer. The entire BeadChip remained submerged during removal of the seals. Using tweezers or powder-free gloved hands, the BeadChip was transferred into the slide rack submerged in the staining dish containing 250 ml Wash E1BC solution. This is the staging area to hold the BeadChips until all coverseals have been removed under the buffer.

12. Using the slide rack handle, the rack was transferred into the staining dish containing High-Temp Wash buffer placed in the waterbath at 55°C. It was Incubated static for 10 minutes. The rack was immediately transferred back into a staining dish containing 250 ml fresh Wash E1BC buffer. Using the slide rack handle, the rack was plunged in and out of the solution 5–10 times. The staining dish was placed on an orbital shaker on medium-low speed at room temperature for 5 minutes.
13. Transfer the rack to a new staining dish containing 250 ml fresh 100% Ethanol. Using the slide rack handle, the rack was plunged in and out of the solution 5–10 times. The staining dish was then shaken on the orbital shaker at room temperature for 10 minutes. It was then transferred to the same staining dish containing 250 ml Wash E1BC buffer and plunged in and out of the solution 5–10 times. It was again shaken on an orbital shaker at room temperature for 2 minutes.
14. The BeadChip was then placed in the wash tray on the rocker mixer and 4 ml Block E1 buffer was added to it. Using tweezers, the BeadChip was transferred face up into the BeadChip wash tray and rock at medium speed for 10 minutes.
15. 2 ml Block E1 buffer with a 1:1,000 dilution of Cy3-Streptavidin (stock of 1 mg/ml) was prepared for each BeadChip in a glass wash tray. The BeadChip was transferred to the wash tray containing Cy3-Streptavidin and covered with the flat lid. The tray was then rocked on medium for 10 minutes.
16. The bead chip was then washed with the E1BC buffer following the same procedure as in step 13.
17. The rack of BeadChip was transferred from the staining dish to a plate centrifuge. It was centrifuged at 1,400 rpm at room temperature for 4 minutes to dry the bead chips.

18. The bead chip was then scanned using the standard settings on the hi-scan system from illumina. The .dmap and .idat files specific for the beadchip were used to annotate the beads on the chip.
19. The data was analysed using the genome studio software ensuring that all controls including the Housekeeping genes, Cy3 Hybridisation control, Low Stringency Hybridisation control, Biotin controls and Negative controls were appropriate.
20. The background was subtracted and the data was normalised using the average normalisation method. The significance analysis for microarray (SAM analysis) for differentially expressed genes was carried out using the MeV module of the TM4 package.
21. Genes were selected for further analysis as direct targets of miR-204 on the basis of the following criteria-
 - a. The top differentially expressed genes found to have downregulation of expression in the miR-204 expressing cells as studied by the gene expression analysis
 - b. Putative direct targets for miR-204 identified using the Targetscan miRNA target prediction software consisting of conserved miR-204 binding sites in their respective 3' UTR region.
22. The downregulation of a select set of genes was carried out by real time RT-PCR analysis. CDNA synthesis was carried out using random primers as described in section 3.5. Real time PCR was carried out using the SYBR green chemistry as described in section 3.7. The table 3.1 shows the sequences of primers used for the realtime PCR.

Gene name	Primer	Sequence (5' to 3')
<i>RAB22A</i>	F	TGTAAGAGAAGTCATGGAGAGAGAT
	R	CAGGTTGGCGTCAGTGGAT
<i>M6PR</i>	F	CAGTTTCCCACGACACGATG

	R	GCCAGGAGTAGTAGTAGCA
<i>EDEM1</i>	F	AAGAAGAGGGCGGGAAGC
	R	CGTTGACATAGAGTGGAGGG
<i>APIS2</i>	F	CAGGAGGATGCGAAAGAAGC
	R	TCATCAACAAGGGAGGAGAGT
<i>EZR</i>	F	TGGATAGTCGTGTTTTTCGGGG
	R	TGGTTTCGGCATTTTCGGTTTCTG
<i>BCL2L2</i>	F	GCCGCCTTGTAGCCTTCT
	R	AGCTGTGAACTCCGCCCA
<i>RAB10</i>	F	CGAAAGACCCCTGTAAAAGAGC
	R	GTGGATGGCAACTGATGGAAC

Table 3.1: List of primers used for real time RT-PCR analysis of miR-204 target genes.

F: Forward, R: Reverse primer.

3.18 Luciferase Reporter Assay

3'-UTR of each of the potential miRNA target genes was amplified from genomic DNA of normal human peripheral blood lymphocytes using Phusion Taq polymerase. The 3'-UTRs were then cloned downstream of firefly luciferase cDNA from pGL3 vector in a pcDNA 3.0 plasmid vector. The genomic region encoding miR-204 was cloned into pGIPZ plasmid vector. The pGIPZ vector now had the miR-204-IRES-turboGFP cassette under CMV promoter. HEK 293T cells were transfected with the luciferase reporter plasmid and either the miR-204-pGIPZ vector or the pGIPZ empty vector using calcium phosphate BES buffer method. Luciferase activity was assessed from the total protein extracted from the transfected HEK293T cells and was normalized against the turboGFP fluorescence.

3.18.1 Generation of Vector Constructs for the 3'UTR Luciferase Reporter assay.

Reagents

Plasmids: pcDNA3.0 (Invitrogen, Life Sciences, Carlsbad, CA, USA); pGL3Basic ((Promega, Madison, WI, USA) and pGIPZ (Open biosystems, Thermo fisher scientific)

Enzymes: Phusion Taq Polymerase, T4 DNA Ligase, standard Taq Polymerase, Restriction enzyme

3'UTR Luciferase Reporter vector: Firefly Luciferase cDNA fragment was removed from pGL3basic vector by using restriction digestion using the HindIII and BamHI enzymes and was ligated into pcDNA3.0 digested with similar restriction enzymes. This created a vector cassette where the MCS from pcDNA3.0 lies downstream to the luciferase cDNA. This vector was used for the cloning of the 3' UTR regions of putative miR-204 gene targets downstream to firefly luciferase cDNA.

3'UTR Luciferase Reporter constructs for putative gene targets: Primers (Table 3.2) with desired restriction sites at their 5' end were designed to amplify 3'UTRs of putative miR-204 target genes namely *ANGPTL2*, *RAB10* and *NRPI* or the known miR-204 target gene *EZR*. 3'UTRs were amplified using Taq polymerase and digested with the appropriate combination of restriction enzymes. These digested amplicons were then ligated into the 3'UTR luciferase reporter vector digested with similar combination of restriction enzymes, using T4 DNA ligase.

Name of the Gene	Primer	Sequence (5' to 3')
EZR	F	CTCGAATTCTAGGAACTCCCTCAGATCCC
	R	ATTCTAGACTGCGGCATGGAATCCACCT
ANGPTL2	F	GGTGAATTCTGTCCCTCCTACTTTCCT
	R	GCACTCGAGGCTTTTATTGCAGATTCGTGTCAT

RAB10	F	TTGGAATTCTGGAAGCATGTGCAGGAGAC
	R	TCCCTCGAGACTTACAGAAAAGGGGCAAAGC
RAB10-SDM	F	CTGCACTTTCTAAATATCAAAAAATCGAAATGAA-GTATAAATCAATTTTGTATAATCTG
	R	CAGATTATACAAAAATTGATTTATACTTCATTTTCG-ATTTTTTGATATTAGAAAGTGCAG

Table 3.2: List of primers for PCR amplification and cloning of 3'UTR regions of putative miR-204 target genes.

F: Forward, R: Reverse primer.

pGIPZ-miR-204: Primers were designed to amplify miR-204 coding genomic region covering at least 200 bp on either side of pri-miR-204 sequence. Amplicon corresponding to 670 bp was amplified using Phusion polymerase and digested with HpaI and XhoI restriction enzymes. This was then ligated with a pGIPZ vector digested with the same enzymes.

Mutant *RAB10* 3'UTR luciferase reporter construct: The miR-204 binding site in the *RAB10* 3'UTR was mutated to yield non-functional binding site by using site directed mutagenesis (SDM) PCR. Nucleotides 5'-AAAGGGA- 3' from wild type miR-204 binding site in *RAB10* 3'UTR were mutated to 5'-AAATCGA-3' making it incapable of binding to mature miR-204. The change in the sequence was confirmed by sequencing.

Method

1. Primers were designed to have (a) T_m more than or equal to 78°C . (b) Primers designed with desired mutation at the centre (c) reverse primer should be exactly complimentary to forward primer, (d) GC content of more than 40% and the primer terminating in G or C.
2. A 50 μl PCR reaction was set up as follows

Components	Volume per 10 μ l Reaction	Final Concentration
5XHF/GC buffer	2 μ l	1X
10 mM dNTPs	0.2 μ l	2 mM
10 pmol/ μ l Forward primer	0.2 μ l	2 pmol
10 pmol/ μ l Reverse Primer	0.2 μ l	2 pmol
Template (vector DNA)	20 ng	-
Phusion Taq Polymerase	0.2 μ l	
DMSO (optional)	0.4 μ l	4%
Autoclaved Milli-Q	Make up to 10 μ l	

The PCR reaction conditions were as follows

Temperature	Time	No. Of. Cycles
98 ⁰ C	3 min	1
98 ⁰ C	1 min	20
56-62 ⁰ C (variable)	45 sec	
72 ⁰ C	1min per kb	
4 ⁰ C	∞	

3. PCR product was digested with DpnI restriction enzyme. The reaction conditions were as follows

Components	Volume	Final Concentration
10X Tango buffer	5 μ l	1X
PCR product	40 μ l	100-200 ng

DpnI (10 U/ μ l)	1 μ l	
Autoclaved Milli-Q	Make up volume to 50 μ l	

4. Reaction mixture was incubated at 37⁰C for 12-16 hr and was inactivated at 80⁰C for 20 min.
5. 5 μ l of PCR product before and equivalent PCR product after DpnI digestion was loaded on 1% agarose gel to ensure persistence of full length PCR product post DpnI digestion.
6. 10 μ l of DpnI digested DNA was transformed in DH5 α competent cells.
7. Plasmid DNA was extracted from 10 DH5 α colonies by alkaline lysis method.
8. The presence of the mutation was confirmed by sequencing of the plasmid DNA.

3.18.2 Luciferase Assay

Reagents

Cell lysis buffer

Components	Volume	Final Concentration
1 M Glycine-glycine pH 7.8	1.25 ml	25 mM
1M MgSO ₄	0.75 ml	15 mM
250 mM EGTA	0.8 ml	4 mM
Triton X-100	0.5 ml	1% (v/v)
100 mM DTT	*	1 mM
Autoclave Milli-Q	Make up to 50 ml	

Luciferase Assay Buffer

Components	Volume	Final Concentration
1 M Potassium phosphate buffer pH 7.8	0.75 ml	15 mM
1 M Glycine-glycine pH 7.8	1.25 ml	25 mM
1 M MgSO ₄	0.75 ml	15 mM
250 mM EGTA	0.8 ml	4 mM
100 mM ATP	*	2 mM
100 mM DTT	*	1 mM
Autoclave Milli-Q	Make up to 50 ml	

(*Note- Add DTT and ATP just before use)

Luciferin Solution

Components	Volume	Final Concentration
1M Glycine-glycine pH 7.8	1.25 ml	25 mM
1M MgSO ₄	0.75 ml	15 mM
250 mM EGTA	0.8 ml	4 mM
20 mM D-Luciferin	*	0.2 mM
100 mM DTT	*	2 mM
Autoclave Milli-Q	Make up to 50 ml	

(*Note- Add DTT, ATP and D-Luciferin just before use)

Method

1. HEK293 cells were trypsinised, counted and seeded as 1×10^4 cells per well of 96 well late

2. 24 hr post seeding, transfection of total of 0.3 μ g DNA per well of 96 well was done using BES buffer method. (Refer section 3.11)
3. DNA mixture was prepared in autoclaved Milli-Q as given below.

Component	Amount (for one well of 96 well plate)
3'UTR reporter plasmid	20 ng
pGIPZ / pGIPZ-miR-204	280 ng
Autoclaved Milli-Q	2.5 μ l
0.5M CaCl ₂	2.5 μ l
2X BBS	5 μ l

4. 72 hr after transfection, medium was removed and cells were washed twice with ice cold 1X PBS.
5. 30 μ l of cell lysis buffer was added to each well of a 96 well plate. The cells were scraped from the plate and lysate was made homogenous by pipetting it up and down several times. The lysate was transferred to an eppendorf tube and stored on ice till the lysates for all the wells are prepared.
6. The eppendorf tubes were centrifuged at 16000 rpm at 4⁰C for 5 min and the supernatant was transferred to fresh eppendorf tubes.
7. The fluorescence and luminescence was measured using Mithras LB940 multimode reader. 10 μ l of sample was added per well of 384 well Optiplate (Cat No. 6007290, Perkin Elmer), and fluorescence was measured at excitation and emission wavelengths of 485 nm and 515 nm. Each sample was assayed in duplicates.

8. 30 µl of assay buffer containing luciferin solution (2:1) was added to each sample and mixed twice by pipetting. The luminescence was read immediately at an exposure time of 1 sec.

3.19 Sodium Bisulphite Treatment of Genomic DNA and Sequencing of the PCR Amplified Gene Fragments

Treatment of genomic DNA with sodium bisulphite results into the conversion of demethylated cytosines in the genomic DNA to thymidine. On the other hand, the methylated cytosines remain as cytosines resisting the sodium bisulphite treatment. This bisulphite converted DNA is used as a template for PCR amplification using bisulphite specific primers. The PCR products are then sequenced to determine the methylation status of the CpG dinucleotides.

Primer designing: Bisulphite converted DNA sequence of the normal genomic DNA sequence corresponding to the concerned genomic region was obtained using the ‘Bisearch’ online software (<http://bisearch.enzim.hu/>). Primers were manually designed to amplify a region of the CpG island such that (1) they include the least possible number (1-2) of CpG dinucleotides in the normal genomic region (2) The amplicon size does not exceed 300 bp and (3) T_m of primers is equal to or greater than 55⁰C and is within 3⁰C of each other. Quality and specificity of PCR primers was checked using OligoAnalyser 1.5 (www.genelink.com) and ePCR feature of Bisearch online software.

Extraction of genomic DNA from medulloblastoma cell lines

Genomic DNA from medulloblastoma cell lines (5x 10⁶ cells) and 25-30 mg fresh frozen tissue was isolated by using Qiaamp DNA mini kit as per the manufacturer’s instructions.

Bisulphite conversion of DNA

Bisulphite conversion of 500 ng genomic DNA isolated from cultured cells or fresh frozen tumour tissues was performed, using EZ DNA Methylation-Gold Kit from Zymo Research,

as per the manufactures instructions. Primer sequences are as given in Table 3.3. Two reverse primers were used since that region constituted of one CpG dinucleotide to enable amplification of either a methylated or an unmethylated DNA sequence.

Gene name	Primer	Sequence (5' to 3')
miR-204 Bisulphite	F	GGGTGGAGAGTAATTTGGGG
	R 1	CGAATCTCCCTCCAACCTA
	R 2	TGAATCTCCCTCCAACCTA

Table 3.3: Primer sequences used for Bisulphite PCR.

F: Forward, R1 and R2: Reverse primer.

PCR Amplification

The reaction was made as follows

Components	Volume	Final Concentration
10X standard Taq buffer	1 μ l	1X
10 mM dNTP mix	0.2 μ l	0.2 mM
Forward primer (10 pmol/ μ l)	0.3 μ l	3 pmol
Reverse primer 1 (10 pmol/ μ l)	0.3 μ l	3 pmol
Reverse primer 2 (10 pmol/ μ l)	0.3 μ l	3 pmol
Taq Polymerase (1 U/ μ l)	0.25 μ l	0.25 U
Genomic DNA		25 ng
Autoclaved Milli-Q water		Make up volume to 10 μ l

PCR Conditions were as follows

Temperature	Time	Cycles
98°C	3 min	1
98°C	30 sec	30
Annealing temperature	45 sec	
72°C	30 sec	
72°C	5min	1

The PCR product was purified using the PCR product purification kit from Qiagen.

Sequencing of the PCR products

In a 0.2 ml PCR tube, 1.5 pmol of either forward or reverse primer and 5-10 ng of purified PCR product were added. The sequencing reactions were carried out in Eppendorf Master Cycler using Big Dye Terminator Kit V 3.1, which has different fluorescent dye for each terminator ddNTP as per manufacturer's instructions. The reactions were cleaned up to remove excess salt. The reactions were run in either a 50 cm or 80 cm capillary filled with POP4 or POP6 polymer (Applied Biosystems, U.S.A) in 3100 Avant Genetic Analyzer (Applied Biosystems, U.S.A). The size of capillary used depended on the PCR product size.

3.20 Survival Analysis for Group 3 and Group 4 Tumors using miR-204 as a Predictor

Event for overall survival was calculated from the date of surgery until death or last follow-up date. The survival data was divided into two groups (high vs. low expression) based on the Average expression value + Confidence Interval (CI) for the normal cerebellum samples as the cut-off. Hazard ratio and its 95 % confidence interval were computed using the Mantel-

Haenszel method in GraphPad Prism v 5.0. Survival percentages were estimated by Kaplan-Meier method and statistical significance between the survival curves was estimated by log-rank test using Graph Pad Prism software.

3.21 Statistical Analysis

The statistical analysis of the data including the student's t-test wherever indicated, the chi square test for the immunohistochemical analysis for ezrin expression in medulloblastoma tumor tissues across the molecular subgroups was carried out using the Graphpad prism 5.0 software.

RESULTS AND DISCUSSION

4.1: Molecular Subgrouping of Medulloblastoma Cell Lines

In order to identify the subgroup affiliation of available medulloblastoma cell lines, the expression of subgroup specific marker genes was studied in the Daoy, D283, D425, D341 and D384 cell lines. Molecular subgrouping of medulloblastoma tumor tissues has been carried out on the basis of differential expression of 12 protein coding genes [15]. Concomitant overexpression of the *WIFI*, *DKK2*, and *MYC* genes is used as a marker for WNT medulloblastomas. Overexpression of *HHIP*, *EYAI* and *MYCN* genes in addition to the underexpression of *OTX2* serve as markers for the SHH subgroup. The overexpression of *EOMES* helps in the identification of Group 3 and Group 4 tumours, while higher expression of *NPR3*, *MYC*, and *IMPG2* and lower expression of *GRM8* and *UNC5D* helped to distinguish Group 3 from Group 4 tumours. Hence, the expression of some of these marker genes in the medulloblastoma cell lines (*viz* Daoy, D283, D425, D341 and D384) was studied by real time RT-PCR analysis. All the cell lines show very low expression of *WIFI*, *MYCN*, *EOMES*, and *GRM8* marker genes (Figure 4.1.1). The expression of the *HHIP* gene is about 10 fold higher in Daoy cells as compared to the other cell lines while that of *OTX2* is 100-1000 fold lower in Daoy cells as compared with the other cell lines as well as the WNT, Group 3 and Group 4 tumors. Also, the Daoy cell line is derived from a tumor with desmoplastic histology and shows chromosome 9 alteration (Table 4.1.1) [69]. The desmoplastic histology and chromosome 9q loss are strongly associated with the SHH pathway tumours [8]. This indicated that the Daoy cell line most likely belongs to the SHH subgroup of medulloblastoma. The ‘D’ series of cell lines D283, D425, D341 and D384 were established at the Duke university (hence the name ‘D’ series) [30,70,71]. These cells show high expression of *OTX2* (R.Q. = 7-27), *MYC* (R.Q. = 50-500) and *IMPG2* (R.Q. = 30-100).The

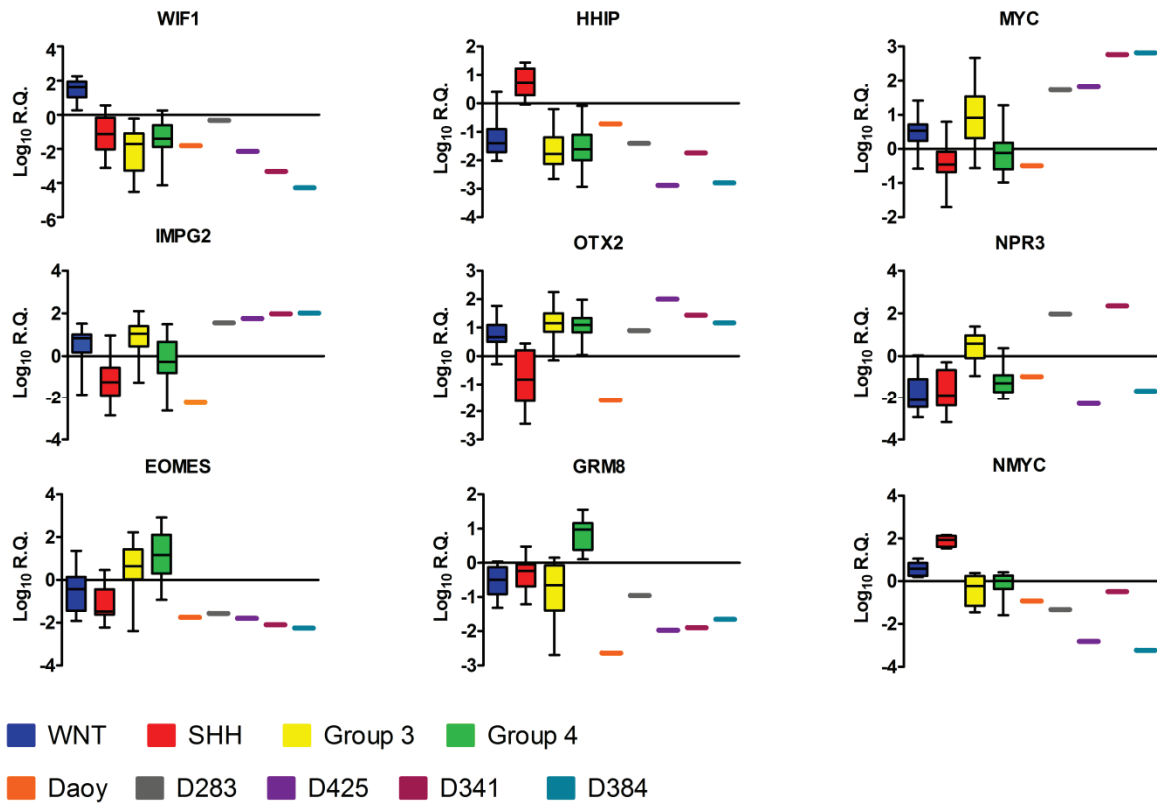


Figure 4.1.1: Expression of subgroup specific marker genes in medulloblastoma cell lines.

The box and whisker plot shows the expression level of the indicated genes in the four subgroups of medulloblastoma and in the medulloblastoma cell lines. The Y-axis represents Log₁₀ of the relative quantity of expression using RNU48 as the control.

No	Cell line	Karyotype [30, 69].
1	Daoy	t (1q5q), t (13q ;?)15p+,7q+, der(9)t(3;9)(p21;q34)
2	D283	der(20)t(1;20)(q12;q13), 8q+ and i(17q)
3	D341	49, XY, + 6, + 8, + 18, -22, + lp, i(17q) , + DMs
4	D384	46, XY, - 8, i(17q) , + 8q +, + DMs
5	D425	46, XY, i(17q) , 10q-, + DMs

Table 4.1.1: Karyotypes of the medulloblastoma cell lines

D283 and D341 cells also show high level of *NPR3* expression. The D283 and D341 cell lines show amplification of the *MYC* gene. This explains the very high expression level of *MYC* in these cell lines. Almost all *MYC* amplifications occur in the Group 3 tumours [8]. All these cell lines are reported to carry isochromosome 17q which is a common feature of Group 3 and Group 4 tumours. However none of these cells show expression of *GRM8* Thus these cell lines may belong to the group 3 of medulloblastoma.

The molecular subgrouping of the medulloblastoma cell lines available in the lab suggests that the Daoy cell line most likely belongs to the SHH subgroup while the D283, D425, D341 and D384 cell lines belong to the group 3 of medulloblastoma. These cell lines were used for the further study on the role of miRNA coding genes in medulloblastoma.

4.2: Role of miR-206 in the Biology of Medulloblastoma

MiRNA expression profiling carried out on 19 medulloblastoma samples and 4 normal cerebellum samples identified miR-206 to be one of the miRNA's downregulated in medulloblastomas belonging to all the four molecular subgroups, as compared to the normal cerebellum samples. It is specifically expressed in the cerebellum of the rat brain which is the site of medulloblastoma occurrence. It is also known to target the *OTX2* gene which is highly expressed in all non-SHH medulloblastomas. Thus, in the present study, the expression of miR-206 in human and mouse medulloblastoma tumor tissues and normal cerebellum samples was studied. Following this, the effect of miR-206 expression on the growth and malignant behaviour of three medulloblastoma cell lines was investigated.

4.2.1 Evaluation of miR-206 Expression in Human Medulloblastoma Tumor Tissues and Normal Cerebellum and Cerebrum Tissues by Real Time RT-PCR analysis

MiR-206 expression was evaluated in human sporadic medulloblastoma tumor tissues, in normal cerebellum and cerebrum tissues by real time RT-PCR. MiR-206 expression in the normal brain cerebrum was found to very low (RQ = 0.006-0.02) while in both developing and adult cerebellar tissues it is about 50-200 fold higher at RQ = 0.91-1.22 (Figure.4.2.1 A). Molecular classification of 44 medulloblastoma tumor tissues into the four subgroups WNT, SHH, Group 3 and Group 4 was carried out using the 12 protein-coding genes and 9 miRNAs as markers by real time RT-PCR assay as described before [15]. MiR-206 expression was found to be downregulated in medulloblastomas belonging to all the four subgroups by 10-10,000 folds ($p \leq 0.0001$). MiR-206 expression was barely

detectable in the five cell lines *viz* Daoy, D425, D283, D384 and D341 established from human sporadic medulloblastomas as well ($p \leq 0.0001$).

4.2.2 Evaluation of miR-206 Expression in Mouse Medulloblastoma Tumor Tissues from the *Smo*^{+/+} Transgenic Mice and the *Ptch1*^{+/-} Knock-out Mice and Normal Cerebellum Tissues by Real Time RT-PCR

The expression of murine homolog of human miR-206 was evaluated in the normal developing cerebellum from the C57BL6 mice at post natal day 5, 7, 14 and 21 and in medulloblastomas from the *Smo*^{+/+} transgenic mice and the *Ptch1*^{+/-} knock-out mice [36, 66]. These mouse models serve as models for SHH subgroup medulloblastomas. The level of miR-206 expression increased during the development of the mouse cerebellum from Day 5 to Day 21. However this increase in miR-206 expression was not found to be statistically significant. MiR-206 expression was found to be downregulated ~10 fold ($p \leq 0.05$) in medulloblastomas from *Smo*^{+/+} transgenic mice and by 10-100 fold ($p \leq 0.01$) in medulloblastomas from *Ptch1*^{+/-} knock-out mice as compared to their normal cerebellar counterparts (Figure 4.2 1 B).

Thus, miR-206 expression was found to be downregulated in all the human medulloblastomas studied, irrespective of the molecular subgroup, as well as in the tumors from the SHH signalling driven medulloblastoma mouse models.

4.2.3 Construction of a Lentiviral Plasmid Vector for Expression of miR-206

The genomic region coding miR-206 along with about 200 nucleotides long 5' and 3' flanking regions was cloned in the pTRIPZ lentiviral vector (Open biosystems, Lafayette, USA) between the HpaI and EcoRI restriction enzyme sites. The miRNA is expressed

under the control of a doxycycline inducible promoter. The pTRIPZ vector consists of the tetracycline response element (TRE) and the reverse tetracycline transactivator 3 (rtTA3)

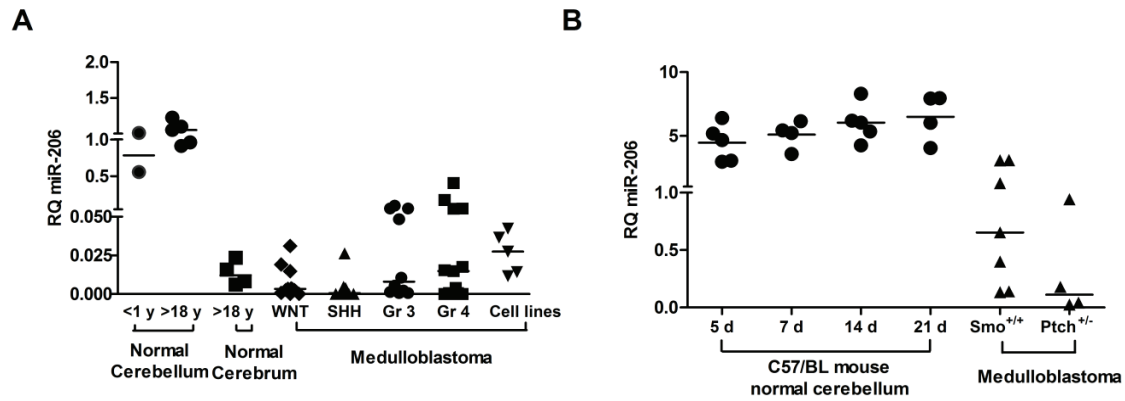


Figure 4.2.1: MiR-206 expression in the normal brain, medulloblastoma tumors, and in the established medulloblastoma cell lines.

(A) The scatter dot plot shows miR-206 expression in normal developing cerebellum (less than 1 yr old infants), adult cerebellum, adult cerebrum, and human sporadic medulloblastomas belonging to the four molecular subgroups and in established medulloblastoma cell lines. (B) The expression of murine homolog of miR-206 in the normal developing cerebellum and in medulloblastoma tissues from *Smo*^{+/+} and *Ptch*^{+/-} medulloblastoma mouse models.

which enable inducible expression of the miRNA. The TRE consists of a string of Tet operators fused to the minimal CMV promoter. The pTRIPZ transactivator, known as the reverse tetracycline transactivator 3 (rtTA3), binds to and activates expression from TRE promoters in the presence of doxycycline. The TRE also drives the expression of a TurboRFP reporter in addition to the miRNA. This enables monitoring of expression from the TRE promoter. This vector construct was used for the stable, inducible expression of miR-206 in medulloblastoma cell lines (Figure 4.2.2 A, B).

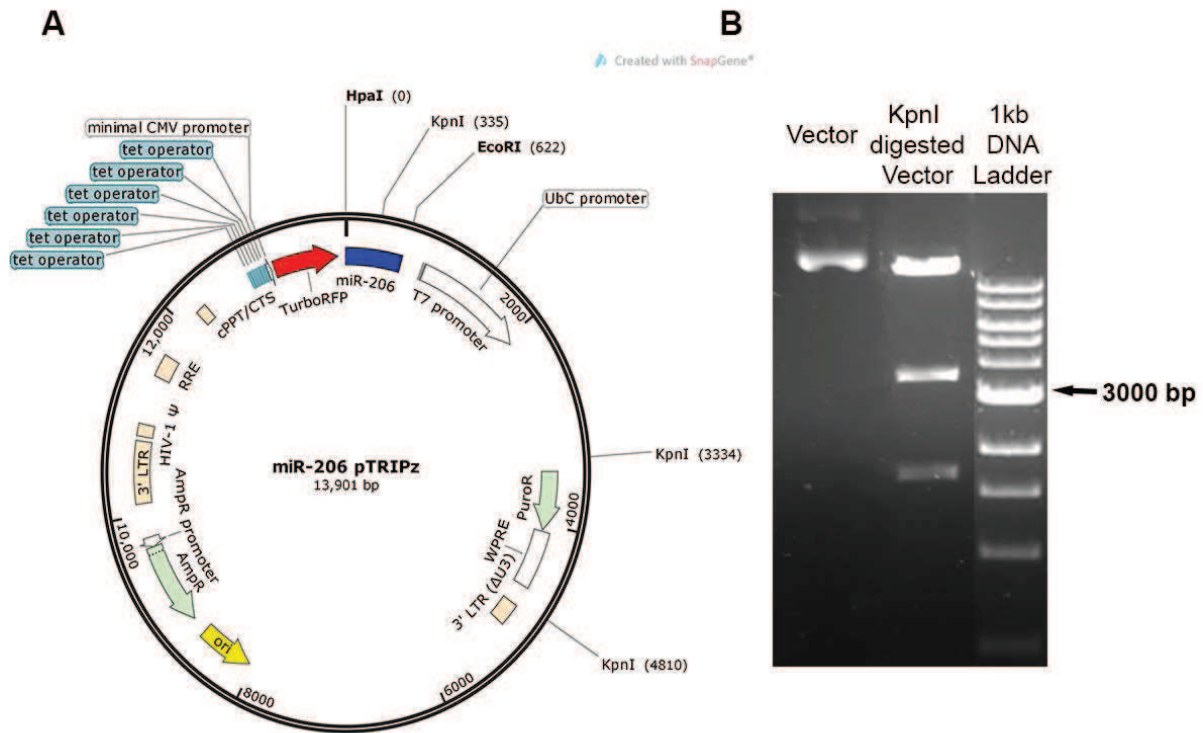


Figure 4.2.2 : miR-206 pTRIPZ vector construct

(A) miR-206 pTRIPZ vector construct map indicating cloning sites HpaI and EcoRI and location of other features of the vector backbone. (B) Agarose gel electrophoresis image of confirmation of the miR-206-pTRIPZ construct. Vector: undigested miR-206 pTRIPZ vector, KpnI digested vector: miR-206 pTRIPZ digested with KpnI.

4.2.4 Effect of miR-206 Expression on the Growth, Clonogenic Potential, Radiation Sensitivity and Anchorage-independent Growth of the Established Medulloblastoma Cell Lines

A. Generation of stable polyclonal populations expressing miR-206 on doxycycline induction

Mir-206 expression was found to be downregulated in all the established medulloblastoma cell lines studied (Figure 4.2.1A). Daoy and D425 / D283 medulloblastoma cell lines belong to SHH, and Group 3 molecular subgroup respectively based on their cytogenetic profiles [70, 72]. Daoy, D425 and D283 medulloblastoma cell lines were transduced with lentiviral particles of pTRIPZ-miR-206 construct that

expressed miR-206 in a doxycycline inducible manner. Two stable polyclonal populations ‘P1, P2’ of each of the three cell lines expressing miR-206 upon doxycycline induction at levels comparable to those in the normal cerebellum were selected in the presence of puromycin (Figure 4.2.3). These cells along with their respective vector control populations ‘C’ were used for different assays for proliferation, clonogenic growth potential, radiation sensitivity, anchorage independent growth potential and sensitivity to the drug All-trans Retinoic acid (ATRA).

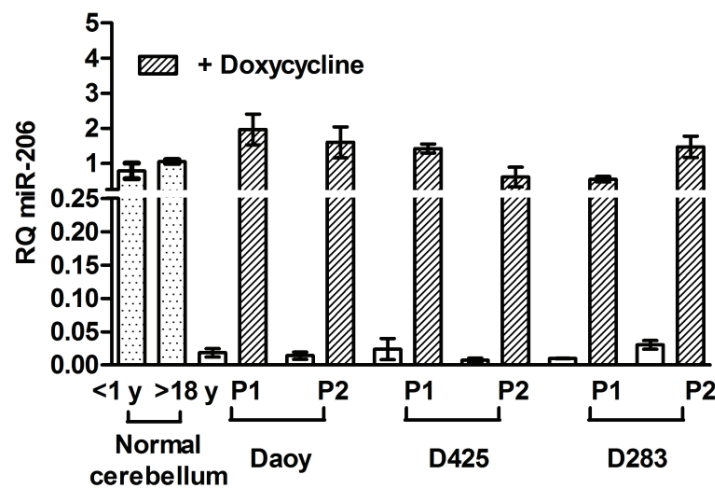


Figure 4.2.3: MiR-206 expression in the normal developing and adult cerebellum and in polyclonal populations ‘P1, P2’ of Daoy, D425 and D283 cell lines.

B. Effect of restoration of miR-206 expression on the growth of medulloblastoma cell lines

The effect of restoration of miR-206 expression on the growth of medulloblastoma cells was studied by the MTT reduction assay. Doxycycline treatment of the vector control population of Daoy, D283 and D425 cells was found to result in 5-10 % growth inhibition as compared to the untreated cells. Restoration of miR-206 expression upon doxycycline treatment of the P1 and P2 populations of the Daoy, D425 and D283 cell lines showed

marginally higher (10-20%) growth inhibition than that brought about by the doxycycline treatment of the control population (Figure 4.2.4 A, B). Thus there was no significant effect of restoration of mir-206 expression on the proliferation of the three medulloblastoma cell lines.

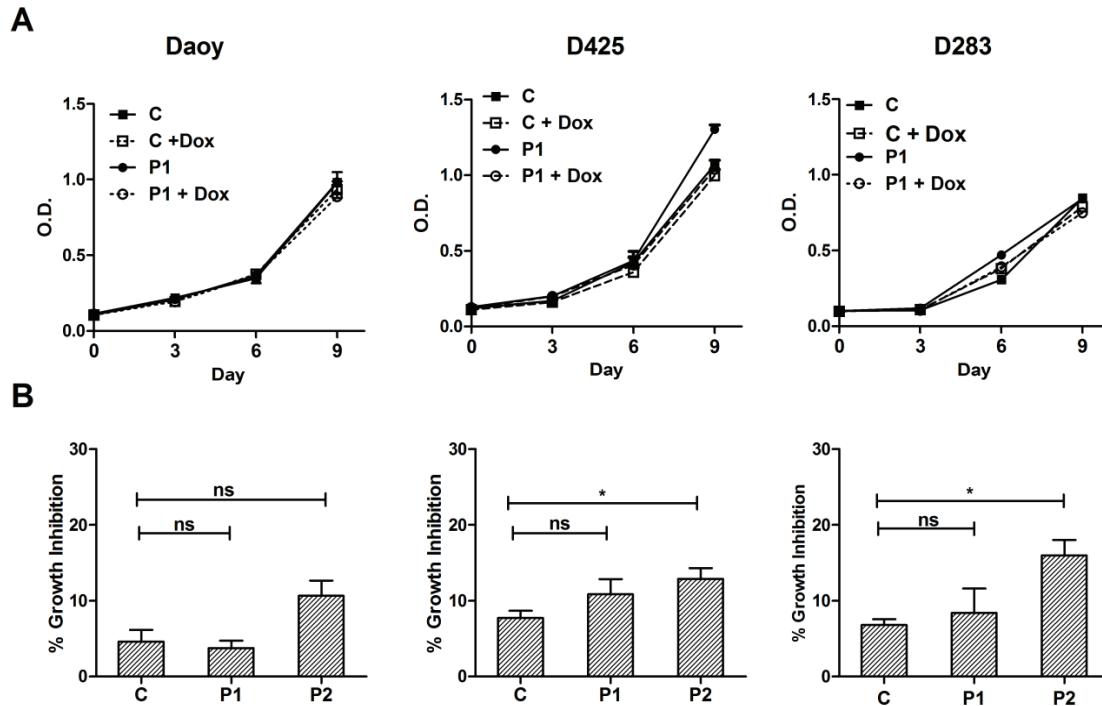


Figure 4.2.4: Effect of miR-206 expression on the growth of medulloblastoma cell lines.

(A) Representative experiments showing growth curves of the indicated medulloblastoma cell line polyclonal populations transduced with control pTRIPZ vector 'C' or pTRIPZ-miR-206 construct 'P1' with (+ DOX) or without doxycycline treatment as studied by the MTT reduction assay over a period of 9 days (B) Y axis denotes the percentage reduction in the growth upon doxycycline treatment of the indicated polyclonal populations compared to the un-treated population as studied by the MTT assay. 'ns' indicates non-significant, * indicates $p \leq 0.05$.

C. Effect of restoration of miR-206 expression on anchorage independent growth potential of medulloblastoma cell lines

The effect of miR-206 expression on the anchorage independent growth potential of Daoy, D425 and D283 cells was studied by the colony formation in soft agar. 10,000 Daoy cells and 1000 cells each of D283 and D425 cells were seeded for the soft agar colony formation assay. Vector control polyclonal populations of Daoy cells formed 400-600 colonies in 2-3 weeks post seeding. The D425 and D283 cells formed ~500 and ~250 colonies respectively. However, there was no significant difference in the number or size of colonies formed in the P1 and P2 populations of miR-206 expressing cells as compared to the vector control cells (Figure 4.2.5 A, B).

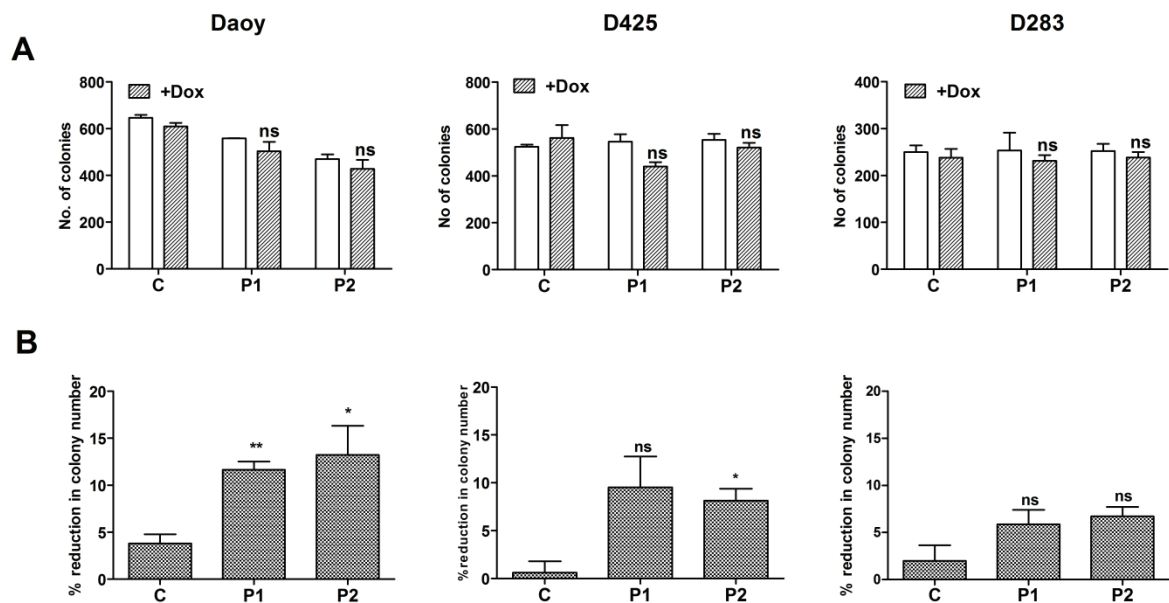


Figure 4.2.5: Effect of miR-206 expression on the anchorage independent growth of medulloblastoma cell lines

(A) Representative experiments showing the number of colonies formed by the indicated medulloblastoma cell line polyclonal populations transduced with control pTRIPZ vector 'C' or pTRIPZ-miR-206 construct 'P1' with (+ DOX) or without doxycycline treatment as studied by the colony formation in soft agar. (B) Y axis denotes the percentage reduction in colony formation upon doxycycline treatment of the indicated polyclonal populations compared to the un-treated population. 'ns' indicates non-significant, * indicates $p \leq 0.05$ ** indicates $p \leq 0.01$.

D. Effect of restoration of miR-206 expression on the clonogenic potential and radiation sensitivity of Daoy cells

The effect of miR-206 expression on the clonogenic potential of Daoy cells was studied by seeding 1000 cells in a 55 mm dish. The control cells formed 400-450 well separated, microscopically visible colonies 8 days post seeding. There was no significant difference observed in the number of colonies formed by the vector control cells and the miR-206 expressing P1 and P2 populations of Daoy cells with or without doxycycline induction (Figure 4.2.6 A, B). The effect of miR-206 expression on the radiation sensitivity of Daoy cells was studied in a clonogenic assay after irradiation of the cells at a dose of 6 Gy. At this dose, clonogenic potential of the parental Daoy cells was found to be reduced by 55-60 %. The clonogenic potential of the P1 and P2 polyclonal populations of Daoy cells was reduced by 75-80 % on irradiation at a dose of 6 Gy before or after induction of miR-206 expression. Thus, there was a marginal increase (~20 %) in the radiation sensitivity of Daoy cells upon miR-206 expression. Thus, the expression of miR-206 at levels equivalent to that in the normal cerebellum did not have a significant effect on the growth characteristics of medulloblastoma cell lines Daoy, D425 and D283.

4.2.5 Effect of Restoration of miR-206 Expression on the Level of OTX2 Protein in the Non-WNT Non-SHH Subgroup Cell Lines

OTX2 is an important oncogene in medulloblastoma. The 3'UTR of the *OTX2* gene carries one conserved binding site for miR-206 and has been reported to be validated as a miR-206 target using luciferase reporter assay and western blot analysis [73]. *OTX2* gene is known to be amplified in the D425 cell line and has a transcript level which is 45 times higher than that in the normal cerebellum. The D283 cell line also shows overexpression of OTX2 protein [64]. In order to study the effect of restoration of miR-206 expression to levels in the normal cerebellum on OTX2 protein expression, western blotting for OTX2 was carried out in the Doxycycline induced and control populations C, P1 and P2 of both

the D425 and D283 cell lines. However, the restoration of mir-206 expression was not found to result in the down-regulation of OTX2 protein levels (Figure 4.2.7 A).

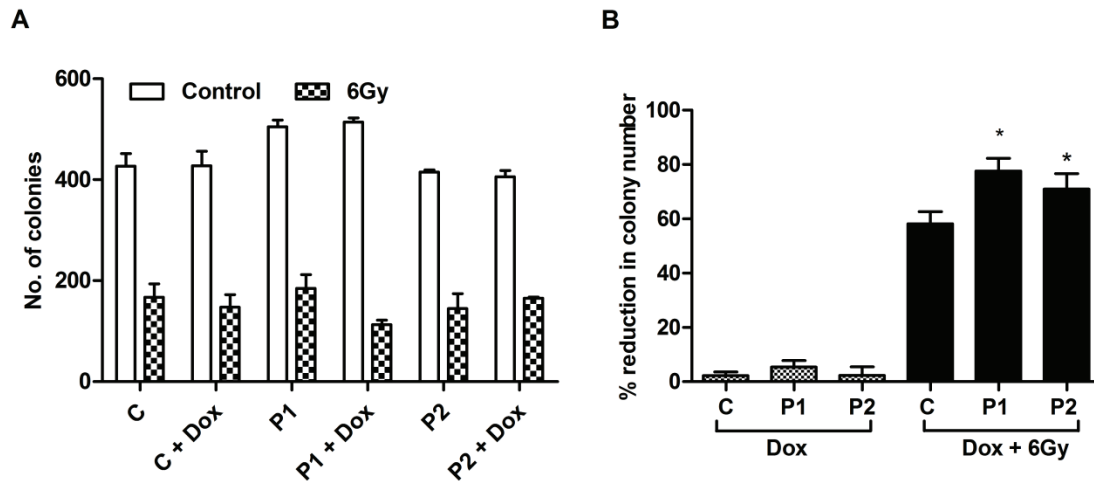


Figure 4.2.6: Effect of miR-206 expression on the clonogenic potential and radiation sensitivity of Daoy cells.

(A) Y axis denotes the number of colonies formed in control ‘C’ and miR-206 expressing P1 and P2 polyclonal population of Daoy cells with or without irradiation (6 Gy) in a clonogenic assay. (B) Y axis denotes the percentage reduction in the number of colonies formed on doxycycline induced expression of miR-206 with or without irradiation as compared to the control un-induced cells of the indicated polyclonal population. * indicates $p \leq 0.05$

4.2.6 Effect of miR-206 Overexpression on the Level of OTX2 Expression and Anchorage Independent Growth of Non-WNT, Non-SHH Medulloblastoma Cell Lines

The amplification and / or overexpression of *OTX2* may hinder the effect of miR-206 on OTX2 expression although it is a known target of miR-206. Therefore, miR-206 was overexpressed in D425 and D283 cell lines using transient transfection with synthetic miRNA mimics. The transfection with miR-206 mimics resulted in about 100 -500 fold overexpression of miR-206 expression as compared to the normal cerebellum. This level of miR-206 expression resulted in the reduction of OTX2 protein levels (Figure 4.2.7 B). The effect of overexpression of miR-206 in D425 and D283 cell lines on the colony formation in soft agar was also studied. MiR-206 mimic transfection resulted in $51.23 \pm 4.11\%$ and $48.93 \pm 4.09 \%$ reduction in the colony formation as compared to the siGLO transfected control cells of D425 and D283 cell lines respectively. Stable polyclonal populations (P3) of D425 and D283 cells overexpressing miR-206 by ~ 80-150 folds at R.Q. levels in the range of 75-150 were also selected in the presence of puromycin by stable transduction with pTRIPZ-miR-206 construct. Doxycycline induction of miR-206 overexpression in the P3 polyclonal populations of D425 and D283 cells also showed 50.54 ± 4.48 and $31.67 \pm 3.79 \%$ reduction in the soft agar colony formation respectively (Figure 4.2.7 C-E). Thus, miR-206 overexpression was found necessary to downregulate OTX2 protein levels and bring about growth inhibition of medulloblastoma cells.

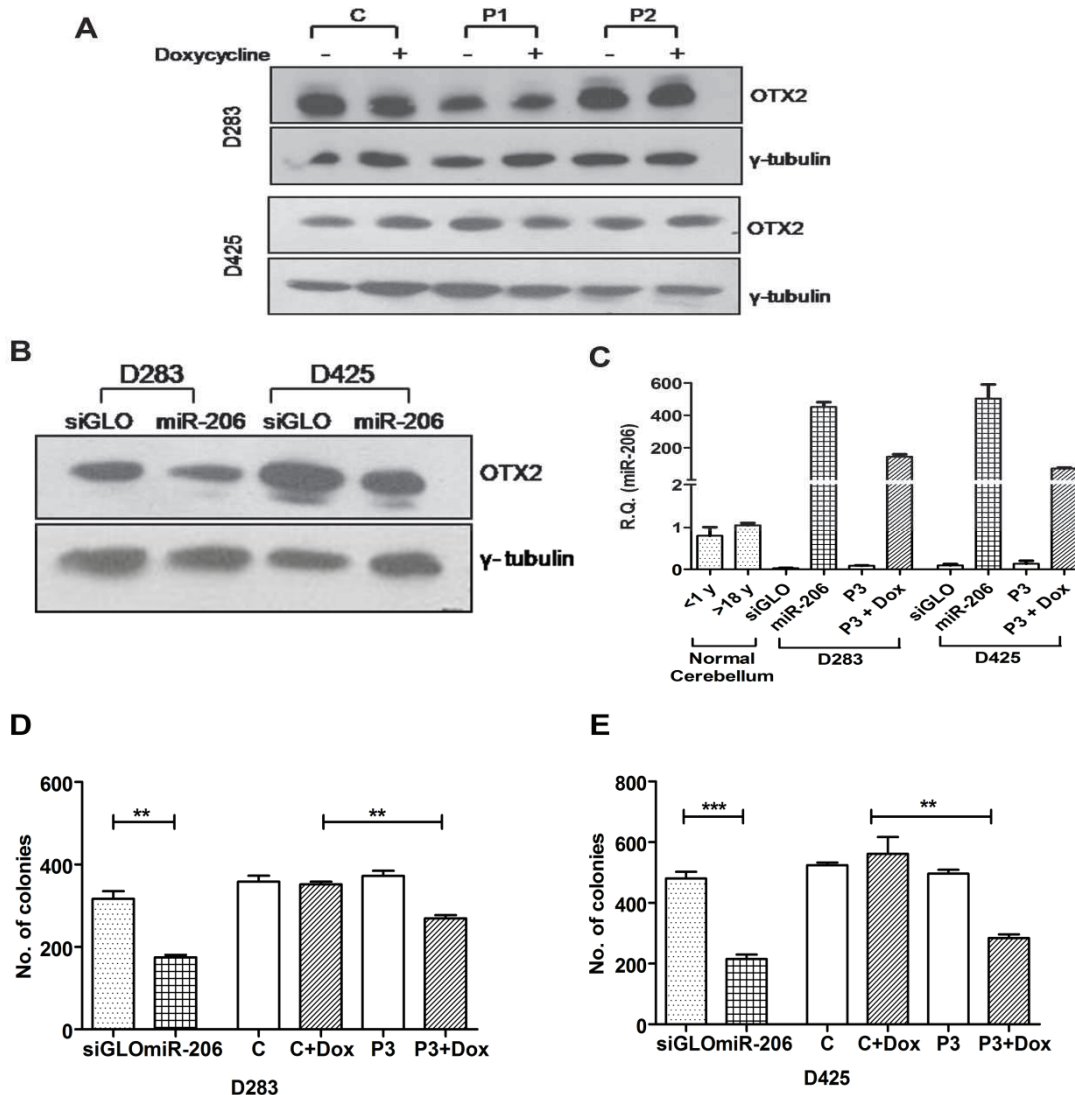


Figure 4.2.7: Effect of restoration and overexpression of miR-206 on OTX2 expression and the effect of miR-206 overexpression on anchorage independent growth of D283 and D425 cells.

(A) Western blot analysis of OTX2 expression in the P1 and P2 polyclonal populations of D283 and D425 cells before and after doxycycline induced miR-206 expression. (B) Western blot analysis of OTX2 expression in siGLO and miR-206 mimic transfected D283 and D425 cells. γ -tubulin was used as a loading control. (C) Level of miR-206 expression in siGLO and miR-206 mimic transfected cells and P3 population of D283 and D425 cells. (D and E) Y axis denotes the number of soft agar colonies formed by siGLO and miR-206 mimic transfected cells and P3 polyclonal population of D283 and D425 cells with (+DOX) or without doxycycline induction. ** indicates $p \leq 0.01$ and *** indicates $p \leq 0.001$.

4.2.7 Synergistic Effect of Restoration of miR-206 Expression and Treatment with All Trans Retinoic Acid (ATRA) on the Growth and OTX2 Expression in D283 Cell Line

ATRA has been shown to downregulate OTX2 expression and inhibit proliferation of medulloblastoma cells. The effect of restoration of miR-206 expression in combination with ATRA treatment on the level of OTX2 expression and growth of medulloblastoma cells was analyzed. The western blot analysis showed reduction of OTX2 protein levels upon treatment with 5 nM and 10 nM ATRA in the P1 population of D283 cells. However, the reduction in the OTX2 protein levels upon ATRA treatment was similar in the absence or presence of restoration of miR-206 expression levels (Figure 4.2.8 B). The treatment of D283 P1 population with 5 nM / 10 nM ATRA resulted in 40-50 % growth inhibition as studied by MTT reduction assay. The level of growth inhibition of D283 cells upon ATRA treatment did not change upon restoration of miR-206 expression, indicating no synergistic effect of ATRA treatment and miR-206 expression at the levels studied (Figure 4.2.8 A).

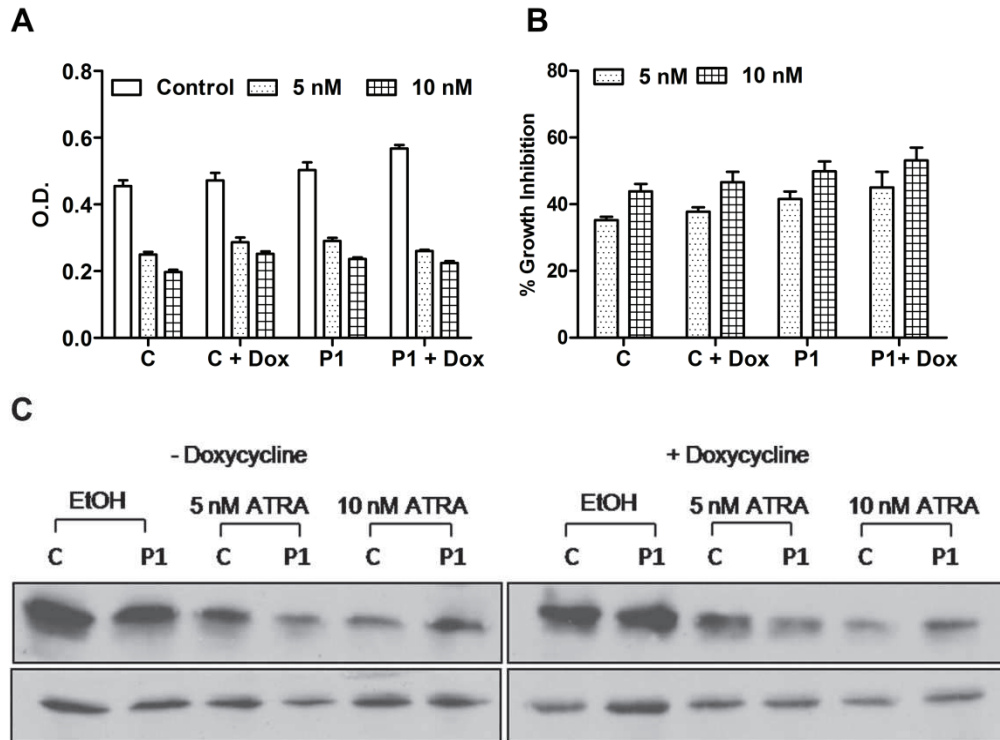


Figure 4.2.8: The effect of ATRA and miR-206 expression on the growth and expression of OTX2 in D283 cells

(A) Representative experiment showing the growth of vector control and the P1 population of D283 cells expressing miR-206 on induction with doxycycline with or without treatment with 5 nM and 10 nM ATRA. (B) Y axis shows the percentage reduction in the growth of control or P1 population of D283 cells on treatment with 5 nM or 10 nM ATRA. (C) Western blot analysis of OTX2 expression. Left panel shows the OTX2 expression in the cells without doxycycline induction and right panel shows OTX2 expression in doxycycline induced cells treated with the indicated concentrations of ATRA. γ -tubulin served as the loading control.

DISCUSSION

MiR-206 was identified as a myomiR along with miR-1 and miR-133a/b, as the expression of these miRNAs was found to be enriched in the muscles [74]. Although miR-206 is enriched in the skeletal muscles, its expression in other tissues such as heart and brain is also known, albeit at lower levels than in the skeletal muscle [75]. In the present study, miR-206 expression was found to be restricted to the human cerebellar brain region that is consistent with its reported enriched expression in rat cerebellum [65]. MiR-206 was found to be expressed during cerebellar development in mice and expressed in both developing and adult human cerebellum suggesting miR-206 role in both cerebellar development and maintenance. MiR-206 expression was found to be downregulated in medulloblastoma tissues belonging to all the four molecular subgroups, as compared to the normal cerebellar tissues. MiR-206 expression is also downregulated in SHH subgroup medulloblastomas from *Ptch1*^{+/-} knock-out and *Smo*^{+/+} transgenic mouse models that is consistent with reported downregulation of miR-206 expression in desmoplastic medulloblastomas belonging to the SHH subgroup [76]. MiR-206 expression is downregulated in all the established medulloblastoma cell lines studied. Thus, down-regulation of miR-206 expression is a consistent feature of all the four molecular subgroups of medulloblastomas well as SHH subgroup medulloblastomas from transgenic mouse models suggesting tumor-suppressive role for miR-206 in medulloblastoma pathogenesis.

Although miR-206 expression is downregulated in medulloblastomas belonging to all the four subgroups, restoration of miR-206 expression in established medulloblastoma cell lines to levels similar to that in normal cerebellar tissues was found to be insufficient to bring about growth inhibition of medulloblastoma cells. Down-regulation of miR-206 expression in medulloblastomas could be necessary for malignant transformation or may

be a consequence of the same. While restoration of miR-206 expression was insufficient, miR-206 expression at levels (~ 100 fold higher) comparable to that in muscle tissues was found to bring about growth inhibition and reduction in the clonogenic potential of medulloblastoma cells. MiR-206 overexpression was found to bring about reduction in protein levels of OTX2, a known target of miR-206. OTX2, a homeobox transcription factor controls cell fate specification during normal brain development [77]. In adults, OTX2 expression is restricted to the retina and is not expressed in the normal cerebellum. OTX2 on the other hand, is overexpressed in all non-SHH medulloblastomas and has been shown to act as an oncogene that is critical for maintenance and progression of these medulloblastomas [78]. Therefore, although downregulation of miR-206 expression may contribute to medulloblastoma pathogenesis, restoration of its expression is insufficient to down-regulate its oncogenic targets like OTX2 that are over-expressed in malignant medulloblastoma cells.

ATRA is a potent inducer of neuronal differentiation and has been evaluated for use as a therapeutic agent for medulloblastoma. ATRA has been shown to downregulate OTX2 expression and thereby inhibit growth of OTX2 expressing medulloblastoma cells [79]. Restoration of miR-206 expression to the levels comparable to those in the normal cerebellum was not found to be sufficient to reduce the OTX2 protein levels by itself and did not enhance the growth inhibitory effect of ATRA in medulloblastoma cells. MiR-206 overexpression at levels comparable to that in muscle tissues downregulated OTX2 levels in medulloblastoma cells and brought about growth inhibition of these cells. While Retinoic acid therapy has been found to be effective in inhibiting growth of medulloblastoma xenografts established subcutaneously, it was ineffective in case of intracranial orthotopic xenografts [80]. Fibroblast growth factor 2 (FGF2) has been implicated in resistance to retinoic acid mediated inhibition of intracranial tumor growth.

Overexpression of miR-206 that targets OTX2 could be an alternative to retinoic acid in the treatment of OTX2 positive medulloblastomas.

A rare variant of medulloblastoma named as medullomyoblastoma which shows features of myogenic differentiation, is known and medulloblastoma cells belonging to classic histology are also known to undergo myogenic differentiation. OTX2 down-regulation has been shown to bring about myogenic differentiation of medulloblastoma cells which is accompanied by upregulation of MYOD1 activity [78, 81]. *MYOD1* has been shown to act as a tumor suppressor gene in medulloblastomas. Loss of one allele of *MYOD1* has been found to promote tumorigenesis in *Smo*^{+/+} transgenic mice [82]. MYOD1 has been found to upregulate miR-206 expression in normal cerebellar neuron progenitor cells (Joyoti Dey Ph. D. thesis, <http://hdl.handle.net/1773/20238>) similar to MYOD1 mediated activation of miR-206 transcription in muscle cells [83]. MiR-206 on the other hand, targets OTX2, indicating feedback inhibitory circuit wherein OTX2 downregulates miR-206 transcription by downregulating MYOD1 expression and miR-206 in turn downregulates OTX2 protein levels. OTX2 overexpression thus may be instrumental in downregulation of miR-206 expression in non-SHH medulloblastomas. In order to evaluate the effect of miR-206 downregulation if any, on the malignant transformation, it would be necessary to downregulate miR-206 expression during the process of malignant transformation in a transgenic mouse model of medulloblastoma.

In summary, expression of miR-206 is enriched in both developing and adult cerebellum and is down-regulated in medulloblastomas belonging to all four molecular subgroups. Over-expression of miR-206 however, was found to be necessary for growth inhibition of medulloblastoma cells and down-regulation of its oncogenic target OTX2, that is known to be overexpressed in all non-SHH medulloblastoma cells.

4.3: Role of miR-204 in the biology of medulloblastoma

4.3.1 Differential expression of miR-204 in molecular subgroups of medulloblastoma

MiRNA expression profiling showed miR-204 expression to be down-regulated 10-100 fold in all SHH tumors and in most group 3 tumors as compared to the normal cerebellum [15]. MiR-204 expression was found to be upregulated in the WNT tumors and most group 4 tumors. This differential miR-204 expression was further validated in a set of 160 medulloblastoma tissues by real time RT-PCR (Figure 4.3.1). The effect of miR-204 expression on growth and malignant behaviour of Daoy medulloblastoma cell line that most likely belongs to SHH subgroup has been studied. MiR-204 expression in Daoy cells brought about ~65-70% reduction in the size of the tumors formed by subcutaneous xenografts as compared to the vector control cells (Pratibha Boga, Ph. D. thesis). As discussed above, apart from SHH subgroup, miR-204 expression is also down regulated in most Group 3 medulloblastomas. In the present study, miR-204 expression was also found to be downregulated 10-100 fold in the group 3 cell lines *viz* D425 and D341 as compared to the normal cerebellum. MiR-204 expression in D283 cell line that also belongs to Group 3 was found to be downregulated by 2-3 fold to the normal cerebellum (R.Q= 25-35) (Figure 4.3.1). Hence, the effect of expression of miR-204 on the growth, tumorigenicity and invasion potential of these Group 3 medulloblastoma cell lines was investigated

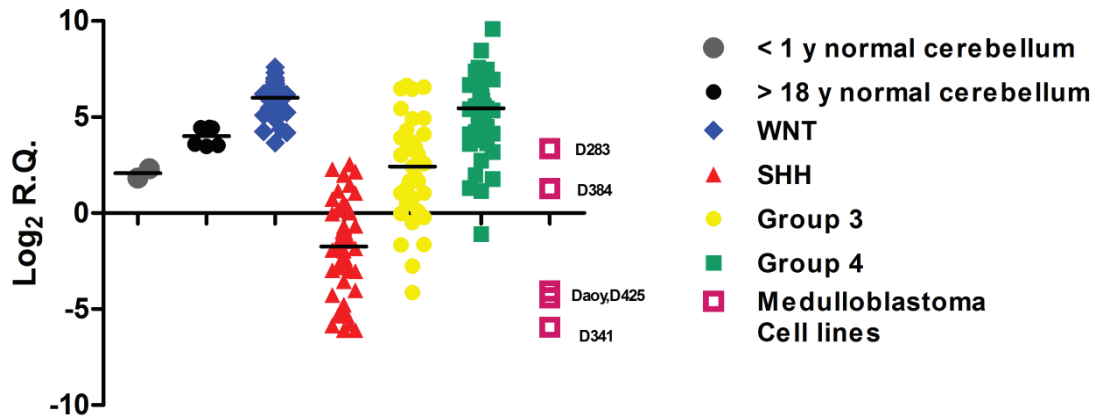


Figure 4.3.1: MiR-204 expression in the normal cerebellum, medulloblastoma tumors, and in the established medulloblastoma cell lines.

The scatter dot plot shows miR-204 expression levels in normal developing cerebellum (< 1 y), normal adult cerebellum (> 18 y), and human sporadic medulloblastomas belonging to the four molecular subgroups and in established medulloblastoma cell lines. The levels are expressed as quantities relative to RNU48, a housekeeping small RNA control.

4.3.2 Correlation of miR-204 expression with survival in the non-WNT, non-SHH medulloblastoma patients

MiR-204 expression across the medulloblastoma subgroups indicates downregulation of its expression in many Group 3 tumors and an upregulation in most of the Group 4 tumors. These subgroups have an overlapping gene expression signature and are often difficult to classify. The group 3 and Group 4 of medulloblastoma are also distinct in their clinical features such as prognosis and overall survival with the group 4 patient's fare much better than the group 3 patients. Kaplan Meier analysis for survival of patients with group 3 (n = 24) and Group 4 (n = 35) tumors with respect to miR-204 as a predictor was conducted. The expression level of miR-204 in the normal cerebellum was used as a median value. The patients with the high miR-204 expression had a survival of 62 % as compared to 23% for those with low miR-204 expression. Thus, the patients with high miR-204 expression had

significantly better survival ($p = 0.01$, hazard ratio = 3.76) as compared to those with low miR-204 expression (Figure 4.3.2).

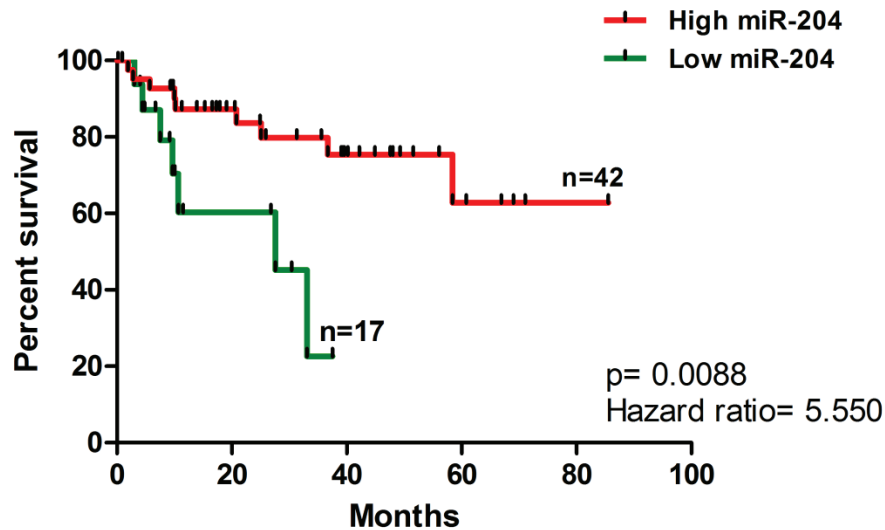


Figure 4.3.2: Kaplan Meier survival analysis

The Y axis indicates percent overall survival for patients with high miR-204 expression as compared to those with low miR-204 expression within the group 3 and group 4 of medulloblastoma. The expression level of miR-204 in the normal cerebellum was used as a median value. The p value indicates level of significant difference in the Kaplan Meier survival curves estimated by the Log Rank Test.

4.3.3 Effect of miR-204 expression on the proliferation, anchorage independent growth and tumorigenicity of medulloblastoma cell lines

A. Generation of stable polyclonal populations / transient expression of miR-204 in medulloblastoma cell lines

The better survival of the patients with higher level of miR-204 expression within the group 3 and group 4 medulloblastoma indicates that miR-204 may play an important role in the biology of medulloblastoma. The genomic region encoding miR-204 cloned in pTRIPZ, a lentiviral vector was used for stable doxycycline inducible miR-204 expression in

medulloblastoma cell lines. The effect of miR-204 expression on the growth characteristics of medulloblastoma cell lines was studied by the generation of stable polyclonal populations of Daoy and D341 cells 'P1 and P2' by transduction with viral particles containing the miR-204-pTRIPZ construct. The cells transduced with the viral particles of the empty pTRIPZ vector of the respective cell lines were used as negative controls 'C'. The level of miR-204 expression in the P1 and P2 populations of both cell lines was found to be in the range of R.Q. =25-45 (Figure 4.3.3 A), which is comparable to that in the normal cerebellum. The effect of miR-204 expression on the growth of D283 and D425 cell lines was studied by transfection of these cells with synthetic miRNA mimics. Transfection with miR-204 mimic resulted in the level of expression (RQ =50-100) (Figure 4.3.3 B), which was comparable to that in the normal cerebellum or in the Group 4 tumors. The non-targeting control siGLO was used for transfection of cells used as a control.

B. Effect of miR-204 expression on proliferation of medulloblastoma cell lines

The effect of miR-204 expression on the proliferation of medulloblastoma cell lines was studied using the MTT reduction assay over a period of 9-12 days. MiR-204 expression in the Daoy cells resulted in 35-45 % reduction ($p \leq 0.01$) in proliferation only on day 12 (Figure 4.3.4 A, B). There was no effect on the proliferation of D341 cells on induction of miR-204 expression as compared to the uninduced control cells (Figure 4.3.4 C, D). Similarly, there was no significant difference in the proliferation of D283 and D425 cells expressing miR-204 as compared to the siGLO transfected control cells (Figure 4.3.4 E, F, G). Thus, the growth of miR-204 expressing Daoy cells was found to be inhibited only on the 12th day and there was no significant effect on proliferative capacity of all three group 3 cell lines.

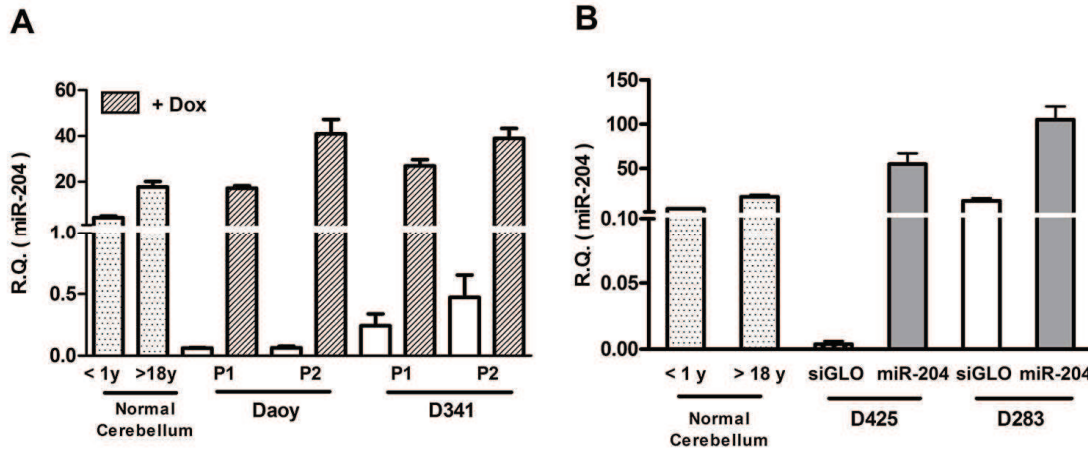


Figure 4.3.3: MiR-204 expression levels in stable polyclonal populations and miR-204 mimic transfected cells.

Relative quantity (R.Q.) of miR-204 expression in (A) the developing (< 1 y) and adult (> 18 y) normal cerebellum, stable polyclonal populations (P1 and P2) of Daoy and D341 cells and in (B) synthetic miR-204 mimic transfected D425 and D283 cells. The miR-204 levels are expressed as relative to levels of RNU48, a housekeeping small RNA control.

C. Effect of miR-204 expression on anchorage independent growth of medulloblastoma cell lines

The anchorage independent growth potential of miR-204 expressing cells was compared to that of the control cells by studying the colony formation in soft agar. 10,000 cells of Daoy polyclonal populations and 1000 cells each of D341 polyclonal populations or D283 and D425 mimic transfected cells were seeded for the assay. The colonies formed were counted after 2-3 weeks. Doxycycline induced miR-204 expression resulted in 30-40 % ($p \leq 0.01$) reduction in number of colonies formed by Daoy cells while the D341 cells showed ~ 40 % ($p \leq 0.01$) reduction in colony number (Figure 4.3.5 A, B, C, D). There was no significant difference in the colony formation in soft agar in D283 cells.

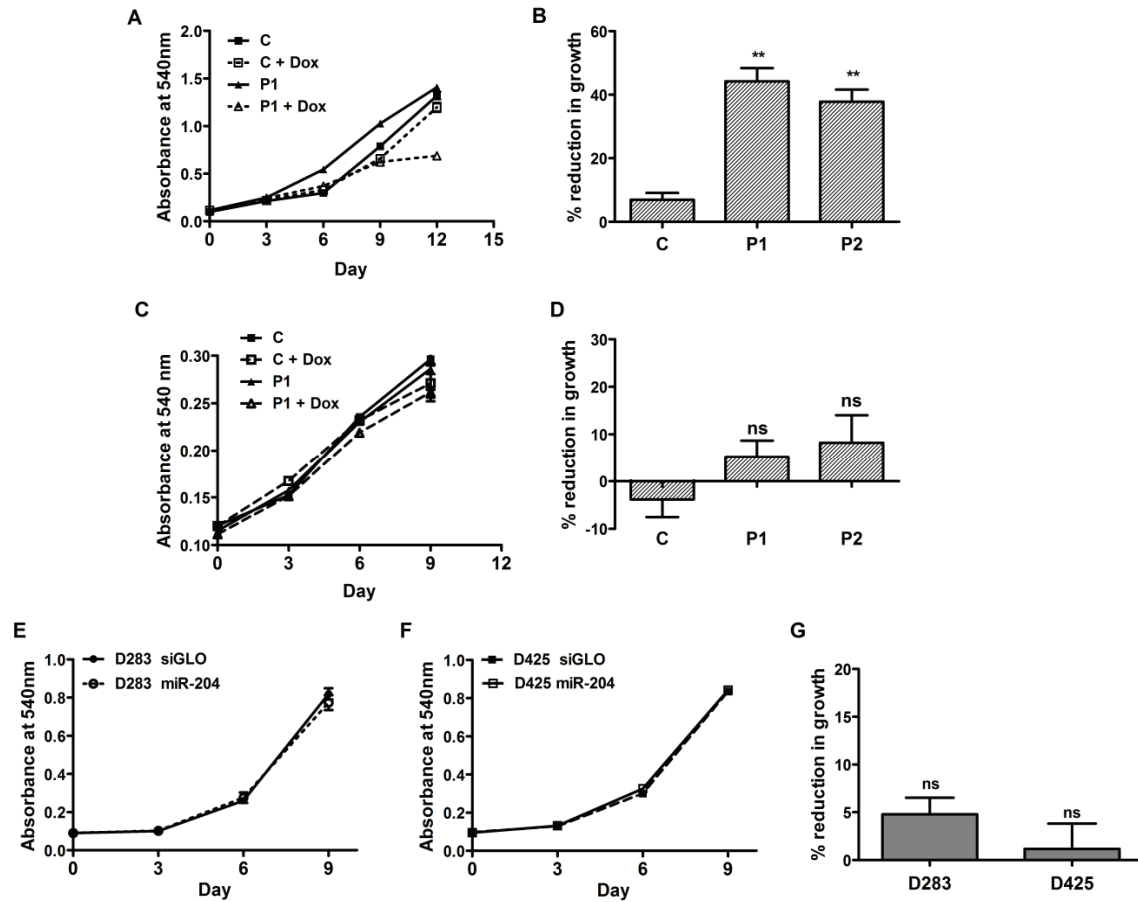


Figure 4.3.4: Effect of miR-204 expression on the growth of medulloblastoma cell lines

(A, C, E, F) Representative experiments showing growth curves of the medulloblastoma cell lines (A) Daoy, (C) D341 polyclonal populations transduced with control pTRIPZ vector ‘C’ or pTRIPZ-miR-204 construct ‘P1’ with (+ DOX) or without doxycycline treatment and in D283 (E), D425 (F) cells transfected with siGLO control or miR-204 mimic as studied by the MTT reduction assay over a period of 9-12 days. In B, D and G the Y axis denotes the percentage reduction in the growth upon doxycycline treatment of the indicated polyclonal populations compared to the un-treated population as studied by the MTT reduction assay. ‘ns’ indicates non-significant

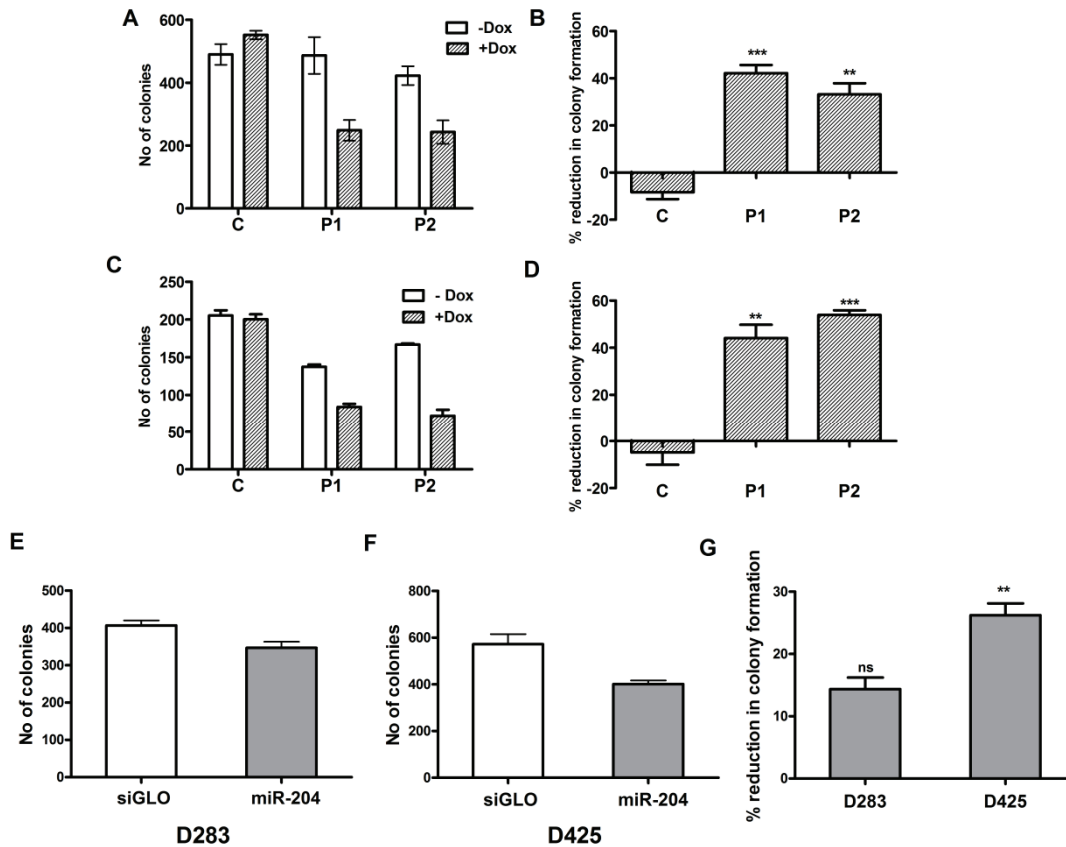


Figure 4.3.5: Effect of miR-204 expression on the anchorage independent growth of medulloblastoma cell lines.

(A, C, E, F) Representative experiments showing the number of colonies formed by the Daoy (A), D341 (C) medulloblastoma cell line polyclonal populations transduced with control pTRIPZ vector 'C' or pTRIPZ-miR-204 construct 'P1 / P2' with (+ DOX) or without doxycycline treatment and in D283 (E), D425 (F) cells transfected with siGLO control or miR-204 mimic as studied by the colony formation in soft agar. In B, D and G the Y axis denotes the percentage reduction in colony formation upon doxycycline treatment of the indicated polyclonal populations compared to the un-treated population. 'ns' indicates non-significant, ** indicates $p \leq 0.01$ and *** indicates $p \leq 0.001$.

expressing miR-204 whereas there was 25-30 % ($p \leq 0.01$) reduction in colony formation of D425 cells expressing miR-204 as compared to the respective control siGLO transfected cells (Figure 4.3.5 E, F, G).

D. Effect of miR-204 expression on invasion potential of medulloblastoma cell lines

The effect of miR-204 expression on the invasion potential of Daoy and D283 cells was studied using matrigel coated Boyden chamber inserts. The D425 and D341 cell lines were not found to invade through these inserts. Hence, the invasion potential of these cell lines could not be studied in this assay. Polyclonal populations of Daoy with or without induction with doxycycline and the siGLO / miR-204 mimic transfected D283 cells were incubated for 36 and 56 hr respectively in the matrigel coated Boyden chamber inserts. The cells were labelled with Calcein AM, a fluorescent dye prior to the termination of the assay. After wiping the cells off the upper side of the membrane, fluorescence intensity of the lower side of the membrane was measured. The fluorescence intensity normalised to the initial number of cells seeded served as a quantitative assessment of the invasion potential. There was no significant difference in the invasion potential of vector control Daoy cells with or without induction with doxycycline. Doxycycline induction of miR-204 expression in the polyclonal populations of Daoy cells resulted in ~50 % ($p \leq 0.001$) (Figure 4.3.6 A, B, D) reduction in invasion as compared to the un-induced control cells. MiR-204 mimic transfected D283 cells also showed ~50 % ($p \leq 0.001$) reduction in invasion as compared to the control siGLO transfected cells (Figure 4.3.6 C, D).

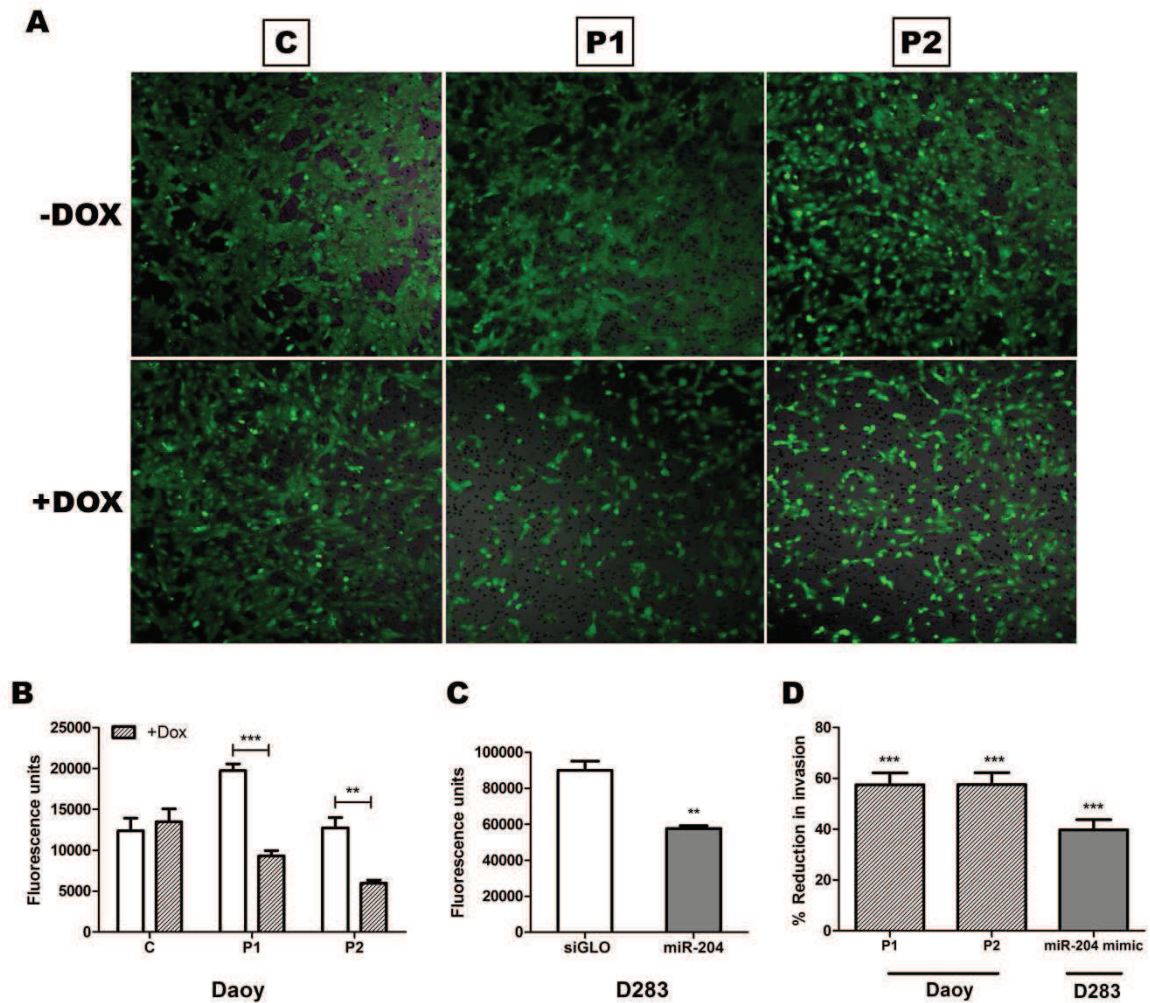


Figure 4.3.6: Effect of miR-204 expression on invasive potential of Daoy and D283 cell lines.

(A) Representative images of Calcein, AM labelled Daoy cells on the lower side of matrigel coated transwell chamber membrane post invasion of the indicated polyclonal populations with or without doxycycline induction of miR-204 expression. In B and C the Y axis denotes total fluorescence intensity of the invaded cells normalised to the total intensity of the initial cell number seeded of the indicated cell populations. D) Y axis indicates percent reduction in the fluorescence of the invaded cells of the P1 and P2 polyclonal populations of Daoy and miR-204 mimic transfected D283 cells. ** indicates $p \leq 0.01$ and *** indicates $p \leq 0.001$.

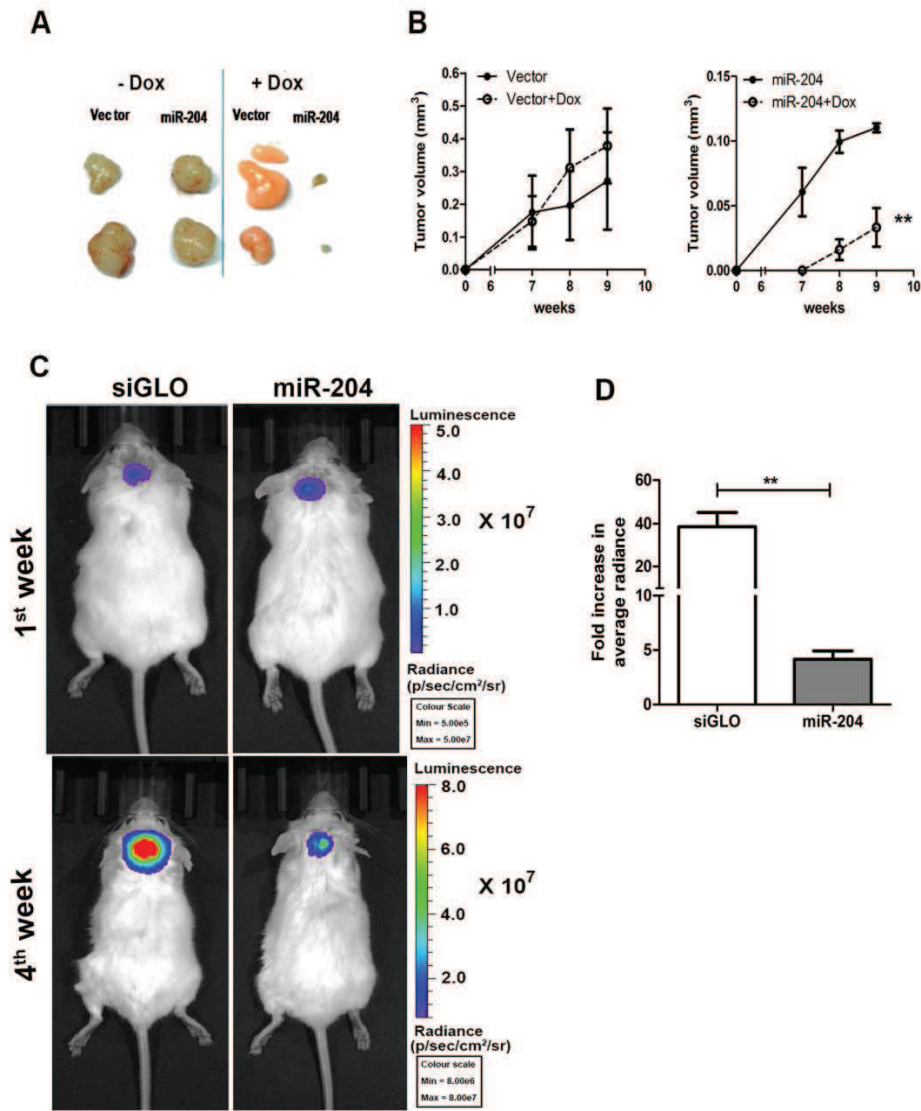


Figure 4.3.7: Effect of miR-204 expression on tumorigenicity of medulloblastoma cell lines.

(A) Representative photographs of the subcutaneous tumors formed 9 weeks post injection of doxycycline induced Daoy P1 polyclonal population (pTRIPZ-miR-204) and vector (pTRIPZ) control population (B) Y axis denotes the volume of tumors formed by the vector and miR-204 expressing cells with or without doxycycline induction in a period of 9 weeks post-injection of tumor cells. (F) Bioluminescence images of NOD/SCID mice orthotopically injected with luciferase labelled D283 cells transfected with siGLO control or miR-204 mimic. The images were captured on 1st and 4th week after the injection. (C) Y axis shows relative fold increase in the average radiance on 4th week as compared to that on 1st week after injection in the indicated cells. ** indicates $p \leq 0.01$.

E. Effect of miR-204 expression on in-vivo tumorigenicity of Daoy and D283 cell lines in immunodeficient mice

In-vivo tumorigenicity of Daoy cells was studied by injecting 4.5×10^5 cells subcutaneously in NOD/SCID mice. The pTRIPZ vector control 'C' and pTRIPZ- miR-204 'P1' population of Daoy cells induced with doxycycline for 72 h were injected on either flank of the same mouse (n = 3). The uninduced cells of the 'C' and 'P1' populations were also injected in a similar manner in a separate set of mice (n = 3). The mice injected with the induced cell populations were fed with 1 mg / ml of doxycycline in 5 % sucrose solution. Visible tumours were seen in the control mice by ~7 weeks post injection. The tumors formed were measured using a vernier calliper and the volume of the tumor calculated. There was ~70 % ($p \leq 0.01$) reduction in the volume of the tumors formed by miR-204 expressing cells as compared to that of the uninduced control cells (Figure 4.3.7 A, B).

D283 cells were engineered to stably express firefly luciferase using the pCAG luciferase vector (Addgene). These cells were transfected with siGLO control / miR-204 mimic and were injected at the midline 3 mm posterior to the lambdoid suture at a depth of 2.5 mm in the cerebellum of NOD/SCID mice using a stereotactic apparatus. The growth of the tumors was monitored using bioluminescence imaging. The normalised luminescence represented as average radiance reflects the tumor growth. There was ~10 fold reduction in the average radiance of the tumors formed by the miR-204 mimic transfected D283 cells as compared to the siGLO transfected control cells 4 weeks post injection as determined by *in vivo* imaging (Figure 4.3.7 C, D).

Thus, miR-204 expression was found to inhibit tumorigenic potential of two medulloblastoma cell lines Daoy and D283 in either subcutaneous xenograft mouse model or intracranial xenograft mouse model system respectively.

4.3.4 Identification of the molecular mechanism underlying the effect of miR-204 by genome wide expression profiling

Genome wide expression analysis of miR-204 expressing Daoy and D283 cells was carried out in order to study the changes in gene expression profile upon miR-204 expression and to identify potential targets of this miRNA. Whole-Genome Gene Expression Direct Hybridization Assay (Illumina, San Diego, USA) was used for the gene expression profiling. The data was normalized by average normalisation using the Genome studio software (Illumina, San Diego, USA). Expression profiles of miR-204 expressing polyclonal populations (P1 and P2) of Daoy was compared with that of Daoy cells stably transduced with pTRIPZ control vector while the expression profile of miR-204 mimic transfected D283 cells was compared with that of siGLO transfected control cells. The validated target genes of miR-204 such as *RAB22A* (Ras family member) , *M6PR* (Mannose-6-phosphate receptor), Ezrin (*EZR*), *APIS2* (adaptor-related protein complex 1, sigma 2 subunit), *EDEMI*(ER degradation enhancer, mannosidase alpha-like 1) and *BCL2L2* (BCL2-like 2) [84-86] were found to be downregulated by 1.5 - 6 folds in the miR-204 expressing Daoy cells as compared to the vector control cells (Figure 4.3.8). The downregulation of expression of these miR-204 target genes in D283 cells was found to be at a lesser extent (fold change = 1.1-1.6 fold). Hence, the validation of expression of the known target genes, *RAB22A*, *M6PR*, *EZR*, *APIS2*, *EDEMI* and *BCL2L2* was validated by real time RT-PCR in the stable polyclonal populations of Daoy and D341 cell lines. The expression of *RAB22A* and *M6PR* was found to be downregulated by ~1.5-2 fold in the miR-204 expressing Daoy and D341 cell lines (Figure 4.3.9 A, B). The expression of *APIS2*, *BCL2L2* and *EDEMI* was found to be very low (R.Q. < 0.5) in Daoy cells and hence there was no significant difference in the expression of these genes in the control and miR-204 expressing Daoy cells (Figure 4.3.9 C, D, F). MiR-204 expressing D341 cells showed 2-10 fold downregulation of *APIS2*, *BCL2L2*

and *EDEMI* gene expression as compared to the uninduced control cells (Figure 4.3.9 C,D,F). There was no significant downregulation of Ezrin expression in Daoy cells, however it was found to be downregulated by 2 fold in D341 cells.

The other target genes for miR-204 including *FOXC1* (forkhead box C1), *SIRT1* (sirtuin 1) and *EZR* are highly expressed in the Daoy medulloblastoma cell line and were found to be downregulated 1.2-1.4 fold in the miR-204 expressing cells as compared to the control cells in the gene expression analysis [87, 88]. MAP1LC3B (Microtubule-Associated Protein 1 Light Chain 3 Beta) is a protein involved in the process of autophagy and has also been shown to be a target of miR-204 [89]. The effect of miR-204 on the expression of these genes was studied by western blot analysis. These genes have been shown to play important roles in cancer enhancing process like stem cell maintenance (*FOXC1*), migration (*EZR*), epigenetic modifications (*SIRT1*) and autophagy (*MAP1LC3B*). MiR-204 was found to bring about downregulation of the *EZR* and *FOXC1* gene expression in the Daoy cells. *EZR* expression was found to be downregulated in the D341 and D283 cell lines as well (Figure 4.3.10 A, C). The group 3 medulloblastoma cell lines have very low levels of *FOXC1* gene expression and cannot be detected by western blot analysis. There was no significant effect of miR-204 expression on the level of *SIRT1* and *MAP1LC3B* in Daoy cells (Figure 4.3.10 A, B).

Most of these genes including *RAB22A*, *M6PR*, *APIS2* and *EDEMI* carry out functions involved in intracellular protein trafficking. *FOXC1* is involved in maintenance of stem cell like characters of cells while Ezrin is involved in the formation of filopodia important for the migration / invasion of cells. This indicates that miR-204 targets genes involved in various cellular processes to bring about the phenotypic effect on medulloblastoma cell lines.

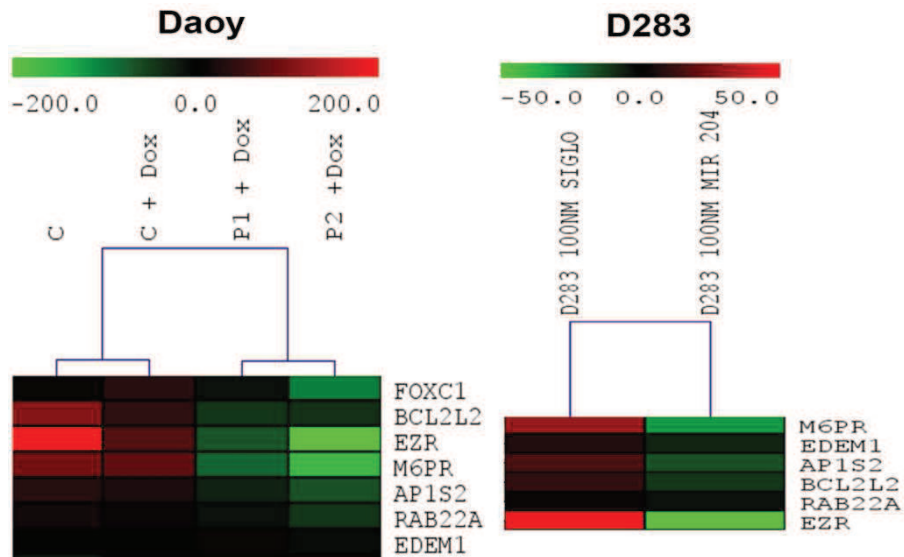


Figure 4.3.8: Gene expression analysis of miR-204 expressing Daoy and D283 cells

The heat maps show the downregulation of miR-204 target genes in the pTRIPZ vector control ‘C’ with or without doxycycline induction and miR-204-pTRIPZ polyclonal populations ‘P1 and P2’ with doxycycline induction of miR-204 expression in Daoy cells and siGLO or miR-204 mimic transfected D283 medulloblastoma cell lines. Heat maps generated using the MeV module of the TM4 package. (<http://www.TM4.org>).

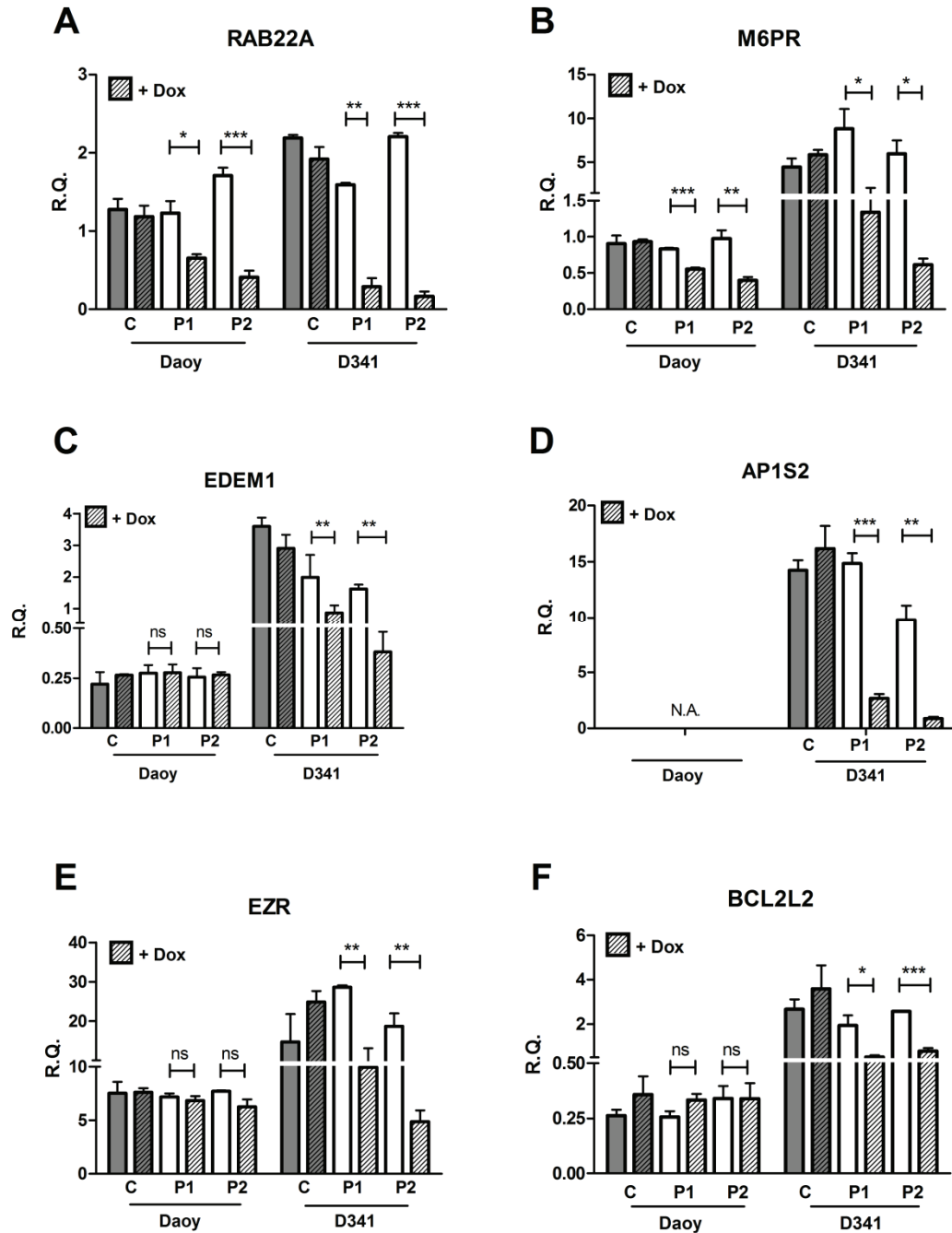


Figure 4.3.9: Effect of miR-204 expression on the mRNA levels of the target genes.

The graphs show real time RT-PCR analysis of the indicated miR-204 target genes. The Y-axis represents the relative quantity (R.Q.) in the pTRIPZ vector control 'C' and miR-204-pTRIPZ polyclonal populations 'P1 and P2' of Daoy and D341 cells before and after doxycycline induction of miR-204 expression. 'ns' indicates non-significant, * indicates $p \leq 0.05$, ** indicates $p \leq 0.01$ and *** indicates $p \leq 0.001$

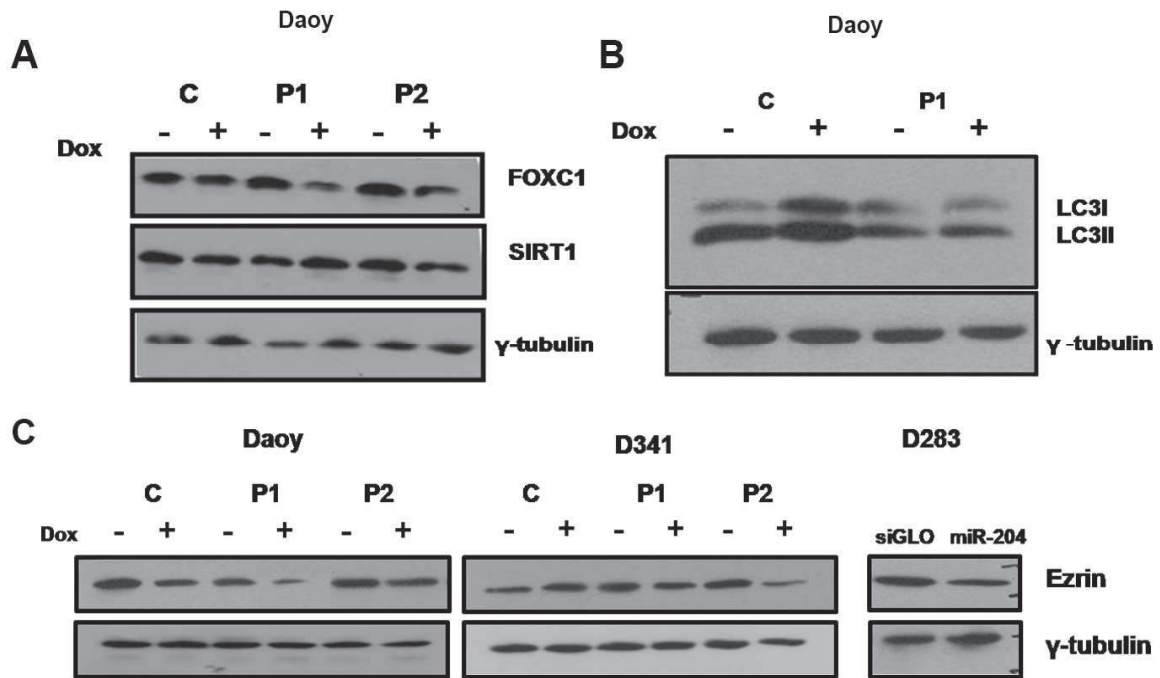


Figure 4.3.10: Effect of miR-204 expression on the expression of target genes

(A) Western blot analysis of the indicated polyclonal populations of Daoy cells for FOXC1 and SIRT1 expression. (B) Western blot analysis of the indicated polyclonal populations of Daoy cells for MAP1LC3B (LC3I and LC3II) expression. (C) Western blot analysis of the indicated polyclonal populations of Daoy and D341 cells and siGLO / miR-204 mimic transfected D283 cells for Ezrin expression.

4.3.5 Ezrin expression in medulloblastomas and its correlation with molecular subgroups and survival

Ezrin, a validated miR-204 target gene, is a cytoskeletal crosslinker protein that has been reported to be overexpressed in all medulloblastoma tumors. SiRNA mediated downregulation of ezrin has been reported to inhibit invasion potential of medulloblastoma cell lines [90]. Ezrin has also been reported to be involved in metastasis of various cancers [90-93]. In this study, Ezrin expression was found to be downregulated in Daoy, D341 and D283 cells expressing miR-204 as compared to the control cells as studied by western blot analysis indicating that effect of miR-204 on inhibition of invasion potential of medulloblastoma cell lines maybe at least partially mediated via the downregulation of ezrin expression. Hence, an immunohistochemical analysis for Ezrin expression was carried out in 108 medulloblastoma tumors tissues to determine its expression across the 4 subgroups which also differ in the incidence of metastasis. The 108 medulloblastoma tumors include tumors belonging to the WNT (23 tumors), SHH (34 tumors), Group 3(20 tumors) and Group 4 (30 tumors) subgroups. The staining intensity was scored by a neuropathologist as ‘negative’ for complete absence of staining, ‘Low’ for weak intensity and focal positive (~10-20 % cells positive) areas, ‘Moderate’ for moderate intensity and more than or equal to 50 % positive area while, ‘High’ for high intensity of staining in more than 80 % of area. Majority of the WNT (100 %) and SHH (91 %) tumors showed negligible to low expression of Ezrin.(Figure 4.3.11 A, B) On the other hand ~35 % Group 3 and Group 4 tumors showed moderate to high level of Ezrin expression. Thus, there was a significant difference in Ezrin expression across the four subgroups of medulloblastoma (Chi square test, $p = 0.0001$) especially with respect to its higher expression in the group 3 and 4 tumors. However, Kaplan Meier analysis did not show significant correlation of Ezrin expression with survival within the group 3 and group 4 patients (Figure 4.3.11 C).

4.3.6 Identification of novel miR-204 target genes

The gene expression analysis of miR-204 expressing medulloblastoma cells showed the downregulation of putative miR-204 target genes along with the validated target genes described above. The genes that were predicted to be miR-204 targets by the miRNA target prediction tool ‘Targetscan’ and their expression level in the miR-204 expressing cells as compared to the vector control cells in the gene expression profiling was analysed. Two genes, *RAB10* and *ANGPTL2* were identified as putative miR-204 target genes which were also found to be downregulated by 1.5 fold and 3-5 fold respectively in miR-204 expressing Daoy cells as compared to the vector control cells in the gene expression analysis. The gene *NRPI* is also a predicted target gene of miR-204 which has recently been shown in our lab to be a target of miR-148a and to play a role in the invasion of medulloblastoma cells [16]. Hence, the 3’ UTR of the *EZR*, *RAB10* and *ANGPTL2* genes was cloned into a luciferase reporter vector to identify the direct targets of miR-204. The *NRPI* 3’ UTR vector construct was already available in the lab. *EZR* is a known target gene of miR-204 and was found to be downregulated in miR-204 expressing medulloblastoma cell lines as studied by western blot analysis. Hence, it was used as a positive control for the luciferase reporter assay. A luciferase reporter construct containing three miR-204 binding sites upstream of the luciferase gene (miR-204 sponge) cloned in the pcDNA3.0 vector was also used as a positive control. The luciferase reporter constructs were co-transfected with either the pGIPZ vector alone or the miR-204 –pGIPZ vector in 293T cells. The pGIPZ vector also expressed GFP which was used for normalisation of the luciferase activity. There was 50-60 % reduction in the luciferase activity of the miR-204 sponge upon co-transfection with the miR-204-pGIPZ vector. The luciferase reporter activity for *EZR* was found to be reduced by ~30 % ($p \leq 0.001$) on co-transfection of the *EZR* 3’ UTR luciferase construct along with miR-204-pGIPz construct (Figure 4.3.12 A). Similarly, the luciferase reporter activity for *RAB10* 3’ UTR

construct was found to be reduced by ~30 % ($p \leq 0.001$) while that of the *NRPI* construct was found to be reduced marginally. There was no significant difference in the luciferase activity of the *ANGPTL2* 3'UTR luciferase reporter vector on cotransfection with miR-204-pGIPz plasmid construct. Thus, *RAB10* was found to be a putative direct target of miR-204, while *ANGPTL2* and *NRPI* may not be direct targets of miR-204. To further validate *RAB10* as a target gene of miR-204, the miR-204 binding site in the 3'UTR of the *RAB10* gene was mutated using site directed mutagenesis (Figure 4.3.12 B). Luciferase reporter assay with the mutant *RAB10* 3'UTR construct carried out in the presence of miR-204 did not result in any change in the luciferase activity, validating RAB10 as a target of miR-204. Western blot analysis for RAB10 expression in Daoy and D341 cells expressing miR-204 was carried out study the effect of miR-204 expression on the level of RAB10 expression. The miR-204 expressing cells showed reduction in the level of RAB10 expression at the protein level (Figure 4.3.12C). Thus, *RAB10* was confirmed to be a direct target of miR-204.

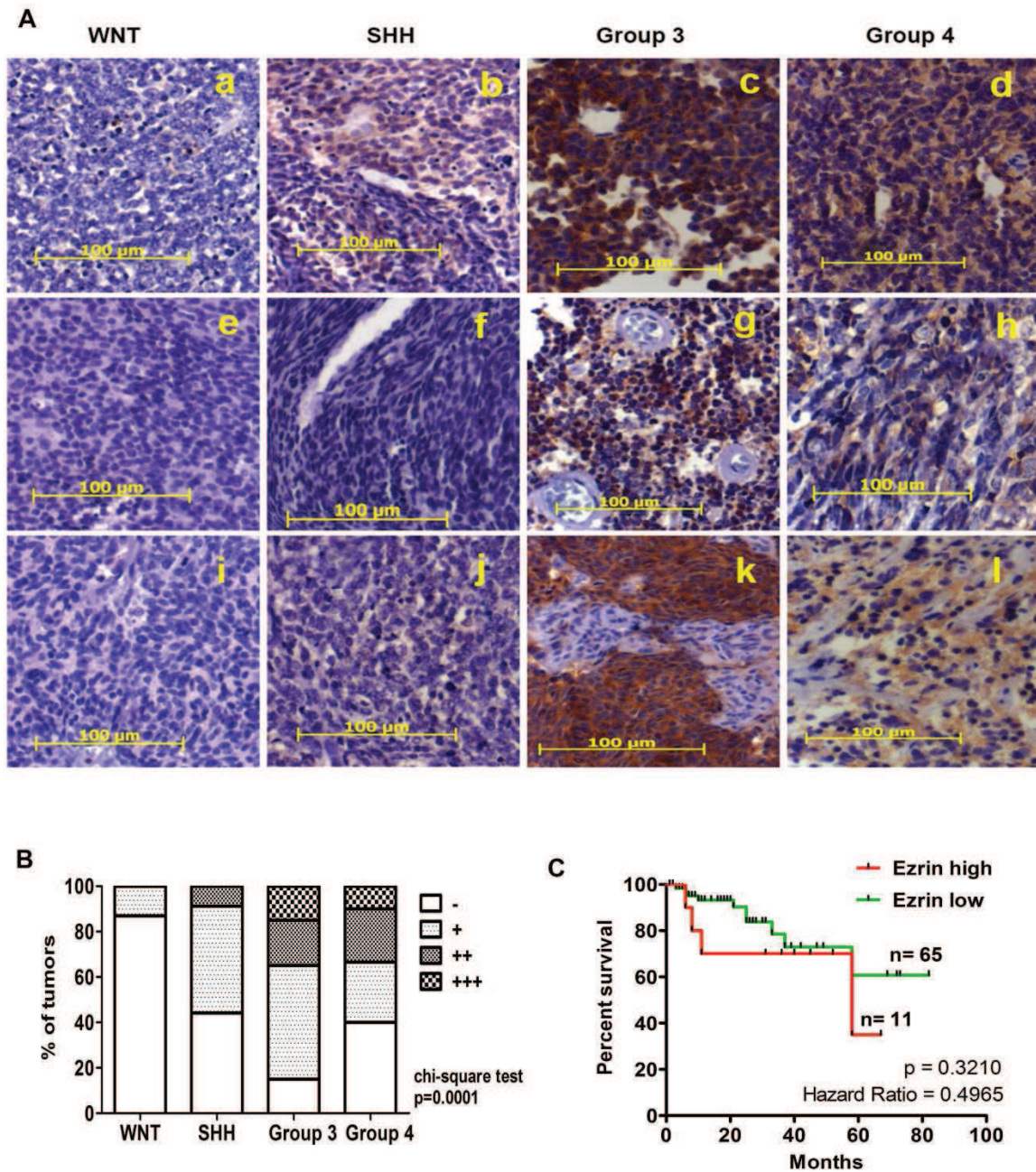


Figure 4.3.11: Immunohistochemical analysis of Ezrin expression in medulloblastoma tumor tissues and its correlation with survival.

(A) Representative images of Ezrin expression in the (a, e, i) WNT subgroup, (b, f, j) SHH subgroup (c, g, k) group 3 and (d, h, l) group 4 medulloblastoma tissues as evaluated by immunohistochemical analysis. (B) Percentage distribution of medulloblastoma tissues having Ezrin expression scored as negative (-), low (+), moderate (++) or high (+++) is shown across the four subgroups of medulloblastomas. (B) Kaplan Meier survival analysis of 76 medulloblastoma patients segregated into two groups based on Ezrin expression. “Ezrin low” group includes medulloblastoma tissues with no or low Ezrin expression while “Ezrin high” group includes tumor tissues with moderate or high Ezrin expression

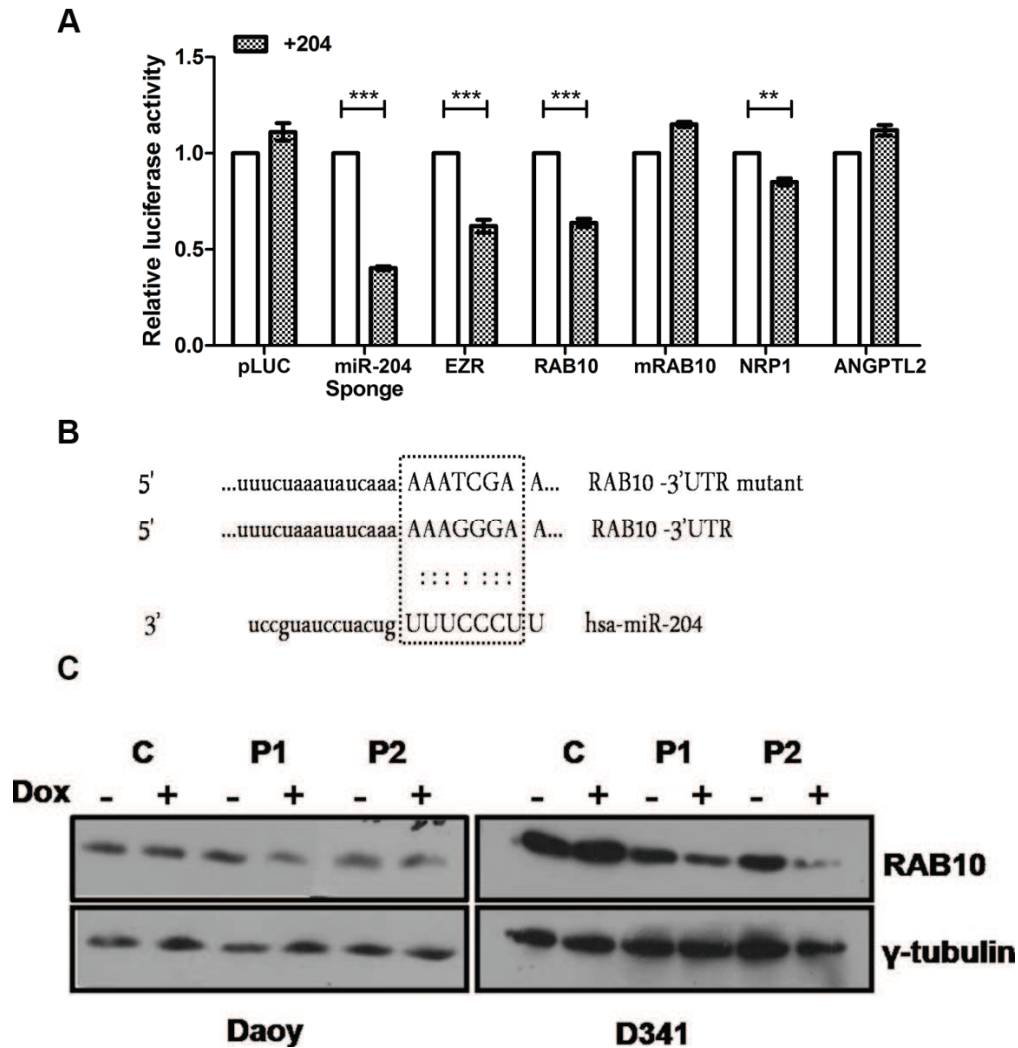


Figure 4.3.12: *RAB10* is a direct target gene of miR-204

(A) Luciferase reporter assay for putative miR-204 target genes *RAB10*, *NRP1* and *ANGPTL2*. The Y-axis represents the luciferase expression relative to the GFP levels (B) Schematic representation of miR-204 binding sequence in the 3' UTR region of *RAB10* gene and position of the mutations in the binding sequence introduced by site directed mutagenesis. (C) Western blot analysis of RAB10 expression in polyclonal populations (P1, P2 and control C) of D341 and Daoy cells with (+) or without (-) doxycycline induction of miR-204 expression. γ -tubulin was used as the loading control. ** indicates $p \leq 0.01$ and *** indicates $p \leq 0.001$

4.3.7 CpG island methylation of miR-204 promoter region

MiR-204 expression is downregulated in all SHH group tumors and in most Group 3 tumors. In order to understand the role of promoter CpG island methylation in the downregulation of miR-204 expression, bisulphite sequencing was carried out on the DNA from the Daoy, D425, D283 and D341 medulloblastoma cell lines. MiR-204 is an intronic miRNA and is known to be co-expressed with the shorter transcripts *TRPM3*-005 and 010 of the *TRPM3* gene. In medulloblastoma tumors, the expression of the *TRPM3* gene and miR-204 is directly correlated with both showing higher expression in the WNT and Group 4 tumors as compared to that in SHH and Group 3 tumors. A 584 bp CpG island upstream of the miR-204 / *TRPM3* gene and close to the known transcription start site of the *TRPM3* gene was predicted by the UCSC genome browser (Figure 4.3.13 A). PCR amplification of a 203 bp region of the CpG island of the bisulphite treated DNA was carried out. The PCR products were sequenced using both the forward and reverse primers. All the 'C' nucleotides which were not a part of the CpG dinucleotide were found to be converted to T indicating complete bisulphite conversion. The 'C' nucleotides constituting the 22 CpG dinucleotides within the PCR product were also found to be converted to 'T' indicating that none of the 22 CpG's were methylated (Figure 4.3.13 B). Thus, the methylation of the CpG island closest to the *TRPM3* / miR-204 promoter may not play an important role in downregulation of miR-204 expression in medulloblastoma.

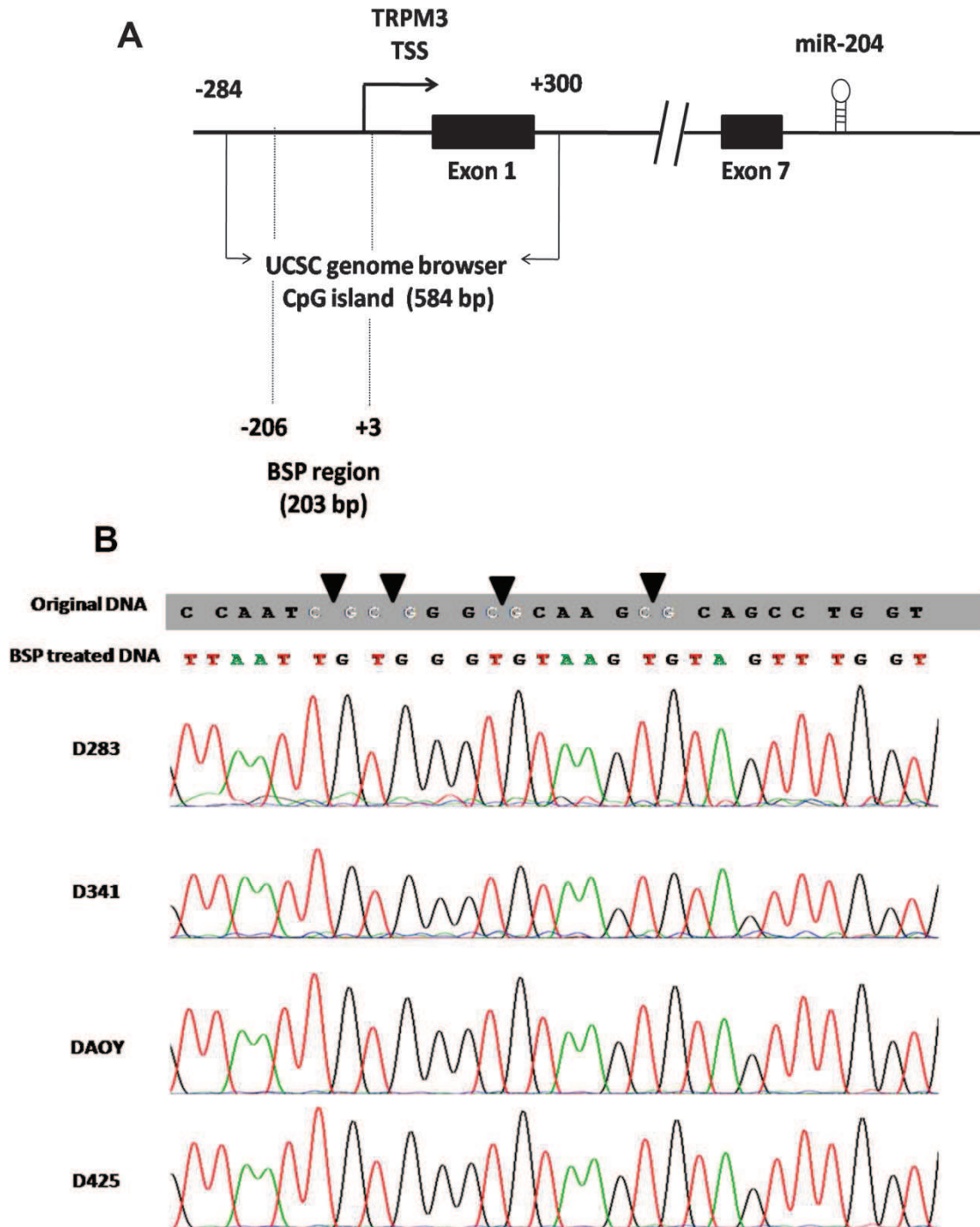


Figure 4.3.13: Methylation status of the miR-204 promoter region.

(A) Schematic representation of the location of the CpG island, and the region sequenced in the promoter region of the *TRPM3* gene. (B) Representative electropherograms showing methylation status of a region of the CpG island of the *TRPM3* gene from the indicated medulloblastoma cell lines. Black arrows indicate the CpG sites within the CpG Island.

DISCUSSION

MiR-204 is located within the sixth intron of the host gene *TRPM3* (transient receptor potential melastatin 3 cation channel) and is transcribed in the same direction as *TRPM3*. Its paralog, miR-211 is located within the *TRPM1* gene at locus 15q13.3. The miR-204 and miR-211 sequences vary only by two nucleotides outside their seed sequences. However the two miRNAs show differential expression across tissues with miR-204 being expressed at a much higher level in most tissues as compared to miR-211[94]. MiR-204 expression is particularly enriched in the brain and kidneys. In the mouse brain, miR-204 expression has been shown to be enriched in the choroid plexus closest to the 4th ventricle, during normal development as well as in adults [95]. It has been shown to play a role in cell differentiation, apoptosis, stress response and inflammation, lens and retinal development and in the maintenance of axonal structure and function [96-98]. MiR-204 is located within the cancer associated genomic region 9q21.1–q22.3 locus that exhibits high frequency of loss of heterozygosity in some types of tumors, such as squamous cell carcinoma of the head and neck [99]. In a large scale study on 3312 tumors, 1107 non-malignant tissues, miR-204-211 family was found to be the top deleted family among all miRNAs [100]. MiR-204 is differentially expressed in the four molecular subgroups of medulloblastomas. It is downregulated in the SHH tumors and in most group 3 tumors as compared to the normal cerebellum. Hence, the present work addressed the role of miR-204 in the biology of medulloblastoma. Kaplan Meier Survival analysis of patients with group 3 and Group 4 tumors indicated a significantly better survival (hazard ratio = 5.55; $p \leq 0.0001$) of patients with high miR-204 expression as compared to those with low miR-204 expression. Group 3 and Group 4 medulloblastomas have overlapping gene expression profiles. However, most Group 3 medulloblastomas have poor survival as compared to that of most Group 4 patients. Some non-WNT, non-SHH medulloblastomas have expression profiles intermediate between that of Group 3 and

Group 4. Accurate risk stratification therefore is urgently required in the non-WNT, non-SHH subgroup tumors. Based on the aforementioned finding of miR-204 expression correlating significantly with the better survival suggests miR-204 as a useful prognostication marker in non-WNT, non-SHH group of medulloblastomas. Further validation of this finding in larger number of medulloblastomas and in relation with other prognostication markers would confirm the utility of miR-204 as a marker for better risk stratification and thereby appropriate treatment design for the non-WNT, non-SHH medulloblastomas.

The positive correlation of miR-204 expression with better survival of medulloblastoma patients suggested a tumor-suppressive role for miR-204, in medulloblastomas. In order to understand the role of miR-204 in medulloblastoma biology, miR-204 was expressed in multiple medulloblastoma cell lines *viz* Daoy, D341, D283 and D425 which show downregulation of mir-204 expression as compared to normal cerebellum tissues. The effect of restoration of miR-204 expression on the growth characteristics of these cell lines was studied. The anchorage independent growth potential of the Daoy, D341 and D425 cells was found to be reduced by 25 - 40 % ($p \leq 0.01$) upon the expression of miR-204. There was a ~50 % ($p \leq 0.001$) decrease in the *in-vitro* invasion potential of Daoy and D283 cells. *In vivo* tumorigenicity of Daoy and D283 cells was also found to be substantially (70-80 %) reduced upon miR-204 expression. MiR-204 has been reported to play a tumor suppressive role in many other cancers. MiR-204 has been shown to inhibit the invasion and migration of glioma and peripheral nerve sheath tumor cells [101, 102]. It has been shown to bring about reduction in the *in-vivo* tumorigenicity of clear cell renal cell carcinoma as well as colorectal cancer cells [84, 89]. Thus, the tumor suppressive role of miR-204 in medulloblastoma cells is consistent with its role in other cancers.

MiRNAs function via binding to their target mRNA's resulting in their degradation or inhibition of translation. A single miRNA can mediate its effects by targeting multiple mRNAs. Gene expression analysis of mir-204 expressing Daoy and D283 cells showed downregulation of eight genes by 1.5 to 6 fold that are known to be miR-204 targets [85-88]. These 8 genes include *EZR*, *RAB22A*, *M6PR*, *EDEMI*, *APIS2*, *BCL2L2*, *FOXC1* and *SIRT1*. The downregulation of *RAB22A* and *M6PR* was further validated in both Daoy and D341 cells by real time RT PCR analysis. *APIS2*, *EDEMI* and *BCL2L2* gene expression was found to be downregulated in D341 cells which express these genes at a 10 fold higher level as compared to Daoy cells. The downregulation of *FOXC1* and Ezrin expression was validated by western blot analysis. Additionally, *RAB10* was identified as a novel miR-204 target by the luciferase reporter assay. Western blotting analysis also showed downregulation of *RAB10* expression in miR-204 expressing Daoy and D341 cells.

The miR-204 target genes including *RAB10*, *RAB22A*, *M6PR*, *APIS2* and *EDEMI* are all involved in a single cellular process i.e. intracellular protein trafficking. Downregulation of these genes indicates to the role of miR-204 in the perturbation of protein trafficking within the cells. Protein trafficking is a process involving a complex interplay of various proteins. Proteins are synthesized in the ER and transported to the Golgi and then to the plasma membrane or other endosomal compartments in what is known as the anterograde protein transport. The trans golgi network (TGN) packages the proteins into specific vesicles for delivery to their destination. The second mode of transport is the retrograde transport wherein proteins are internalised from the membrane and move via the early endosomes to the late endosomes and finally to the lysosomes for degradation. The proteins may also get recycled back to plasma membrane via recycling endosomes in a retrograde transport pathway.[103]

The *RAB10* and *RAB22A* genes are members of the RAB family of small GTPase's. The GTP bound active RAB proteins recruit effector complexes which are involved in transport vesicle formation, tethering of vesicles at their target membranes and microtubule-dependent organelle motility [104]. Several studies have shown changes in RAB protein expression, some of which correlate with tumour aggression or metastasis [105]. RAB10 is known to localise in the golgi, ER and recycling endosomes in different cell types. In MDCK (Madin–Darby Canine Kidney) epithelial cells RAB10 is known to play a role in the polarised transport of cargo in the basolaterally polarised cells. RAB10 GTPase activated mutants have been shown to retain the cargo at the trans-Golgi network (TGN) as well as mistarget cargo to the apical surface instead of the basolateral surface in these epithelial cells thus altering the polarity of the cells [106]. Such changes in polarity are known to promote migration and invasion of epithelial cells and are a key step in the process of epithelial to mesenchymal transition [107]. RAB10 has also been shown to play a role in directional membrane insertion during axonal development in neurons again indicating its role in polarised trafficking [108, 109]. It has been found to be one of the genes upregulated during invasion of hepatocellular carcinoma cells in an *in vitro* study [110]. Knockdown of RAB10 using siRNAs increases cell surface hyaluronan synthase 3 localisation in turn stimulating hyaluronan synthesis, and reducing cell adhesion to type I collagen [111]. Thus, RAB10 downregulation is likely to contribute to the inhibition of invasion of Daoy and D283 cells upon miR-204 expression.

The *RAB22A* gene is known to localise in the recycling endosomes, indicating to its role in receptor recycling at the cell surface and in retrograde transport. Ligand bound receptors internalised via this process may be recycled back to the plasma membrane while their ligands are directed to the lysosomes for degradation. In this process, RAB22A is known to interact with the early endosomal antigen 1 (EEA1) protein which is a marker of the early endosomes [25]. Inactive RAB22A results in improper recycling of receptors such as the

transferrin receptor and the epidermal growth factor receptor (EGFR) to the plasma membrane [26, 27]. MiR-204 mediated downregulation of RAB22A may be involved in the reduced recycling of cell surface receptors like EGFR resulting in decreased cellular growth and communication. One of the mechanisms of internalisation of proteins is via the formation of clathrin coated vesicles at the plasma membrane. The AP1S2 protein is a part of the AP1 complex involved in the formation of clathrin coated vesicles important in both anterograde and retrograde transport. Thus, miR-204 expression may perturb the formation of clathrin coated vesicles via the downregulation of AP1S2 expression. The function of these target genes indicate a role of miR-204 in regulation of the intercellular protein trafficking. Indeed, perturbations in the vesicular trafficking have been reported to have important implications in loss of cellular polarity, inappropriate trafficking of junctional and / or cell adhesion molecules which is involved in the early steps of malignant transformation [105].

The Mannose-6-Phosphate Receptor (M6PR) is important for the transport of lysosomal enzymes from the ER to lysosomes. The enzymes synthesized in the ER are tagged with Mannose-6-phosphate (M6P) group in the golgi and transported to the lysosomes through the TGN. The TGN is the main sorting centre where the cargo proteins are packaged into specific vesicles for delivery to their destinations. The M6P tagged lysosomal enzymes are recognised by the M6PR which mediates its specific transport to the lysosomes. The M6PR's are recycled back to the TGN after their dissociation from the lysosomal enzymes [112]. Expression of an inactive RAB22A mutant has also been shown to result in abnormal accumulation of lysosomal enzymes in vacuole like structures [113]. This indicates that RAB22A may also function in the movement of lysosomal enzymes. Thus, the downregulation of RAB22A and M6PR by miR-204 suggests a compromised lysosomal enzyme transport leading to an inhibition of lysosomal function. In ccRCC (clear cell Renal Cell Carcinoma), miR-204 has been shown to inhibit autophagy by directly targeting

MAP1LC3B, a protein important in the initialisation of autophagy [89]. However, miR-204 was not found to bring about downregulation of MAP1LC3B levels in Daoy cells as studied by western blot analysis. Nonetheless, miR-204 expression may still have an effect on the autophagy in medulloblastoma cells via inhibition of the lysosomal function rather than by directly targeting MAP1LC3B.

MiR-204 expression was also found to bring about downregulation of FOXC1, a transcription factor involved in eye and cerebellum development, in Daoy medulloblastoma cells. During the cerebellum development, the loss of FOXC1 expression results into decrease in ventricular zone radial glial cell proliferation and an increase in cerebellar neuronal differentiation [114]. In basal like breast cancer cells FOXC1 expression increases the invasion potential of endometrial and breast cancer cell lines [87, 115]. Thus, the downregulation of FOXC1 expression is also likely to contribute to the effect of miR-204 expression on the growth and malignant behaviour of Daoy cells.

Ezrin is another target gene of miR-204 that was found to be downregulated in Daoy, D283 and D341 cells at the protein level. It is a cytoskeletal crosslinker protein and is a part of the ezrin-radixin-moesin complex which is involved in the formation of filopodia which enables the migration of cells. Downregulation of Ezrin expression in medulloblastoma cells has been reported to result in inhibition of the migration potential of medulloblastoma cell lines [90]. Therefore, the downregulation of Ezrin expression by miR-204 may additionally contribute to the reduction in the invasion potential of Daoy and D283 cells. The study of Ezrin expression across medulloblastoma subgroups carried out using immunohistochemistry showed none to negligible expression in all the WNT tumors studied, while the highest expression was seen in the group 3 tumors. The Group 3 medulloblastomas are known to have the highest degree of metastasis while the WNT tumors rarely metastasize. On the other hand, the metastasis rate in the group 4 tumors is moderately higher than that in SHH tumors. Thus, the expression

of Ezrin across the medulloblastoma subgroups may correlate with the degree of metastasis. This observation needs to be further validated by investigating the correlation of Ezrin expression to the metastatic status in medulloblastoma patients. This may help determine if the degree of Ezrin staining may be useful as a marker for the metastatic potential of tumors especially in group 3 and group 4 tumors. Although, we did not find any correlation of Ezrin expression with survival of patients, its correlation with metastasis could not be studied due to the unavailability of relevant clinical data.

The level of miR-204 expression in the WNT and group 4 tumors is 2-4 fold higher than that in the normal cerebellum. In the SHH and most group 3 tumors on the other hand, miR-204 expression is downregulated as compared to that in the normal cerebellum. 47 % of SHH tumors and 21 % of group 3 tumors show loss of the chromosome 9q on which the miR-204 gene is located [8]. This loss of chromosome 9q would contribute to the downregulation of miR-204 expression in these subgroups. However the mechanism of downregulation in the rest of the medulloblastomas is not understood. Bisulphite sequencing of the CpG island in the promoter region of miR-204 gene from one SHH pathway cell line (Daoy) and other group 3 cell lines (D283, D425 and D341) did not find the CpG island to be methylated. The promoter of the *TRPM3* gene was not found to be methylated in the whole genome bisulphite sequencing analysis of 34 human and 5 murine medulloblastoma tissues along with 8 normal and 5 murine normal tissues corroborating with our results [116]. Methylation of the CpG island in the promoter region of the miR-204 gene has been shown to occur only in gliomas [101]. In ccRCC, the expression of miR-204 has been shown to be regulated by the Von Hippel Lindau (VHL) protein, which is frequently lost in these tumors leading to a downregulation of miR-204 expression as well. The mechanism underlying downregulation of MiR-204 expression in other malignancies such as neuroblastoma, peripheral nerve sheath tumors, and colorectal cancer is not understood. Thus, while downregulation of miR-204

expression in SHH subgroup medulloblastomas could be due to loss of chr 9q, the mechanism of its downregulation in the non-WNT, non-SHH subgroup medulloblastomas is not understood.

In summary, miR-204 which is differentially expressed across the four medulloblastoma subgroups, acts as a tumor suppressor miRNA in medulloblastoma. It targets multiple genes involved in intracellular protein trafficking and genes known to be involved in cellular invasion and migration. This study draws attention to the underexplored area of the role of vesicle trafficking in the biology of cancer, especially in medulloblastoma. In terms of its clinical relevance, the higher expression of miR-204 in tumors may contribute at least in part to the better survival of the patients within the non-WNT, non-SHH medulloblastomas i.e. the group 3, group 4 tumors. This is important in the light of the lack of complete understanding of the biology of the non-WNT, non-SHH tumors and the need for prognostication markers for appropriate treatment design in these subsets of medulloblastomas. It also provides a novel mechanism for therapy in these subgroup tumors which show lower level of miR-204 expression.

SUMMARY AND CONCLUDING REMARKS

The genomics era has seen a significant improvement in the understanding of medulloblastoma biology. It identified the molecular basis of this clinically heterogeneous disease. The identification of the four molecular subgroups and their association with clinical characteristics has shifted the focus of ongoing research towards identification of subgroup specific mechanisms of pathogenesis. In spite of the technological advances in genomic studies that identified genetic alterations in the medulloblastoma subgroups right upto the single nucleotide level, the biology of the non-WNT non-SHH subgroups in particular still remain poorly understood. In the present study, the role of two miRNAs in the biology of medulloblastoma was studied especially with relevance to their role in the pathogenesis of the non-WNT non-SHH medulloblastoma. The salient features of this study are described below:

Subgroup association of medulloblastoma cell lines

Genome wide expression profiling identified four core molecular subgroups of medulloblastomas. However, the subgroup association of the established medulloblastoma cell lines was not known. The differential expression of a select set of subgroup specific genes (*WIF1*, *HHIP*, *CMYC*, *NMYC*, *OTX2*, *EOMES*, *IMPG2*, *NPR3* and *GRM8*) enables the subgrouping of medulloblastomas into the four subgroups. Based on the expression profile of these genes as well as known chromosomal alterations in these cell lines, the **Daoy cell line** was assigned to the SHH subgroup while all the other cell lines were found to belong to the Group 3 with very high expression of the *MYC* gene.

Role of miR-206 in the pathogenesis of medulloblastoma

- MiR-206 expression was found to be downregulated 10-10,000 fold in most medulloblastoma tumor tissues and cell lines as compared to the normal cerebellum. Its expression was also found to be downregulated ~10 fold in *Smo*^{+/+} transgenic mice tumors and 10-100 folds in *Ptch1*^{+/-} knock-out mice tumors as compared to their

normal cerebellar counterparts. Thus, **miR-206 expression was found to be downregulated in all subgroups of medulloblastoma and in established medulloblastoma cell lines.**

- MiR-206 expression was found to be 50-200 folds lower in the normal cerebrum as compared to that in the normal cerebellum in the human brain. This indicates that **miR-206 is specifically expressed in the cerebellum in the human brain.**
- Although the restoration of miR-206 expression did not affect the growth characteristics of medulloblastoma cell lines, ~50-100 fold overexpression of miR-206 in the Group 3 cell lines D425 and D283 resulted in downregulation of OTX2 expression and ~ 50 % inhibition of colony formation in soft agar. Thus, miR-206 downregulation although is likely to be important during the process of malignant transformation, its overexpression is necessary to bring about downregulation of OTX2 expression and inhibit the growth of medulloblastoma cells.

In summary, expression of miR-206 is enriched in both developing and adult cerebellum and is down-regulated in medulloblastomas belonging to all the four molecular subgroups. Downregulation of miR-206 expression upon malignant transformation suggests its role in medulloblastoma pathogenesis. However, **the tumor suppressive potential of miR-206 appears to be inhibited by the aberrant high expression and / or amplification of its target genes such as OTX2 in medulloblastoma cells**

Role of miR-204 in the pathogenesis of medulloblastoma

- MiR-204 expression was found to be downregulated in the SHH subgroup tumors and in most group 3 tumors as compared to the WNT and Group 4 medulloblastomas. MiR-204 expression was also found to be downregulated in the SHH subgroup cell line, Daoy as well as in the Group 3 cell lines, D283, D425 and D341.

- **MiR-204 expression in the non-WNT, non-SHH tumors was found to correlate with the significantly better survival (hazard ratio = 5.55; p = 0.01) of these patients as studied by Kaplan Meier survival analysis.** This indicates the potential of this miRNA as a marker of better prognosis within the poorly understood non-WNT non-SHH medulloblastoma subgroups.
- Expression of miR-204 in the medulloblastoma cell lines resulted in 30-40% decrease in the anchorage independence potential, ~ 50% reduction in the invasion capacity through matrigel and a substantial (70-80 %) reduction in the tumorigenicity as judged by xenograft formation in immunodeficient mice. These results and the positive correlation of miR-204 expression with better survival of medulloblastoma patients indicate a **tumor suppressive role for miR-204 in medulloblastoma biology.**
- MiR-204 expression resulted in downregulation of its target gene, Ezrin in the Daoy, D283 and D341 medulloblastoma cell lines. Ezrin is highly expressed in medulloblastoma tumors and is known to be associated with the increased metastatic potential of many cancers [85, 90-93, 117]. Thus, **the reduction in invasion potential of medulloblastoma cell lines upon miR-204 expression is likely to be partially mediated by the downregulation of Ezrin expression.**
- Ezrin expression across 108 medulloblastoma tumor tissues from the four molecular subgroups showed differential expression across the subgroups. The highest level of Ezrin expression was seen in the group 3 tumors followed by the group 4 tumors. On the other hand, the WNT and the SHH tumors showed negligible Ezrin expression. Thus, **the high Ezrin expression is observed in the poor prognosis non-WNT non-SHH subgroups of medulloblastoma.**

- A number of genes involved in intracellular protein trafficking including *RAB22A* and *M6PR* among others were found to be downregulated upon miR-204 expression in both the Daoy and D341 medulloblastoma cell lines. These genes are important players in the retrograde transport of proteins, receptor recycling at the cell surface and lysosomal enzyme transport. Thus, **the tumor suppressive effect of miR-204 may be mediated by the perturbation of protein trafficking in medulloblastoma cell lines.**
- ***RAB10* was identified as a novel miR-204 target gene in the present study.** *RAB10* is also a member of the RAB family of proteins involved in intracellular protein trafficking and has been shown to be involved in polarised transport of proteins which is important for maintaining the polarity of epithelial cells and thus is likely to play a role in their migration potential.

In conclusion, miR-204 acts as a tumor suppressor miRNA in medulloblastoma by inhibiting the medulloblastoma cell invasion and tumorigenicity. Group 3 and group 4 medulloblastomas have overlapping gene expression profiles. However, most group 3 medulloblastomas have poor survival as compared to that of most Group 4 patients. Accurate prognostication of these non-WNT, non-SHH medulloblastomas is therefore necessary for appropriate treatment strategies. MiR-204 expression correlating significantly with the better survival suggests miR-204 as a useful marker for accurate risk stratification and thereby appropriate treatment design of the non-WNT, non-SHH medulloblastoma patients. The downregulation of a number of genes involved in a single cellular pathway of intracellular protein trafficking upon miR-204 expression in medulloblastoma cell lines points to a novel molecular mechanism underlying tumor suppressive activity of this miRNA. It brings to attention the relatively less explored field of protein trafficking playing a role in the pathogenesis and growth of cancer, particularly in medulloblastoma. The therapeutic

potential of this miRNA may be explored for targeted treatment of the poor prognosis medulloblastomas having downregulation of miR-204 expression.

BIBLIOGRAPHY

1. Rossi, A., Caracciolo, V., Russo, G., Reiss, K., and Giordano, A. (2008). **Medulloblastoma: From molecular pathology to therapy**. *Clinical cancer research : an official journal of the American Association for Cancer Research* 14, 971-976.
2. Louis, D.N., Ohgaki, H., Wiestler, O.D., Cavenee, W.K., Burger, P.C., Jouvet, A., Scheithauer, B.W., and Kleihues, P. (2007). **The 2007 who classification of tumours of the central nervous system**. *Acta neuropathologica* 114, 97-109.
3. Polkinghorne, W.R., and Tarbell, N.J. (2007). **Medulloblastoma: Tumorigenesis, current clinical paradigm, and efforts to improve risk stratification**. *Nature clinical practice. Oncology* 4, 295-304.
4. Ris, M.D., Packer, R., Goldwein, J., Jones-Wallace, D., and Boyett, J.M. (2001). **Intellectual outcome after reduced-dose radiation therapy plus adjuvant chemotherapy for medulloblastoma: A children's cancer group study**. *Journal of clinical oncology : official journal of the American Society of Clinical Oncology* 19, 3470-3476.
5. Ning, M.S., Perkins, S.M., Dewees, T., and Shinohara, E.T. (2015). **Evidence of high mortality in long term survivors of childhood medulloblastoma**. *Journal of neuro-oncology* 122, 321-327.
6. Taylor, M.D., Northcott, P.A., Korshunov, A., Remke, M., Cho, Y.J., Clifford, S.C., Eberhart, C.G., Parsons, D.W., Rutkowski, S., Gajjar, A., et al. (2012). **Molecular subgroups of medulloblastoma: The current consensus**. *Acta neuropathologica* 123, 465-472.
7. Gottardo, N.G., Hansford, J.R., McGlade, J.P., Alvaro, F., Ashley, D.M., Bailey, S., Baker, D.L., Bourdeaut, F., Cho, Y.J., Clay, M., et al. (2014). **Medulloblastoma down under 2013: A report from the third annual meeting of the international medulloblastoma working group**. *Acta neuropathologica* 127, 189-201.
8. Kool, M., Korshunov, A., Remke, M., Jones, D.T., Schlanstein, M., Northcott, P.A., Cho, Y.J., Koster, J., Schouten-van Meeteren, A., van Vuurden, D., et al. (2012). **Molecular subgroups of medulloblastoma: An international meta-analysis of transcriptome, genetic aberrations, and clinical data of wnt, shh, group 3, and group 4 medulloblastomas**. *Acta neuropathologica* 123, 473-484.
9. Pugh, T.J., Weeraratne, S.D., Archer, T.C., Pomeranz Krummel, D.A., Auclair, D., Bochicchio, J., Carneiro, M.O., Carter, S.L., Cibulskis, K., Erlich, R.L., et al. (2012). **Medulloblastoma exome sequencing uncovers subtype-specific somatic mutations**. *Nature* 488, 106-110.
10. Jones, D.T., Jager, N., Kool, M., Zichner, T., Hutter, B., Sultan, M., Cho, Y.J., Pugh, T.J., Hovestadt, V., Stutz, A.M., et al. (2012). **Dissecting the genomic complexity underlying medulloblastoma**. *Nature* 488, 100-105.
11. Northcott, P.A., Shih, D.J., Peacock, J., Garzia, L., Morrissy, A.S., Zichner, T., Stutz, A.M., Korshunov, A., Reimand, J., Schumacher, S.E., et al. (2012). **Subgroup-specific structural variation across 1,000 medulloblastoma genomes**. *Nature* 488, 49-56.
12. Bartel, D.P. (2004). **Micrnas: Genomics, biogenesis, mechanism, and function**. *Cell* 116, 281-297.
13. Calin, G.A., and Croce, C.M. (2006). **Micrna signatures in human cancers**. *Nature reviews. Cancer* 6, 857-866.
14. Gokhale, A., Kunder, R., Goel, A., Sarin, R., Moiyadi, A., Shenoy, A., Mamidipally, C., Noronha, S., Kannan, S., and Shirsat, N.V. (2010). **Distinctive micrna signature of medulloblastomas associated with the wnt signaling pathway**. *Journal of cancer research and therapeutics* 6, 521-529.
15. Kunder, R., Jalali, R., Sridhar, E., Moiyadi, A., Goel, N., Goel, A., Gupta, T., Krishnatry, R., Kannan, S., Kurkure, P., et al. (2013). **Real-time pcr assay based on the differential expression of micrnas and protein-coding genes for molecular classification of formalin-fixed paraffin embedded medulloblastomas**. *Neuro-oncology* 15, 1644-1651.

16. Yogi, K., Sridhar, E., Goel, N., Jalali, R., Goel, A., Moiyadi, A., Thorat, R., Panwalkar, P., Khire, A., Dasgupta, A., et al. (2015). **Mir-148a, a microRNA upregulated in the wnt subgroup tumors, inhibits invasion and tumorigenic potential of medulloblastoma cells by targeting neuropilin 1.** *Oncoscience* 2, 334-348.
17. Crawford, J.R., MacDonald, T.J., and Packer, R.J. (2007). **Medulloblastoma in childhood: New biological advances.** *The Lancet. Neurology* 6, 1073-1085.
18. Sarkar, C., Deb, P., and Sharma, M.C. (2006). **Medulloblastomas: New directions in risk stratification.** *Neurology India* 54, 16-23.
19. Nicholson, J.C., Ross, F.M., Kohler, J.A., and Ellison, D.W. (1999). **Comparative genomic hybridization and histological variation in primitive neuroectodermal tumours.** *British journal of cancer* 80, 1322-1331.
20. Pomeroy, S.L., Tamayo, P., Gaasenbeek, M., Sturla, L.M., Angelo, M., McLaughlin, M.E., Kim, J.Y., Goumnerova, L.C., Black, P.M., Lau, C., et al. (2002). **Prediction of central nervous system embryonal tumour outcome based on gene expression.** *Nature* 415, 436-442.
21. Cowan, R., Hoban, P., Kelsey, A., Birch, J.M., Gattamaneni, R., and Evans, D.G. (1997). **The gene for the naevoid basal cell carcinoma syndrome acts as a tumour-suppressor gene in medulloblastoma.** *British journal of cancer* 76, 141-145.
22. Taylor, M.D., Liu, L., Raffel, C., Hui, C.C., Mainprize, T.G., Zhang, X., Agatep, R., Chiappa, S., Gao, L., Lowrance, A., et al. (2002). **Mutations in sufu predispose to medulloblastoma.** *Nature genetics* 31, 306-310.
23. Lam, C.W., Xie, J., To, K.F., Ng, H.K., Lee, K.C., Yuen, N.W., Lim, P.L., Chan, L.Y., Tong, S.F., and McCormick, F. (1999). **A frequent activated smoothened mutation in sporadic basal cell carcinomas.** *Oncogene* 18, 833-836.
24. Hamilton, S.R., Liu, B., Parsons, R.E., Papadopoulos, N., Jen, J., Powell, S.M., Krush, A.J., Berk, T., Cohen, Z., Tetu, B., et al. (1995). **The molecular basis of turcot's syndrome.** *The New England journal of medicine* 332, 839-847.
25. Huang, H., Mahler-Araujo, B.M., Sankila, A., Chimelli, L., Yonekawa, Y., Kleihues, P., and Ohgaki, H. (2000). **Apc mutations in sporadic medulloblastomas.** *The American journal of pathology* 156, 433-437.
26. Dahmen, R.P., Koch, A., Denkhaus, D., Tonn, J.C., Sorensen, N., Berthold, F., Behrens, J., Birchmeier, W., Wiestler, O.D., and Pietsch, T. (2001). **Deletions of axin1, a component of the wnt/wingless pathway, in sporadic medulloblastomas.** *Cancer research* 61, 7039-7043.
27. Zurawel, R.H., Chiappa, S.A., Allen, C., and Raffel, C. (1998). **Sporadic medulloblastomas contain oncogenic beta-catenin mutations.** *Cancer research* 58, 896-899.
28. Malkin, D. (2011). **Li-fraumeni syndrome.** *Genes & cancer* 2, 475-484.
29. Biegel, J.A., Rorke, L.B., Packer, R.J., Sutton, L.N., Schut, L., Bonner, K., and Emanuel, B.S. (1989). **Isochromosome 17q in primitive neuroectodermal tumors of the central nervous system.** *Genes, chromosomes & cancer* 1, 139-147.
30. Bigner, S.H., Friedman, H.S., Vogelstein, B., Oakes, W.J., and Bigner, D.D. (1990). **Amplification of the c-myc gene in human medulloblastoma cell lines and xenografts.** *Cancer research* 50, 2347-2350.
31. Herms, J., Neidt, I., Luscher, B., Sommer, A., Schurmann, P., Schroder, T., Bergmann, M., Wilken, B., Probst-Cousin, S., Hernaiz-Driever, P., et al. (2000). **C-myc expression in medulloblastoma and its prognostic value.** *International journal of cancer. Journal international du cancer* 89, 395-402.
32. Ramaswamy, V., Remke, M., Bouffet, E., Faria, C.C., Perreault, S., Cho, Y.J., Shih, D.J., Luu, B., Dubuc, A.M., Northcott, P.A., et al. (2013). **Recurrence patterns across medulloblastoma subgroups: An integrated clinical and molecular analysis.** *The Lancet. Oncology* 14, 1200-1207.

33. Northcott, P.A., Jones, D.T., Kool, M., Robinson, G.W., Gilbertson, R.J., Cho, Y.J., Pomeroy, S.L., Korshunov, A., Lichter, P., Taylor, M.D., et al. (2012). **Medulloblastomics: The end of the beginning**. *Nature reviews. Cancer* 12, 818-834.
34. Northcott, P.A., Korshunov, A., Witt, H., Hielscher, T., Eberhart, C.G., Mack, S., Bouffet, E., Clifford, S.C., Hawkins, C.E., French, P., et al. (2011). **Medulloblastoma comprises four distinct molecular variants**. *Journal of clinical oncology : official journal of the American Society of Clinical Oncology* 29, 1408-1414.
35. Dey, J., Ditzler, S., Knoblaugh, S.E., Hatton, B.A., Schelter, J.M., Cleary, M.A., Mecham, B., Rorke-Adams, L.B., and Olson, J.M. (2012). **A distinct smoothened mutation causes severe cerebellar developmental defects and medulloblastoma in a novel transgenic mouse model**. *Molecular and cellular biology* 32, 4104-4115.
36. Corcoran, R.B., and Scott, M.P. (2001). **A mouse model for medulloblastoma and basal cell nevus syndrome**. *Journal of neuro-oncology* 53, 307-318.
37. Hatton, B.A., Villavicencio, E.H., Tsuchiya, K.D., Pritchard, J.I., Ditzler, S., Pullar, B., Hansen, S., Knoblaugh, S.E., Lee, D., Eberhart, C.G., et al. (2008). **The smo/smo model: Hedgehog-induced medulloblastoma with 90% incidence and leptomeningeal spread**. *Cancer research* 68, 1768-1776.
38. Kim, J.Y., Nelson, A.L., Algon, S.A., Graves, O., Sturla, L.M., Goumnerova, L.C., Rowitch, D.H., Segal, R.A., and Pomeroy, S.L. (2003). **Medulloblastoma tumorigenesis diverges from cerebellar granule cell differentiation in patched heterozygous mice**. *Developmental biology* 263, 50-66.
39. Rausch, T., Jones, D.T., Zapatka, M., Stutz, A.M., Zichner, T., Weischenfeldt, J., Jager, N., Remke, M., Shih, D., Northcott, P.A., et al. (2012). **Genome sequencing of pediatric medulloblastoma links catastrophic DNA rearrangements with tp53 mutations**. *Cell* 148, 59-71.
40. Rudin, C.M., Hann, C.L., Laterra, J., Yauch, R.L., Callahan, C.A., Fu, L., Holcomb, T., Stinson, J., Gould, S.E., Coleman, B., et al. (2009). **Treatment of medulloblastoma with hedgehog pathway inhibitor gdc-0449**. *The New England journal of medicine* 361, 1173-1178.
41. Buonamici, S., Williams, J., Morrissey, M., Wang, A., Guo, R., Vattay, A., Hsiao, K., Yuan, J., Green, J., Ospina, B., et al. (2010). **Interfering with resistance to smoothened antagonists by inhibition of the pi3k pathway in medulloblastoma**. *Science translational medicine* 2, 51ra70.
42. Kawauchi, D., Robinson, G., Uziel, T., Gibson, P., Reh, J., Gao, C., Finkelstein, D., Qu, C., Pounds, S., Ellison, D.W., et al. (2012). **A mouse model of the most aggressive subgroup of human medulloblastoma**. *Cancer cell* 21, 168-180.
43. Northcott, P.A., Lee, C., Zichner, T., Stutz, A.M., Erkek, S., Kawauchi, D., Shih, D.J., Hovestadt, V., Zapatka, M., Sturm, D., et al. (2014). **Enhancer hijacking activates gfi1 family oncogenes in medulloblastoma**. *Nature* 511, 428-434.
44. Swartling, F.J., Savov, V., Persson, A.I., Chen, J., Hackett, C.S., Northcott, P.A., Grimmer, M.R., Lau, J., Chesler, L., Perry, A., et al. (2012). **Distinct neural stem cell populations give rise to disparate brain tumors in response to n-myc**. *Cancer cell* 21, 601-613.
45. Robinson, G., Parker, M., Kranenburg, T.A., Lu, C., Chen, X., Ding, L., Phoenix, T.N., Hedlund, E., Wei, L., Zhu, X., et al. (2012). **Novel mutations target distinct subgroups of medulloblastoma**. *Nature* 488, 43-48.
46. Lee, R.C., Feinbaum, R.L., and Ambros, V. (1993). **The c. Elegans heterochronic gene lin-4 encodes small rnas with antisense complementarity to lin-14**. *Cell* 75, 843-854.
47. Di Leva, G., Garofalo, M., and Croce, C.M. (2014). **Micronas in cancer**. *Annual review of pathology* 9, 287-314.

48. Chen, J.F., Mandel, E.M., Thomson, J.M., Wu, Q., Callis, T.E., Hammond, S.M., Conlon, F.L., and Wang, D.Z. (2006). **The role of microrna-1 and microrna-133 in skeletal muscle proliferation and differentiation.** *Nature genetics* 38, 228-233.
49. Faraoni, I., Antonetti, F.R., Cardone, J., and Bonmassar, E. (2009). **Mir-155 gene: A typical multifunctional microrna.** *Biochimica et biophysica acta* 1792, 497-505.
50. He, Y., Jiang, X., and Chen, J. (2014). **The role of mir-150 in normal and malignant hematopoiesis.** *Oncogene* 33, 3887-3893.
51. Winter, J., Jung, S., Keller, S., Gregory, R.I., and Diederichs, S. (2009). **Many roads to maturity: Microrna biogenesis pathways and their regulation.** *Nature cell biology* 11, 228-234.
52. Kent, O.A., and Mendell, J.T. (2006). **A small piece in the cancer puzzle: Micrnas as tumor suppressors and oncogenes.** *Oncogene* 25, 6188-6196.
53. Calin, G.A., Dumitru, C.D., Shimizu, M., Bichi, R., Zupo, S., Noch, E., Aldler, H., Rattan, S., Keating, M., Rai, K., et al. (2002). **Frequent deletions and down-regulation of micro- rna genes mir15 and mir16 at 13q14 in chronic lymphocytic leukemia.** *Proceedings of the National Academy of Sciences of the United States of America* 99, 15524-15529.
54. Davis-Dusenbery, B.N., and Hata, A. (2010). **Mechanisms of control of microrna biogenesis.** *Journal of biochemistry* 148, 381-392.
55. Ferretti, E., De Smaele, E., Po, A., Di Marcotullio, L., Tosi, E., Espinola, M.S., Di Rocco, C., Riccardi, R., Giangaspero, F., Farcomeni, A., et al. (2009). **Microrna profiling in human medulloblastoma.** *International journal of cancer. Journal international du cancer* 124, 568-577.
56. Cho, Y.J., Tsherniak, A., Tamayo, P., Santagata, S., Ligon, A., Greulich, H., Berhoukim, R., Amani, V., Goumnerova, L., Eberhart, C.G., et al. (2011). **Integrative genomic analysis of medulloblastoma identifies a molecular subgroup that drives poor clinical outcome.** *Journal of clinical oncology : official journal of the American Society of Clinical Oncology* 29, 1424-1430.
57. Northcott, P.A., Fernandez, L.A., Hagan, J.P., Ellison, D.W., Grajkowska, W., Gillespie, Y., Grundy, R., Van Meter, T., Rutka, J.T., Croce, C.M., et al. (2009). **The mir-17/92 polycistron is up-regulated in sonic hedgehog-driven medulloblastomas and induced by n-myc in sonic hedgehog-treated cerebellar neural precursors.** *Cancer research* 69, 3249-3255.
58. Uziel, T., Karginov, F.V., Xie, S., Parker, J.S., Wang, Y.D., Gajjar, A., He, L., Ellison, D., Gilbertson, R.J., Hannon, G., et al. (2009). **The mir-17~92 cluster collaborates with the sonic hedgehog pathway in medulloblastoma.** *Proceedings of the National Academy of Sciences of the United States of America* 106, 2812-2817.
59. Bai, A.H., Milde, T., Remke, M., Rolli, C.G., Hielscher, T., Cho, Y.J., Kool, M., Northcott, P.A., Jugold, M., Bazhin, A.V., et al. (2012). **Microrna-182 promotes leptomeningeal spread of non-sonic hedgehog-medulloblastoma.** *Acta neuropathologica* 123, 529-538.
60. Weeraratne, S.D., Amani, V., Teider, N., Pierre-Francois, J., Winter, D., Kye, M.J., Sengupta, S., Archer, T., Remke, M., Bai, A.H., et al. (2012). **Pleiotropic effects of mir-183~96~182 converge to regulate cell survival, proliferation and migration in medulloblastoma.** *Acta neuropathologica* 123, 539-552.
61. Andolfo, I., Liguori, L., De Antonellis, P., Cusanelli, E., Marinaro, F., Pistollato, F., Garzia, L., De Vita, G., Petrosino, G., Accordi, B., et al. (2012). **The micro-rna 199b-5p regulatory circuit involves hes1, cd15, and epigenetic modifications in medulloblastoma.** *Neuro-oncology* 14, 596-612.
62. Venkataraman, S., Birks, D.K., Balakrishnan, I., Alimova, I., Harris, P.S., Patel, P.R., Handler, M.H., Dubuc, A., Taylor, M.D., Foreman, N.K., et al. (2013). **Microrna 218 acts as a tumor suppressor by targeting multiple cancer phenotype-associated genes in medulloblastoma.** *The Journal of biological chemistry* 288, 1918-1928.

63. Silber, J., Hashizume, R., Felix, T., Hariono, S., Yu, M., Berger, M.S., Huse, J.T., VandenBerg, S.R., James, C.D., Hodgson, J.G., et al. (2013). **Expression of mir-124 inhibits growth of medulloblastoma cells.** *Neuro-oncology* 15, 83-90.
64. Boon, K., Eberhart, C.G., and Riggins, G.J. (2005). **Genomic amplification of orthodenticle homologue 2 in medulloblastomas.** *Cancer research* 65, 703-707.
65. Olsen, L., Klausen, M., Helboe, L., Nielsen, F.C., and Werge, T. (2009). **Micrnas show mutually exclusive expression patterns in the brain of adult male rats.** *PloS one* 4, e7225.
66. Hallahan, A.R., Pritchard, J.I., Hansen, S., Benson, M., Stoeck, J., Hatton, B.A., Russell, T.L., Ellenbogen, R.G., Bernstein, I.D., Beachy, P.A., et al. (2004). **The smoa1 mouse model reveals that notch signaling is critical for the growth and survival of sonic hedgehog-induced medulloblastomas.** *Cancer Res* 64, 7794-7800.
67. Lowry, O.H., Rosebrough, N.J., Farr, A.L., and Randall, R.J. (1951). **Protein measurement with the folin phenol reagent.** *J Biol Chem* 193, 265-275.
68. Laemmli, U.K. (1970). **Cleavage of structural proteins during the assembly of the head of bacteriophage t4.** *Nature* 227, 680-685.
69. Jacobsen, P.F., Jenkyn, D.J., and Papadimitriou, J.M. (1985). **Establishment of a human medulloblastoma cell line and its heterotransplantation into nude mice.** *Journal of neuropathology and experimental neurology* 44, 472-485.
70. Friedman, H.S., Burger, P.C., Bigner, S.H., Trojanowski, J.Q., Wikstrand, C.J., Halperin, E.C., and Bigner, D.D. (1985). **Establishment and characterization of the human medulloblastoma cell line and transplantable xenograft d283 med.** *Journal of neuropathology and experimental neurology* 44, 592-605.
71. Friedman, H.S., Burger, P.C., Bigner, S.H., Trojanowski, J.Q., Brodeur, G.M., He, X.M., Wikstrand, C.J., Kurtzberg, J., Berens, M.E., Halperin, E.C., et al. (1988). **Phenotypic and genotypic analysis of a human medulloblastoma cell line and transplantable xenograft (d341 med) demonstrating amplification of c-myc.** *The American journal of pathology* 130, 472-484.
72. Keles, G.E., Berger, M.S., Srinivasan, J., Kolstoe, D.D., Bobola, M.S., and Silber, J.R. (1995). **Establishment and characterization of four human medulloblastoma-derived cell lines.** *Oncol Res* 7, 493-503.
73. Wang, R., Hu, Y., Song, G., Hao, C.J., Cui, Y., Xia, H.F., and Ma, X. (2012). **Mir-206 regulates neural cells proliferation and apoptosis via otx2.** *Cellular physiology and biochemistry : international journal of experimental cellular physiology, biochemistry, and pharmacology* 29, 381-390.
74. Koutsoulidou, A., Mastroiannopoulos, N.P., Furling, D., Uney, J.B., and Phylactou, L.A. (2011). **Expression of mir-1, mir-133a, mir-133b and mir-206 increases during development of human skeletal muscle.** *BMC developmental biology* 11, 34.
75. McCarthy, J.J. (2008). **Microrna-206: The skeletal muscle-specific myomir.** *Biochimica et biophysica acta* 1779, 682-691.
76. Lucon, D.R., Rocha Cde, S., Craveiro, R.B., Dilloo, D., Cardinalli, I.A., Cavalcanti, D.P., Aguiar Sdos, S., Maurer-Morelli, C., and Yunes, J.A. (2013). **Downregulation of 14q32 micrnas in primary human desmoplastic medulloblastoma.** *Frontiers in oncology* 3, 254.
77. Frantz, G.D., Weimann, J.M., Levin, M.E., and McConnell, S.K. (1994). **Otx1 and otx2 define layers and regions in developing cerebral cortex and cerebellum.** *The Journal of neuroscience : the official journal of the Society for Neuroscience* 14, 5725-5740.
78. Adamson, D.C., Shi, Q., Wortham, M., Northcott, P.A., Di, C., Duncan, C.G., Li, J., McLendon, R.E., Bigner, D.D., Taylor, M.D., et al. (2010). **Otx2 is critical for the maintenance and progression of shh-independent medulloblastomas.** *Cancer research* 70, 181-191.

79. Di, C., Liao, S., Adamson, D.C., Parrett, T.J., Broderick, D.K., Shi, Q., Lengauer, C., Cummins, J.M., Velculescu, V.E., Fuets, D.W., et al. (2005). **Identification of otx2 as a medulloblastoma oncogene whose product can be targeted by all-trans retinoic acid.** *Cancer Res* 65, 919-924.
80. Bai, R., Siu, I.M., Tyler, B.M., Staedtke, V., Gallia, G.L., and Riggins, G.J. (2010). **Evaluation of retinoic acid therapy for otx2-positive medulloblastomas.** *Neuro-oncology* 12, 655-663.
81. Bunt, J., Hasselt, N.E., Zwijnenburg, D.A., Hamdi, M., Koster, J., Versteeg, R., and Kool, M. (2012). **Otx2 directly activates cell cycle genes and inhibits differentiation in medulloblastoma cells.** *Int J Cancer* 131, E21-32.
82. Dey, J., Dubuc, A.M., Pedro, K.D., Thistrup, D., Mecham, B., Northcott, P.A., Wu, X., Shih, D., Tapscott, S.J., LeBlanc, M., et al. (2013). **Myod is a tumor suppressor gene in medulloblastoma.** *Cancer research* 73, 6828-6837.
83. Rosenberg, M.I., Georges, S.A., Asawachaicharn, A., Analau, E., and Tapscott, S.J. (2006). **Myod inhibits fstl1 and utrn expression by inducing transcription of mir-206.** *The Journal of cell biology* 175, 77-85.
84. Yin, Y., Zhang, B., Wang, W., Fei, B., Quan, C., Zhang, J., Song, M., Bian, Z., Wang, Q., Ni, S., et al. (2014). **Mir-204-5p inhibits proliferation and invasion and enhances chemotherapeutic sensitivity of colorectal cancer cells by downregulating rab22a.** *Clinical cancer research : an official journal of the American Association for Cancer Research* 20, 6187-6199.
85. Lam, E.K., Wang, X., Shin, V.Y., Zhang, S., Morrison, H., Sun, J., Ng, E.K., Yu, J., and Jin, H. (2011). **A microrna contribution to aberrant ras activation in gastric cancer.** *American journal of translational research* 3, 209-218.
86. Li, G., Luna, C., Qiu, J., Epstein, D.L., and Gonzalez, P. (2011). **Role of mir-204 in the regulation of apoptosis, endoplasmic reticulum stress response, and inflammation in human trabecular meshwork cells.** *Investigative ophthalmology & visual science* 52, 2999-3007.
87. Chung, T.K., Lau, T.S., Cheung, T.H., Yim, S.F., Lo, K.W., Siu, N.S., Chan, L.K., Yu, M.Y., Kwong, J., Doran, G., et al. (2012). **Dysregulation of microrna-204 mediates migration and invasion of endometrial cancer by regulating foxc1.** *International journal of cancer. Journal international du cancer* 130, 1036-1045.
88. Zhang, L., Wang, X., and Chen, P. (2013). **Mir-204 down regulates sirt1 and reverts sirt1-induced epithelial-mesenchymal transition, anoikis resistance and invasion in gastric cancer cells.** *BMC cancer* 13, 290.
89. Mikhaylova, O., Stratton, Y., Hall, D., Kellner, E., Ehmer, B., Drew, A.F., Gallo, C.A., Plas, D.R., Biesiada, J., Meller, J., et al. (2012). **Vhl-regulated mir-204 suppresses tumor growth through inhibition of lc3b-mediated autophagy in renal clear cell carcinoma.** *Cancer cell* 21, 532-546.
90. Osawa, H., Smith, C.A., Ra, Y.S., Kongkham, P., and Rutka, J.T. (2009). **The role of the membrane cytoskeleton cross-linker ezrin in medulloblastoma cells.** *Neuro-oncology* 11, 381-393.
91. Elliott, B.E., Meens, J.A., SenGupta, S.K., Louvard, D., and Arpin, M. (2005). **The membrane cytoskeletal crosslinker ezrin is required for metastasis of breast carcinoma cells.** *Breast cancer research : BCR* 7, R365-373.
92. Khanna, C., Wan, X., Bose, S., Cassaday, R., Olomu, O., Mendoza, A., Yeung, C., Gorlick, R., Hewitt, S.M., and Helman, L.J. (2004). **The membrane-cytoskeleton linker ezrin is necessary for osteosarcoma metastasis.** *Nature medicine* 10, 182-186.
93. Yu, Y., Khan, J., Khanna, C., Helman, L., Meltzer, P.S., and Merlino, G. (2004). **Expression profiling identifies the cytoskeletal organizer ezrin and the developmental homeoprotein six-1 as key metastatic regulators.** *Nature medicine* 10, 175-181.

94. Wang, F.E., Zhang, C., Maminishkis, A., Dong, L., Zhi, C., Li, R., Zhao, J., Majerciak, V., Gaur, A.B., Chen, S., et al. (2010). **Microrna-204/211 alters epithelial physiology**. *FASEB journal : official publication of the Federation of American Societies for Experimental Biology* 24, 1552-1571.
95. Deo, M., Yu, J.Y., Chung, K.H., Tippens, M., and Turner, D.L. (2006). **Detection of mammalian microrna expression by in situ hybridization with rna oligonucleotides**. *Developmental dynamics : an official publication of the American Association of Anatomists* 235, 2538-2548.
96. Huang, J., Zhao, L., Xing, L., and Chen, D. (2010). **Microrna-204 regulates runx2 protein expression and mesenchymal progenitor cell differentiation**. *Stem cells* 28, 357-364.
97. Courboulain, A., Paulin, R., Giguere, N.J., Saksouk, N., Perreault, T., Meloche, J., Paquet, E.R., Biardel, S., Provencher, S., Cote, J., et al. (2011). **Role for mir-204 in human pulmonary arterial hypertension**. *The Journal of experimental medicine* 208, 535-548.
98. Conte, I., Carrella, S., Avellino, R., Karali, M., Marco-Ferreres, R., Bovolenta, P., and Banfi, S. (2010). **Mir-204 is required for lens and retinal development via meis2 targeting**. *Proceedings of the National Academy of Sciences of the United States of America* 107, 15491-15496.
99. Abou-Elhamd, K.E., Habib, T.N., Moussa, A.E., and Badawy, B.S. (2008). **The role of genetic susceptibility in head and neck squamous cell carcinoma**. *European archives of oto-rhino-laryngology : official journal of the European Federation of Oto-Rhino-Laryngological Societies* 265, 217-222.
100. Volinia, S., Galasso, M., Costinean, S., Tagliavini, L., Gamberoni, G., Drusco, A., Marchesini, J., Mascellani, N., Sana, M.E., Abu Jarour, R., et al. (2010). **Reprogramming of mirna networks in cancer and leukemia**. *Genome research* 20, 589-599.
101. Ying, Z., Li, Y., Wu, J., Zhu, X., Yang, Y., Tian, H., Li, W., Hu, B., Cheng, S.Y., and Li, M. (2013). **Loss of mir-204 expression enhances glioma migration and stem cell-like phenotype**. *Cancer research* 73, 990-999.
102. Gong, M., Ma, J., Li, M., Zhou, M., Hock, J.M., and Yu, X. (2012). **Microrna-204 critically regulates carcinogenesis in malignant peripheral nerve sheath tumors**. *Neuro-oncology* 14, 1007-1017.
103. Johannes, L., and Popoff, V. (2008). **Tracing the retrograde route in protein trafficking**. *Cell* 135, 1175-1187.
104. Stenmark, H., and Olkkonen, V.M. (2001). **The rab gtpase family**. *Genome biology* 2, S3007.
105. Goldenring, J.R. (2013). **A central role for vesicle trafficking in epithelial neoplasia: Intracellular highways to carcinogenesis**. *Nature reviews. Cancer* 13, 813-820.
106. Schuck, S., Gerl, M.J., Ang, A., Manninen, A., Keller, P., Mellman, I., and Simons, K. (2007). **Rab10 is involved in basolateral transport in polarized madin-darby canine kidney cells**. *Traffic* 8, 47-60.
107. Etienne-Manneville, S. (2008). **Polarity proteins in migration and invasion**. *Oncogene* 27, 6970-6980.
108. Wang, T., Liu, Y., Xu, X.H., Deng, C.Y., Wu, K.Y., Zhu, J., Fu, X.Q., He, M., and Luo, Z.G. (2011). **Lgl1 activation of rab10 promotes axonal membrane trafficking underlying neuronal polarization**. *Developmental cell* 21, 431-444.
109. Xu, X.H., Deng, C.Y., Liu, Y., He, M., Peng, J., Wang, T., Yuan, L., Zheng, Z.S., Blackshear, P.J., and Luo, Z.G. (2014). **Marcks regulates membrane targeting of rab10 vesicles to promote axon development**. *Cell research* 24, 576-594.
110. Chen, R.X., Song, H.Y., Dong, Y.Y., Hu, C., Zheng, Q.D., Xue, T.C., Liu, X.H., Zhang, Y., Chen, J., Ren, Z.G., et al. (2014). **Dynamic expression patterns of differential proteins during early invasion of hepatocellular carcinoma**. *PloS one* 9, e88543.

111. Deen, A.J., Rilla, K., Oikari, S., Karna, R., Bart, G., Hayrinen, J., Bathina, A.R., Ropponen, A., Makkonen, K., Tammi, R.H., et al. (2014). **Rab10-mediated endocytosis of the hyaluronan synthase has3 regulates hyaluronan synthesis and cell adhesion to collagen.** *The Journal of biological chemistry* 289, 8375-8389.
112. Coutinho, M.F., Prata, M.J., and Alves, S. (2012). **Mannose-6-phosphate pathway: A review on its role in lysosomal function and dysfunction.** *Molecular genetics and metabolism* 105, 542-550.
113. Kauppi, M., Simonsen, A., Bremnes, B., Vieira, A., Callaghan, J., Stenmark, H., and Olkkonen, V.M. (2002). **The small gtpase rab22 interacts with eea1 and controls endosomal membrane trafficking.** *Journal of cell science* 115, 899-911.
114. Haldipur, P., Gillies, G.S., Janson, O.K., Chizhikov, V.V., Mithal, D.S., Miller, R.J., and Millen, K.J. (2014). **Foxc1 dependent mesenchymal signalling drives embryonic cerebellar growth.** *eLife* 3.
115. Sizemore, S.T., and Keri, R.A. (2012). **The forkhead box transcription factor foxc1 promotes breast cancer invasion by inducing matrix metalloprotease 7 (mmp7) expression.** *The Journal of biological chemistry* 287, 24631-24640.
116. Hovestadt, V., Jones, D.T., Picelli, S., Wang, W., Kool, M., Northcott, P.A., Sultan, M., Stachurski, K., Ryzhova, M., Warnatz, H.J., et al. (2014). **Decoding the regulatory landscape of medulloblastoma using DNA methylation sequencing.** *Nature* 510, 537-541.
117. Leiphrahpam, P.D., Rajput, A., Mathiesen, M., Agarwal, E., Lazenby, A.J., Are, C., Brattain, M.G., and Chowdhury, S. (2014). **Ezrin expression and cell survival regulation in colorectal cancer.** *Cellular signalling* 26, 868-879.

PUBLICATIONS